Development 134, 1454 (2007) doi:10.1242/dev.02841

β-catenin, MAPK and Smad signaling during early *Xenopus* development

Anne Schohl and François Fagotto

The link for the supplementary material published in *Development* **129**, 37-52 is incorrect.

The correct link is http://dev.biologists.org/cgi/content/full/129/1/37/DC1.

The authors apologise to readers for this mistake.

Development 129, 37-52 (2002)
Printed in Great Britain © The Company of Biologists Limited 2002
DEV2792

β-catenin, MAPK and Smad signaling during early *Xenopus* development

Anne Schohl and François Fagotto*

Department of Cell Biology, Max Planck Institute for Developmental Biology, Spemannstrasse 35, D-72076 Tübingen, Germany
*Author for correspondence (e-mail: francois.fagotto@tuebingen.mpg.de)

Accepted 8 October 2001

SUMMARY

Knowledge of when and where signaling pathways are activated is crucial for understanding embryonic development. In this study, we have systematically analyzed and compared the signaling pattern of four major pathways by localization of the activated key components β-catenin (Wnt proteins), MAPK (tyrosine kinase receptors/FGF), Smad1 (BMP proteins) and Smad2 (Nodal/activin/Vg1). We have determined semi-quantitatively the distribution of these components at 18 consecutive stages in *Xenopus* development, from early blastula to tailbud stages, by immunofluorescence on serial cryosections. The image obtained is that of very dynamic and widespread activities, with very few inactive regions. Signaling fields can vary from large gradients to restricted areas with sharp borders. They do not respect tissue boundaries. This direct visualization of active signaling verifies several predictions inferred from previous functional data. It also reveals unexpected signal patterns, pointing to some poorly understood aspects of early development. In several instances, the patterns strikingly overlap, suggesting extensive interplay between the various pathways. To test this possibility, we have manipulated maternal β-catenin signaling and determined the effect on the other pathways in the blastula embryo. We found that the patterns of P-MAPK, P-Smad1 and P-Smad2 are indeed strongly dependent on β-catenin at this stage.

Supplementary material:
http://www.eb.tuebingen.mpg.de/papers/fagotto_dev_2002.html

Key words: Signal transduction, Wnt, Activin, Vg1, Nodal, FGF, *Xenopus laevis*

INTRODUCTION

Embryonic induction relies on a relatively small number of signal transduction pathways, which are used repeatedly and in various combinations during development. The set of gene targets affected by a given pathway depends on the intensity of the signal, the history of the cell (competence), and the cross-talk with other signals. A precise activation of these pathways in space, time and intensity is thus crucial for proper embryonic patterning. Our present knowledge of these parameters is still very fragmentary. It is essentially inferred from the expression patterns of secreted inducers and of target genes, and from functional data on the requirement for certain pathways. Yet, many secreted factors can activate the same pathways, only a few have been so far characterized, and comparative data on their relative abundance are virtually non-existent. Moreover, mRNA localization provides no information on the actual activity of the secreted factors and their range of diffusion. These depend on a variety of parameters such as processing, secretion, retention (and/or activation) by binding to the extracellular matrix, presence of extracellular inhibitors/competitors, affinity for a given receptor, or functional state of the receptor and of the downstream components. The expression pattern of target genes may reflect more directly the signaling activities, but the available information is incomplete, and its interpretation is complicated by the fact that most genes are targets of more than one pathway. Also, the transcripts may survive long after disappearance of the signal, obscuring the dynamics of the inductive pathways.

The most reliable method of characterizing signaling activities in the embryo is the direct detection of downstream components in their active state. In many cases, these downstream components are resident cytoplasmic proteins, which enter the nucleus specifically upon stimulation of the corresponding pathway. We have chosen to study four such components: β-catenin, Smad1, Smad2 and MAPK. Each of these components transduces a specific pathway, triggered by a family of secreted factors. (1) β-catenin is stabilized/activated by Wnts (Cadigan and Nusse, 1997); (2) the Smads are phosphorylated upon stimulation by TGFβ-related factors (Massague, 1998; Heldin et al., 1997), by BMPs for Smad1, by activin, Vg1 and Nodal-related proteins (Xnrs) for Smad2. (3) Finally, one of the members of the MAPK family, ERK, is phosphorylated/activated in response to various ligands of tyrosine kinase receptors, including FGF (Cobb and Goldsmith, 2000).

Numerous functional studies have provided evidence indicating essential roles for these four pathways in early patterning of the vertebrate embryos, roles that appear to be at least partly conserved from fish to mammals. The β-catenin pathway determines the body axis (Heasman et al., 1994; Heasman, 1997; Harland and Gerhart, 1997). This early β-catenin signaling is activated by an unknown maternal dorsalizing determinant that is anchored to the vegetal cortex

of the egg and is asymmetrically re-localized at fertilization (Darras et al., 1997; Harland and Gerhart, 1997; Marikawa et al., 1997). Zygotic Wnt8 is involved in determination of the paraxial mesoderm (somites) and inhibition of anterior and axial mesoderm (Christian and Moon, 1993; Hoppler et al., 1996; Leyns et al., 1997; Wang et al., 1997; Niehrs, 1999). Various Wnts are expressed at later stages, and function in particular in neural patterning (Joyner, 1996; Ikeya et al., 1997).

FGF/MAPK signaling plays an essential, but not fully understood role in mesoderm formation (Amaya et al., 1991; Harland and Gerhart, 1997). FGF may act as a competence factor for mesoderm induction (Kimelman et al., 1992; Cornell et al., 1995; Harland and Gerhart, 1997; LaBonne and Whitman, 1997), or may only function in mesoderm maintenance (Isaacs et al., 1994; Schulte-Merker and Smith, 1995; Harland and Gerhart, 1997). FGF can later also induce/posteriorize the neuroderm (Cox and Hemmati-Brivanlou, 1995; Lamb and Harland, 1995; Isaacs et al., 1998). Some other activators of MAPK, such as PDGF, are also expressed during early development (Ataliotis et al., 1995).

Mesoderm and endoderm formation requires activin-like signals emanating from the vegetal pole (Hemmati-Brivanlou and Melton, 1992; Schulte-Merker et al., 1994; Harland and Gerhart, 1997), which may act as morphogens, activating distinct genes at different doses (Green et al., 1992; Gurdon et al., 1994). The egg contains the maternal factors activin (Oda et al., 1995) and the vegetally localized Vg1 (Weeks and Melton, 1987). The current models, however, attribute a crucial role to Xnrs, induced by the maternal transcription factor VegT in the vegetal hemisphere of late blastulae (Zhang et al., 1998; Clements et al., 1999; Kofron et al., 1999; Sun et al., 1999; Agius et al., 2000; Takahashi et al., 2000; Yasuo and Lemaire, 1999). Whether the VegT-Xnrs pathway is responsible alone for endoderm-mesoderm induction, or whether it synergizes with another maternal factor such as Vg1 is still unclear (Zhang et al., 1998; Clements et al., 1999).

The function of BMP signaling during gastrulation is to impose a ventral fate (Sasai and De Robertis, 1997; Lemaire and Yasuo, 1998; Dale and Wardle, 1999). BMPs are strongly expressed during gastrulation in the ventral and lateral ectoderm and mesoderm, except in the dorsal region corresponding to the prospective neuroderm and the Spemann Organizer (Fainsod et al., 1994; Hemmati-Brivanlou and Thomsen, 1995; Schmidt et al., 1995). BMPs can act as morphogens, and induce lateral to ventral fates in a dose dependent manner. The Organizer antagonizes BMP signaling both by transcriptional repression of BMPs, and through secretion of soluble inhibitors of BMP ligands, such as Noggin and Chordin (Lemaire and Yasuo, 1998; Dale and Wardle, 1999). At later stages, BMPs are expressed in the dorsal neural tube and the overlaying ectoderm. They can dorsalize the neural tissue, and antagonize the ventralizing activity of Sonic hedgehog emanating from the notochord (Sasai and De Robertis, 1997).

Activation of these four pathways can be detected biochemically and histologically: in non-stimulated cells, β-catenin is restricted to the plasma membrane, and cytoplasmic levels are maintained very low. In activated cells, the soluble pool is increased, and nuclear accumulation is conspicuous (Cadigan and Nusse, 1997). Nuclear β-catenin has been detected in the dorsal cells of *Xenopus* and zebrafish blastulae, in agreement with its role in axis induction (Schneider et al., 1996). Upon stimulation, Smad1, Smad2 and MAPK become phosphorylated and accumulate in the nucleus (Cobb and Goldsmith, 2000; Heldin et al., 1997; Massague, 1998). These phosphorylated forms are recognized by specific antibodies (Christen and Slack, 1999; Faure et al., 2000). Localization of Smad1 and Smad2 at the early gastrula stage have been recently reported (Faure et al., 2000), but phosphorylated MAPK is the only component that has received a thorough examination during development (Christen and Slack, 1999; Curran and Grainger, 2000). All previous immunolocalization data were obtained using whole-mount staining procedures, which are not ideally suited for the study of large embryos. Immunofluorescence on cryosections (Fagotto and Gumbiner, 1994; Fagotto, 1999) has allowed us to perform a detailed, semi-quantitative and comparative analysis of the four signaling pathways. This is to our knowledge the first systematic description of signal transduction pattern during vertebrate development.

MATERIALS AND METHODS

Immunofluorescence

Embryos were fixed in paraformaldehyde, postfixed in DMSO/methanol, embedded in fish gelatin and 10 μm serial cryosections were prepared as described (Fagotto, 1999). Sections were stained with the following antibodies: affinity purified rabbit anti-β-catenin (Schneider et al., 1996) (1 μg/ml), mouse anti-P-ERK (1/250; Sigma), rabbit anti-P-Smad1 (1/500) and anti-P-Smad2 (1/250; kindly provided by Peter ten Dijke, NKI, Amsterdam). Secondary and tertiary antibodies were donkey anti-mouse Alexa488 (1/100, Molecular Probes), goat-anti-donkey Alexa488 (1/100) and donkey anti-rabbit Cy3 (1/100, Dianova). The nuclei were counterstained with DAPI, and the yolk with Eriochrome Black (Sigma).

Image acquisition and analysis (Fig. 1)

To obtain comparable signal intensities, sections from different stages were stained simultaneously, and the images were collected and processed identically. The samples were observed with a 25× water-immersion objective (NA 0.8) on an Axiovert fluorescence microscope (Zeiss). Three filter sets were used: a DAPI filter; a FITC-filter set with a long pass emission filter allowing simultaneous collection of the green Alex488 image and the red Eriochrome image; a Cy3 filter set with narrow orange emission filter, which excludes the red Eriochrome signal. Images were collected with a DXC-950P 3CCD video camera (Sony). Composite images of whole sections were produced by collecting 20-40 contiguous images using an automated stage and AnalySIS software (Soft Imaging System).

Image processing was performed using Photoshop (Adobe Systems Inc.) and AnalySIS programs. Images were first adjusted for background and intensity, such that the absolute strongest signal during early development was set to 100%. Cross-reactivity signals from the vitellin membrane with Smad1 and Smad2 antibodies were removed digitally. Except for images showing Eriochrome counterstaining, all images were transformed in monochrome RGB images (red for Cy3, green for Alexa488, blue for DAPI). Red, green and blue images were then merged. Nuclear images were obtained by using the blue channel (DAPI staining) as a mask (Fig. 1). The use of a DAPI mask was especially important for β-catenin staining, since the strong plasma membrane signal complicated, and

sometimes obscured, the nuclear staining. The other three signals were almost exclusively nuclear, except for P-MAPK in animal caps of blastulae, where a significant cytoplasmic staining was also observed [see also Curran and Grainger (Curran and Grainger, 2000)]. To minimize overlap of β-catenin signal from the plasma membrane, which can occur in the small cells of late stages, the areas of the masks were shrunk (1 pixel/radius of each nucleus) using an 'erosion function'. The nuclei were finally re-expanded (2-3 pixels/radius) in the final nuclear images for better visibility. For estimation of the signal intensities, pseudocolors were used on nuclear images (Fig. 1). The intensity range was divided into four equal parts, and translated into four colors in the drawings, from white (no signal) to red (strongest signal). In some cases, a very weak or spotted signal was reproducibly observed, which is depicted in pale yellow.

In control experiments, embryos overexpressing Axin, a downregulator of β-catenin, or dominant negative receptors (MAPK and Smad) showed strong reduction of the corresponding nuclear signals (supplementary Fig. S1). Controls demonstrating the absence of bleed-through between the green and Cy3 channels in our double-staining experiments are also shown in the supplementary material (Fig. S2).

Embryo manipulation

30 minutes after fertilization, eggs were UV-irradiated from the vegetal side using a UV-Stratalinker 1800 (Statagene; energy: 85 mJ). The degree of ventralization (dorsoanterior index) (Kao and Elinson, 1988) measured at early tadpole stages was <0.5 (5 is normal, 0 is maximal ventralization). 32-cell stage embryos were incubated for 30 minutes in 133 mM LiCl, which produces a strong dorsalization phenotype. 1 ng Myc-tagged β-catenin mRNA was injected ventrally in 4-cell stage embryos.

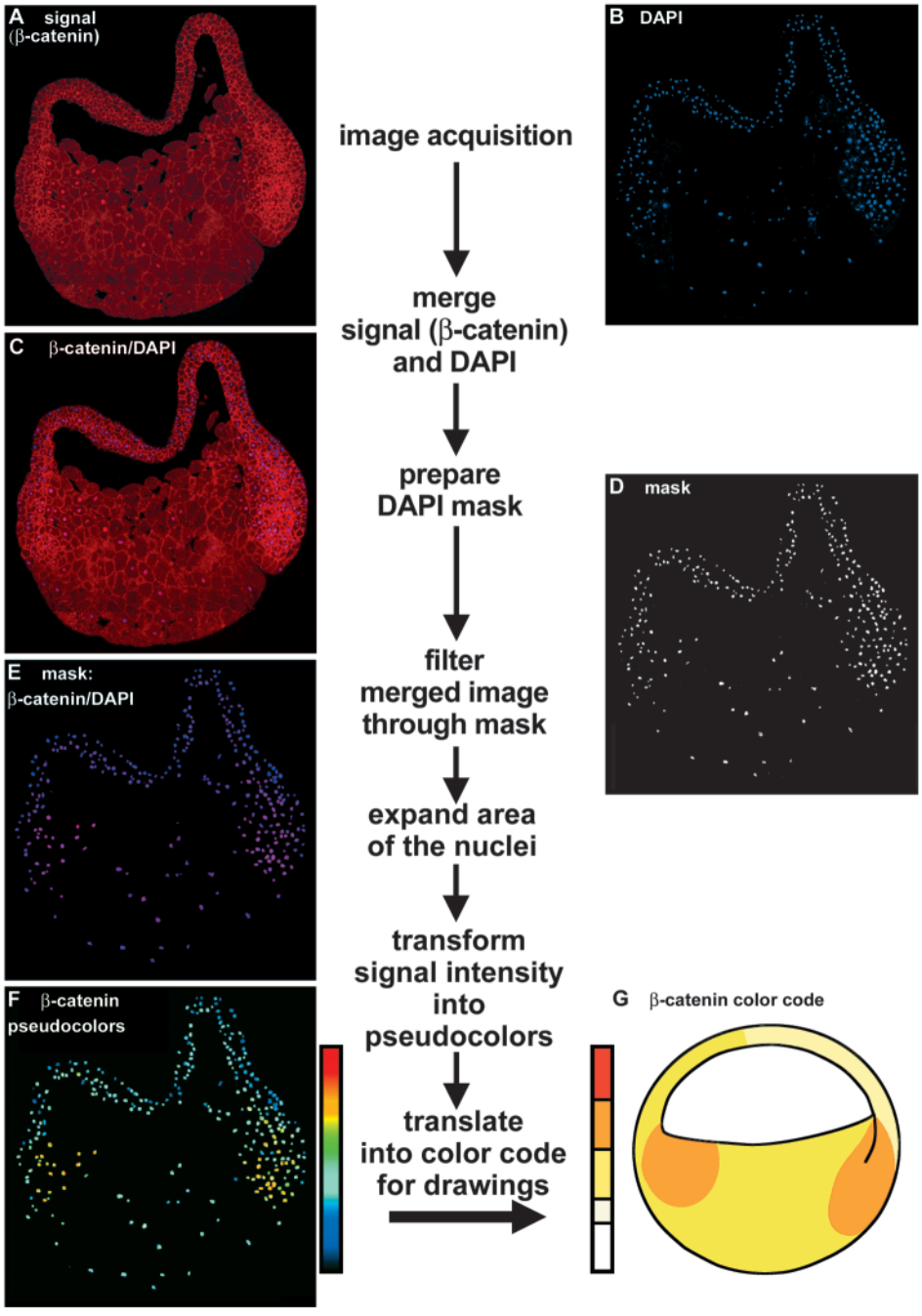

Fig. 1. Example of image processing for the analysis of nuclear signals: β-catenin staining of a parasagittal section, stage 10.25. 25 consecutive images of β-catenin signal (A, red channel) and of DAPI staining (B, blue channel) were collected and collated automatically. The two images were merged (C), and filtered through a mask (D) created from the DAPI image. Because nuclei are small and their intensity difficult to visualize at low magnification, the nuclear area was expanded (E). To obtain semi-quantitative information, the intensity of the β-catenin signal was translated into pseudocolors (F). The intensities were divided into five categories and translated into a color code (red to white) used for our drawings (G). Note that pale yellow can represent very weak or inhomogeneous signals. An identical procedure was used to analyze signals for P-Smad2 (red channel), P-Smad1 and P-MAPK (green channel).

RESULTS AND DISCUSSION

Methodology

Previous data on β-catenin, Smad or MAPK localization in *Xenopus* have been obtained using whole-mount based techniques. These methods are widely used for in situ hybridization, and provide good information for the superficial structures of the embryo. However, they suffer from the very limited penetration of large molecules, in particular antibodies, through the thickness of the embryonic tissues. In attempts to circumvent this limitation, whole-mount staining of embryo halves have been used (Faure et al., 2000), but, even then, the deep, yolk-rich cells are still poorly stained (compare Smad

staining in Faure et al. and in the present work) (Faure et al., 2000).

To obtain unequivocal results, we have localized β-catenin, Smad1, Smad2 and MAPK by indirect immunofluorescence on cryosections. Owing to the complexity and the dynamics of the signals, it was important to collect a large number of images of consecutive stages, using serial sections and sections obtained along different axes. The distribution of the four signaling components could be directly compared by double staining and staining of adjacent sections. For each pathway, the relative intensity at various stages was estimated using image processing (see Materials and Methods and Fig. 1). For each stage (stages 8-20) an average distribution obtained by comparing different embryos was represented in schematic drawings. These results are summarized in Fig. 8, Fig. 9, Fig. 10, Fig. 11, Fig. 12. Examples of selected stages are presented in Fig. 2, Fig. 3, Fig. 4, Fig. 5, Fig. 6, Fig. 7. A collection of immunofluorescence images for each staining, which also includes later stages not represented in the drawings, is available as supplementary material at http://www.eb.tuebingen.mpg.de/papers/fagotto_dev_2002.html. Also included in the supplementary material are animated drawings of these signals during early development.

A detailed discussion of each pattern is beyond our scope. We limit our presentation to the most striking features of each pathway, and discuss some specific aspects in relationship to previous data and current models. The comparison of these patterns suggests a possible subdivision in three phases, early (before gastrulation), gastrulation, and later stages, which we have largely followed in our presentation of each pathway. Finally, we highlight some general features emerging from this study.

β-catenin

β-catenin staining in blastulae (Fig. 2, Fig. 3, Fig. 4, summary Fig. 9)

At stage 8-8.5, β-catenin accumulation is prominent in the dorsal nuclei (Fig. 2A-B, Fig. 4A′, double arrowheads). Dorsal accumulation is prevented when cortical rotation is inhibited by UV irradiation (Fig. 4). β-catenin is then strongest in vegetal

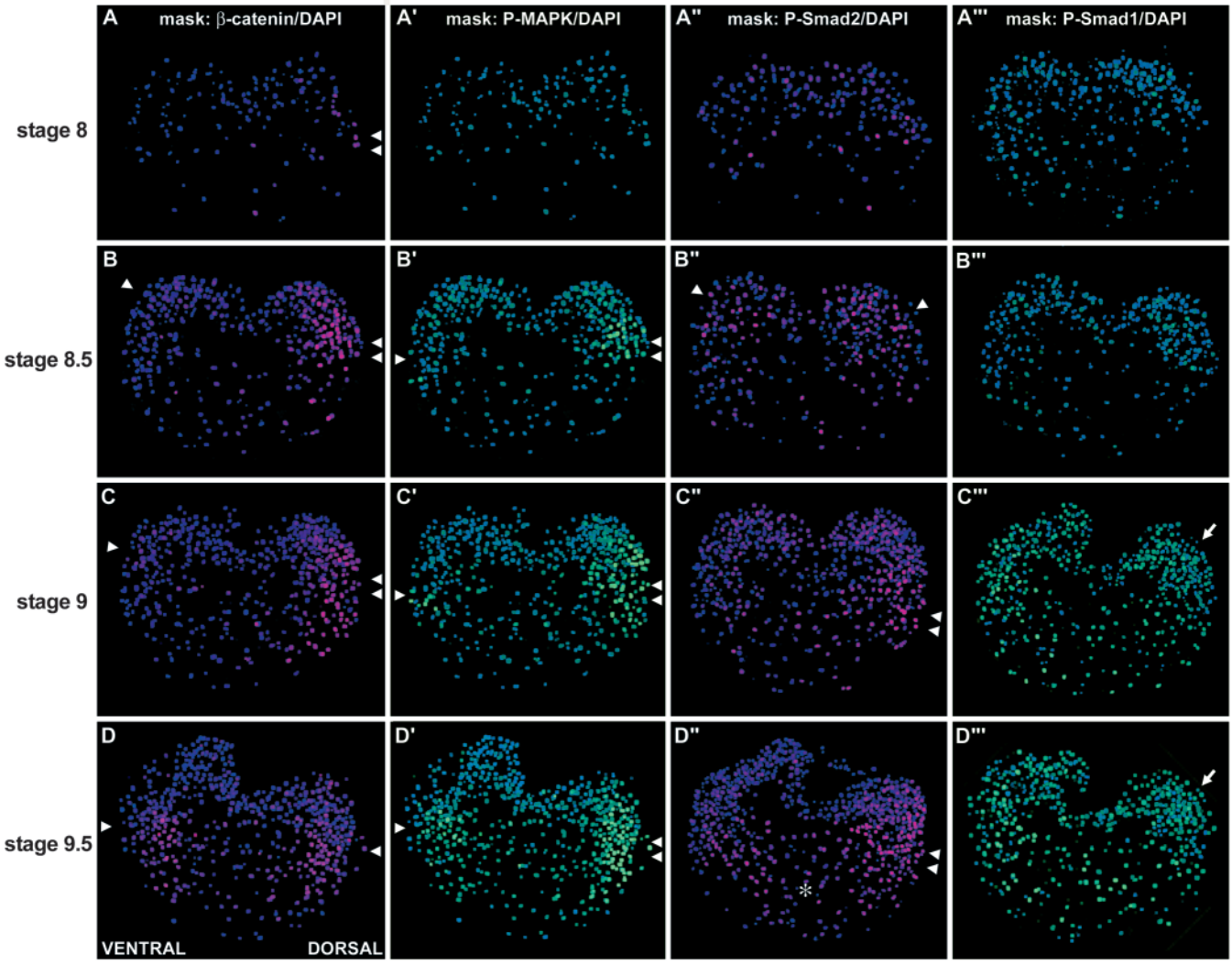

Fig. 2. Distribution of nuclear β-catenin, P-MAPK and P-Smads during blastula stages. Because there are only few nuclei per section at early stages, nuclear images of several sections were superimposed (number of sections: stages 8 and 8.5=5; stage 9=3-4; stage 9.5=3). β-catenin and P-MAPK images are from double-stained sections. Arrows and arrowheads point at particular aspects of the patterns discussed in the text.

nuclei (Fig. 4B′, asterisk). Previous observations had suggested that activation of maternal β-catenin occurred near the surface of the embryo (Schneider et al., 1996). However, nuclear β-catenin clearly extends to the deep layers in our on-section staining, both in normal and in UV-irradiated embryos. Thus, activation of β-catenin is not restricted to the cortex of the embryo, but must spread toward the interior after cortical rotation. Surprisingly, lower levels of nuclear β-catenin are also present throughout the embryo. Perhaps, activation of the dorsalizing pathway 'leaks' out of the dorsal region. Alternatively, a ubiquitous basal activity might be induced by maternal Wnts such as Wnt8b (Cui et al., 1995).

From stage 8.5 to stage 9.5, nuclear β-catenin also increases progressively on the ventral and lateral sides to form a ring (Fig. 2B-D, Fig. 3B′, Fig. 4C′, Fig. 4E′, arrowheads). This ring overlaps with the prospective mesoderm, but is wider than the ring of P-MAPK (see below), and includes dorsal vegetal cells. It shifts progressively lower, a likely consequence of epiboly. This ring-shaped signal was unexpected. During early development, β-catenin is classically thought to be activated by two consecutive signals with opposite effects: the maternal dorsalizing activity, and the zygotic ventrolateral Wnt8, which has a ventralizing function during gastrulation (Christian and Moon, 1993; Hoppler et al., 1996). It is unlikely that the ring might represent the overlap of both early and late signals. It appears earlier than expected for induction by Wnt8, and persists longer than the maternal dorsalizing activity (Jones and Woodland, 1987; Harland and Gerhart, 1997). Alternatively, this ring may reveal the existence of a third intermediate signal. In UV-irradiated embryos, β-catenin activity at stage 9.5 was shifted more vegetal, occupying the lower marginal zone and the vegetal mass (Fig. 4D′,F′, asterisks). Thus, the late blastula pattern seems to depend on the position of the early maternal signal: the signal seems to spread from dorsal to ventral along the equator in normal embryos, and to radiate from the vegetal pole in UV-irradiated embryos.

β-catenin staining during gastrulation (Fig. 5, Fig. 6, summary Fig. 9)

At stage 10.25, β-catenin is still present all around the marginal zone (Fig. 5B′,C′,D′, small arrowheads), except for a narrow area of the most dorsal side (Fig. 5B′,D′, arrows). Soon thereafter (stage 10.5), a strong signal appears at the dorsal blastoporal lip (Fig. 6A′, arrowhead). This signal further strengthens and spreads to the ventral lip in subsequent stages (Fig. 6B, arrow, D-D′, arrowheads), and persists until the end of gastrulation. The endoderm also displays prominent nuclear β-catenin staining (Fig. 6D′, asterisk), which fades toward the dorsal anterior region. This endodermal signal peaks at the end of gastrulation (Fig. 6E′, asterisk, Fig. 9, stages 12-14), and disappears at late neurula stages (Fig. 9, stage 20). The animal pole has variable, low to moderate levels. The only region devoid of nuclear β-catenin is the most dorsal part of the neurectoderm (Fig. 6A′,D′,E′, carets) and of the adjacent anterior mesoderm.

The ventrolateral crescent at stage 10.25 fits well with the

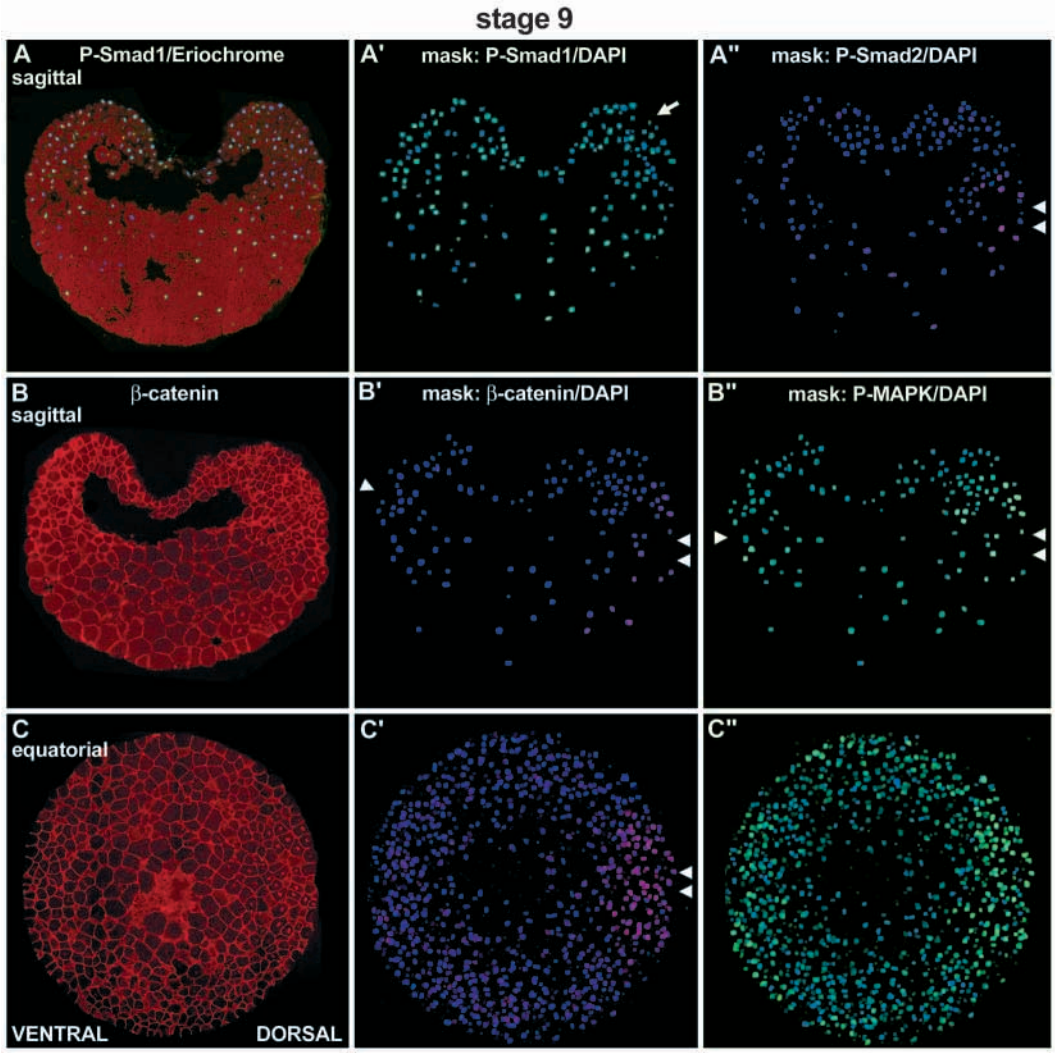

Fig. 3. Examples of staining at stage 9 (blastula). (A-C) Original images; (A′-C′,A″-C″) nuclear images. β-catenin and P-MAPK images are from double-stained sections. In the Smad1 image (A), the yolk was counterstained with Eriochrome Black (red). (C′,C″) Nuclear images of 4 equatorial sections, superimposed. Arrows and arrowheads: prominent patterns, see explanations in the text.

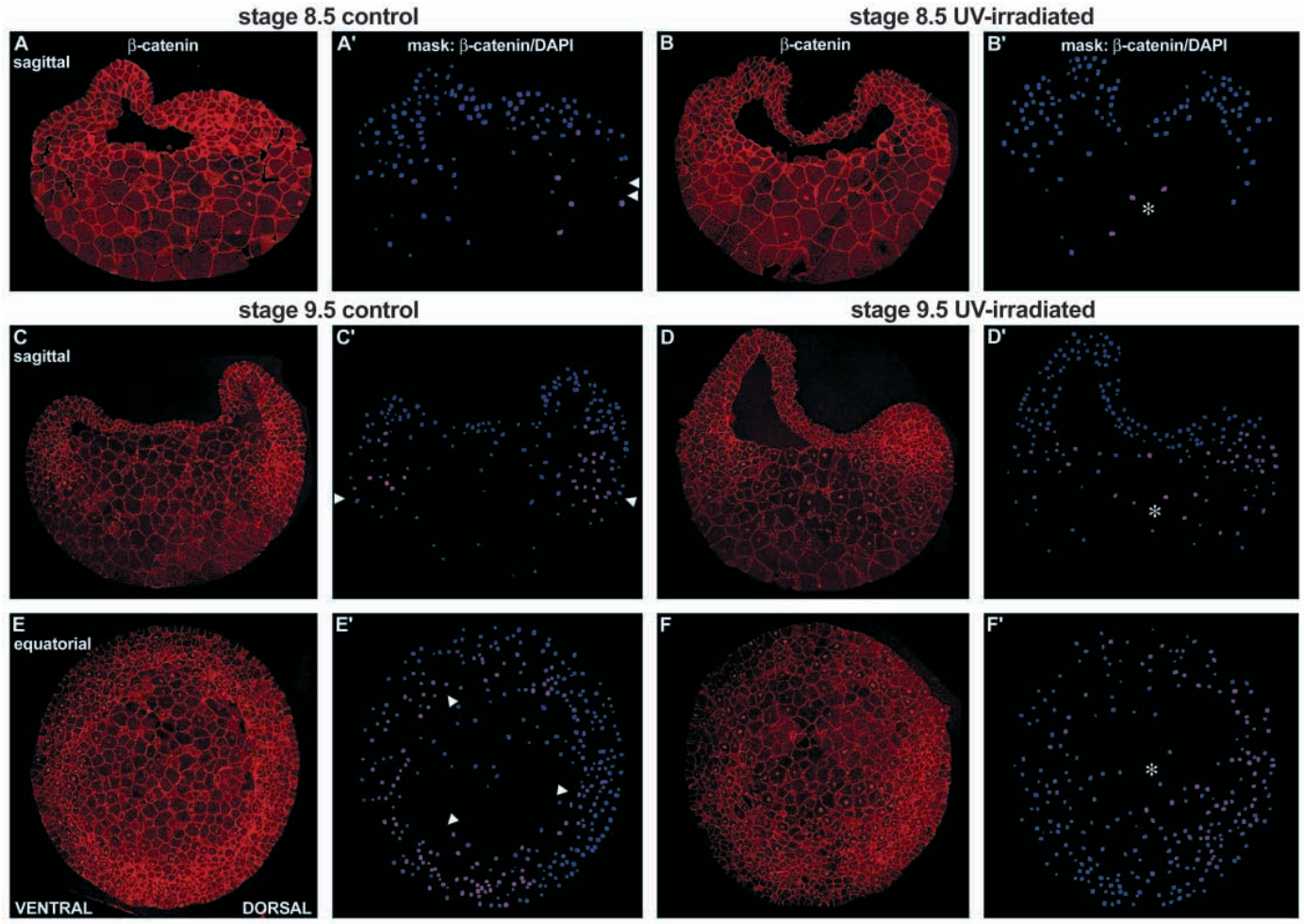

Fig. 4. β-catenin distribution at mid (8.5) and late blastula (9.5) stages in normal and UV-irradiated embryos. (A-F) Original images; (A′-F′) nuclear images. Arrows, arrowheads and asterisks: prominent patterns, see explanations in the text.

expression of Wnt8 (Christian and Moon, 1993). However, the dorsal 'gap' is surprisingly small, narrower than the prospective axial mesoderm field, and extremely transient, as the next strong signal soon appears at the blastopore lip. It is presently unclear how this may be fully reconciled with the proposed inhibitory role of Wnt8 in notochord formation (Christian and Moon, 1993). Our data are however consistent with head formation being incompatible with Wnt signaling (Niehrs, 1999), as β-catenin is low or absent from the dorsal anterior region during gastrulation.

The complex pattern during gastrulation indicates that other Wnts must act in addition to Wnt8, and suggests that important functions of β-catenin signaling have probably been overlooked. The appearance of β-catenin at the blastoporal lip coincides with the start of convergence extension in the dorsal side and archenteron spreading both in the dorsal and in the ventral side. Its pattern is reminiscent of Xbra and Wnt11 expression. Wnt11 is a direct target of Xbra (Saka et al., 2000), which regulates cell polarity and gastrulation movements via a β-catenin-independent pathway (Heisenberg et al., 2000). Wnt11 shows some axis-inducing activity (Ku and Melton, 1993), indicating that it may also activate β-catenin signaling. The intense signal in the endoderm is also unexpected, but may be related to the role of Sox17 in endoderm development (Hudson et al., 1997). Indeed, similar to TCFs, Sox are HMG-box transcription factors, which bind directly to β-catenin (Zorn et al., 1999). It is tempting to speculate that a Sox-β-catenin pathway is involved in endoderm formation.

β-catenin at neurula and tailbud stages (Fig. 7, summary Fig. 9, supplementary material)

At the end of gastrulation, β-catenin staining remains intense around the posterior circumblastoporal region, until the end of neurulation (Fig. 7A,B, cc and asterisk). The endodermal signal shrinks toward the ventral posterior region (Fig. 7A,B, en and star), and disappears at stage 20. New patterns appear, in particular in the neural tissue, consistent with the expression of various Wnts in this tissue. Note in particular the stripe in the prospective midbrain area (Fig. 7B,D, arrowhead), which is perfectly complementary to the MAPK staining (Fig. 7C,D, carets). Both the ligand, Wnt1, and the target, engrailed, are specifically expressed in this area, and this pathway is required for proper development of this part of the brain (Joyner, 1996). Other prominent signals include, at neurula stages, the lateral regions of the neural plate, consistent with a function of the pathway in neural crest formation (Ikeya et al., 1997; Dorsky et al., 2000), and, at early tailbud stages, dorsal cells such as neural crest cells and

dermatome (Fan et al., 1997), as well as the inner layer of the epithelium (supplementary material). At stage 31, β-catenin signal has strongly diminished in most regions of the embryo (supplementary material).

MAPK

MAPK activation has been studied previously by whole-mount immunochemistry (Christen and Slack, 1999; Curran and Grainger, 2000). Our data confirm most of the published patterns, with some notable exceptions in early stages.

MAPK at blastula stages (Fig. 2, Fig. 3, summary Fig. 10)

At stage 8, MAPK is weakly, ubiquitously activated (dark blue-green nuclei in Fig. 2A′). It is then further activated in the marginal zone (stages 8.5-9.5), first stronger dorsally (Fig. 2B′,C′ and Fig. 3B″, double arrowheads) than ventrally (arrowheads). The vegetal region maintains low-moderate levels, while the animal cap shows weak signal. The marginal ring has been reported previously (Christen and Slack, 1999; Curran and Grainger, 2000). The weaker, and somewhat variable, activation in the vegetal cells had not been detected by whole-mount staining, but is consistent with earlier biochemical data (LaBonne and Whitman, 1997).

MAPK during gastrulation (Fig. 5, Fig. 6, summary Fig. 10)

During gastrulation, MAPK is strongly activated at the blastoporal lips (Fig. 5B″,C″ and Fig. 6D″, arrowheads). Compared to previous reports, our staining gives a more precise and dynamic pattern. It shows in particular that the MAPK signal is not initially confined to the blastopore lip, but is more widespread, as weaker signals are observed in the posterior neuroderm and the dorsal endoderm (Fig. 5B″,C″, caret and asterisks, Fig. 10, stage 10-10.25). MAPK activity then progressively retracts from the animal/anterior regions while becoming increasingly restricted to the lips (Fig. 6D″, arrowheads, Fig. 10, stages 10.5-12). This sharpening of the activity domain probably partly reflects the positive feedback loop involving Xbra-eFGF (Isaacs et al., 1994; Schulte-Merker and Smith, 1995).

MAPK at later stages (Fig. 7, summary Fig. 10, and supplementary material)

At the end of gastrulation, a different pattern appears. Activity re-spreads from the dorsal lip to a wide posterior area (Fig. 7C,D, asterisk, see summary Fig. 10). Other discrete areas are activated, including a small region at the anterior tip of the neuroderm, followed by a second stripe at the level of the prospective anterior hindbrain and the tip of the notochord (Fig. 7C,D, carets, supplementary material). As mentioned above, MAPK signal tends to be complementary to β-catenin signal in the anterior neuroderm (Fig. 7D), while both signals coexist in the posterior mesoderm. This pattern fits well with the expression of FGF8 in the anterior ridge (forebrain) and

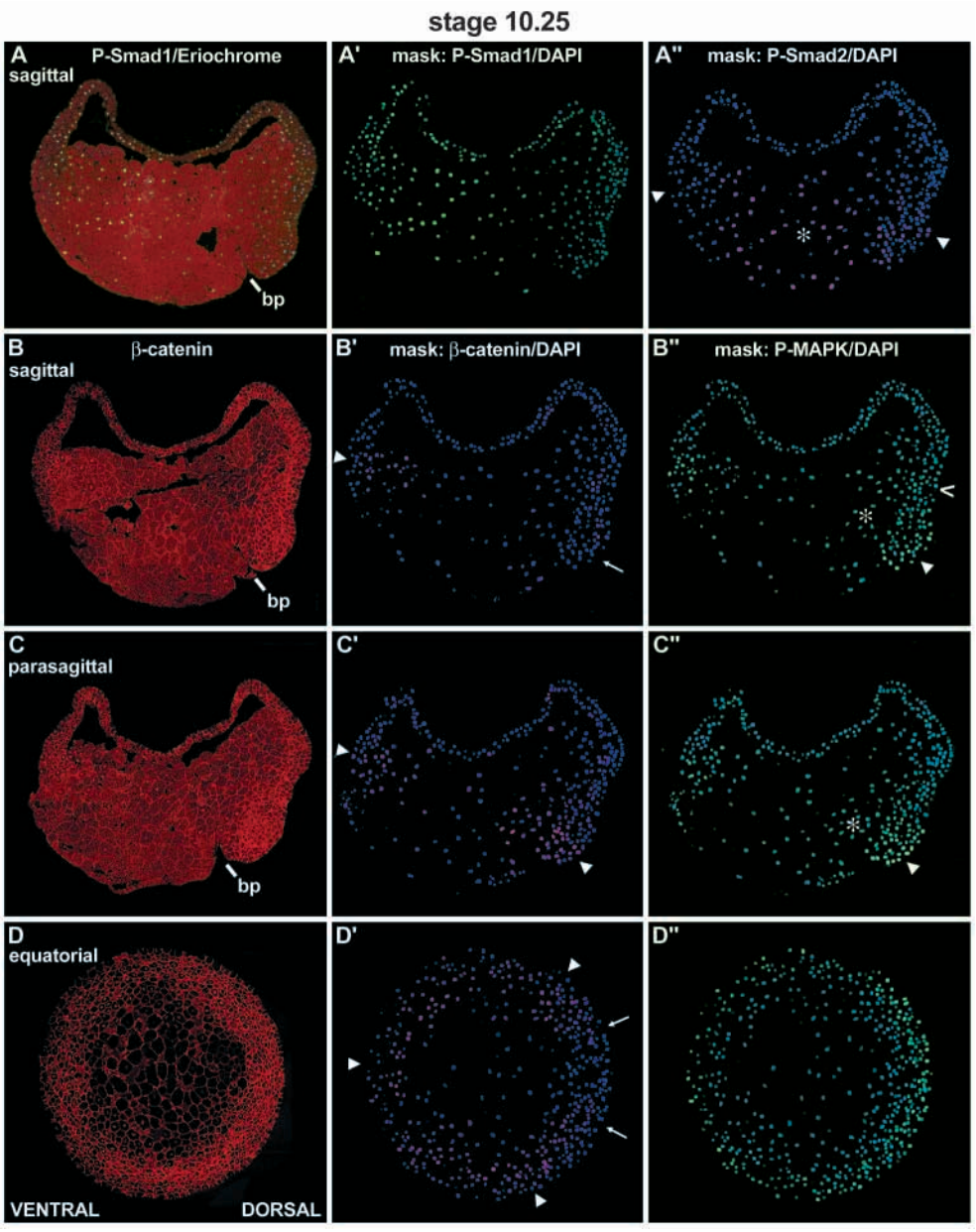

Fig. 5. Examples of staining at early gastrula stage. (A-D) Original images; (A′-D′,A″-D″) nuclear images. β-catenin and P-MAPK images are from double-stained sections. bp, dorsal blastopore lip. Other symbols: see explanations in the text.

at the midbrain-hindbrain boundary, and its role in patterning of the brain (Shanmugalingam et al., 2000; Joyner et al., 2000).

Smad2 (Fig. 2, Fig. 3, Fig. 5, Fig. 6, summary Fig. 11)

Smad2 shows a very dynamic pattern during early development. At stage 8, significant levels of Smad2 are detected ubiquitously (Fig. 2A″). The signal is however somewhat inhomogeneous. At stage 8.5, the signal increases transiently in a wide supraequatorial ring (Fig. 2B″, arrowheads), already observed for β-catenin. The activity then increases in the vegetal hemisphere (Fig. 2D″, asterisk), starting dorsally (Fig. 2C″,D″ and Fig. 3A″, double arrowheads). P-Smad2 signal remains high in the vegetal region and moderate in the marginal zone during early gastrulation (Fig. 5A″, respectively asterisk and arrowheads), then decreases rapidly (Fig. 6C″, summary Fig. 11, and supplementary material). At stage 14 only a weak signal with a variable distribution remains. Nuclear Smad2 later reappears in several areas of the embryo. The most prominent late patterns are the endodermal signal at stages 16-20, and the very strong activity in the somites, which at tailbud stages reaches levels higher than during gastrulation (supplementary material).

These data show a significant early general Smad2 activation (stage 8-8.5). This early activation has not been previously detected biochemically (Faure et al., 2000), perhaps owing to a lower sensitivity of the method. This pattern was unexpected, since most potential sources of signal, i.e. maternal Vg1 and zygotic Xnrs, are considered to be vegetally localized (see general discussion below). The predicted vegetal signal is eventually observed, but surprisingly late, at the beginning of gastrulation. Its progressive spreading from dorsal to ventral is in agreement with expression of nodal-related factors (Jones et al., 1995; Joseph and Melton, 1997; Sun et al., 1999; Kofron et al., 1999; Clements et al., 1999; Agius et al., 2000; Takahashi et al., 2000), but with a temporal delay of 1-2 hours, likely required for secretion of the Xnrs. No obvious

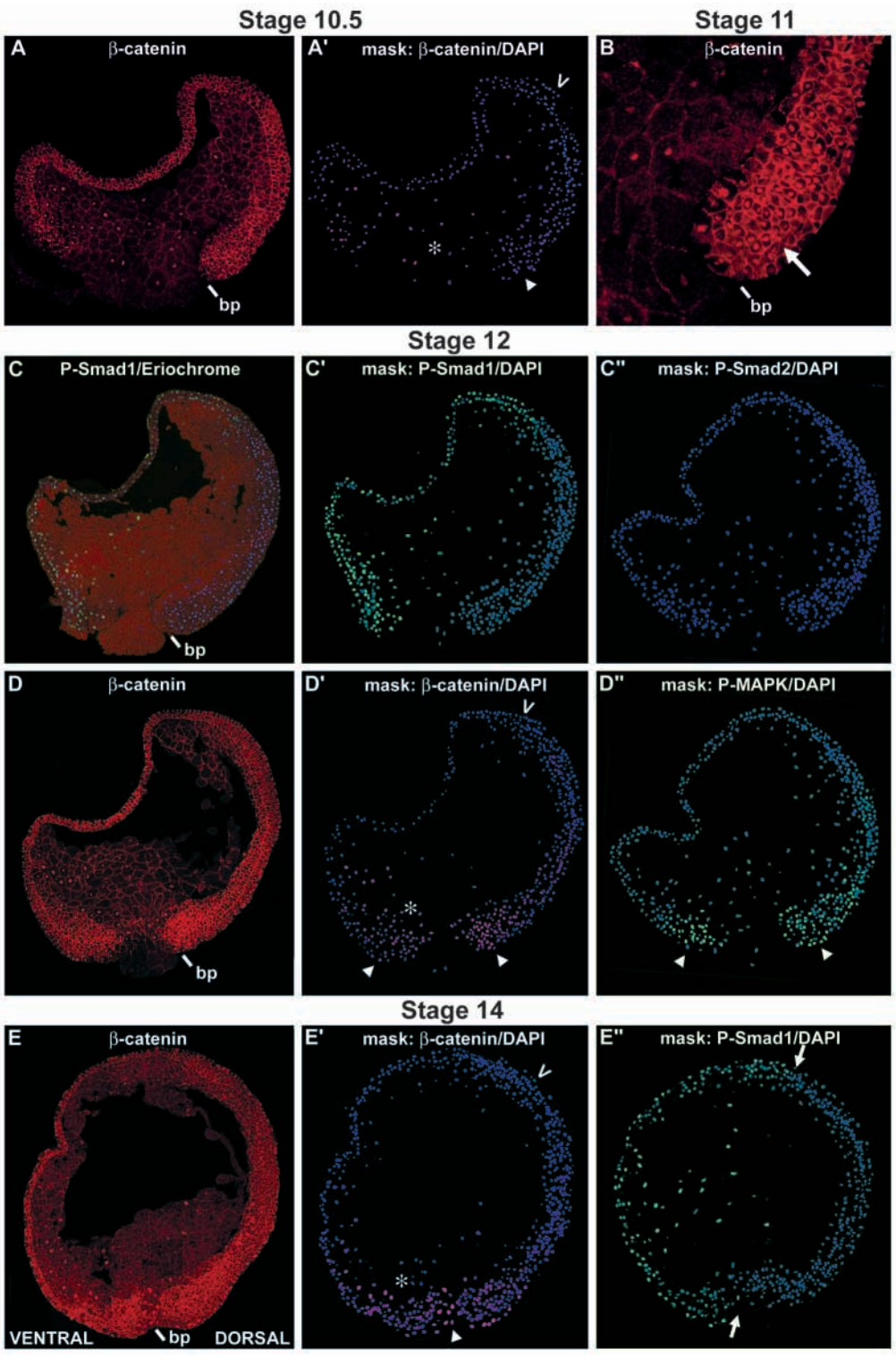

Fig. 6. Examples of staining at various gastrula stages. (A-E) Original images; (A′,C′-E′,C″-E″) nuclear images. C″ and D″ are from a double-stained section. All sections are sagittal. bp, dorsal blastopore lip. Other symbols: see explanations in the text.

vegetal-animal gradient is detected in the vegetal mass. However, P-Smad2 is increased where β-catenin signal peaks (dorsally at stages 9-10, Fig. 2C″,D″, Fig. 3A″, double arrowheads, summary Fig. 11, and at the ventral corner of the blastocoel floor at stage 10, summary Fig. 11), consistent with activation of Xnrs by β-catenin (Agius et al., 2000; Hyde and Old, 2000) (see also below). Note that in the previously published image of stage 10.25, the vegetal signal was conspicuously weak (Faure et al., 2000), a probable artifact of whole-mount staining.

We are not aware of any known activin/Nodal-dependent process that can be correlated to the strong Smad2 activation found in the somites at late stages. On the other hand, nodals have been implicated in determination of left-right assymetry, and Xnr1 is asymmetrically expressed in the left lateral region of tailbud stages (Lowe et al., 1996; Lustig et al., 1996). We have not been able to detect a corresponding asymmetric P-Smad2 signal in this region. Perhaps levels of Smad2 activation were below detection. Alternatively, Xnr1 might act via other transducing molecules in this process.

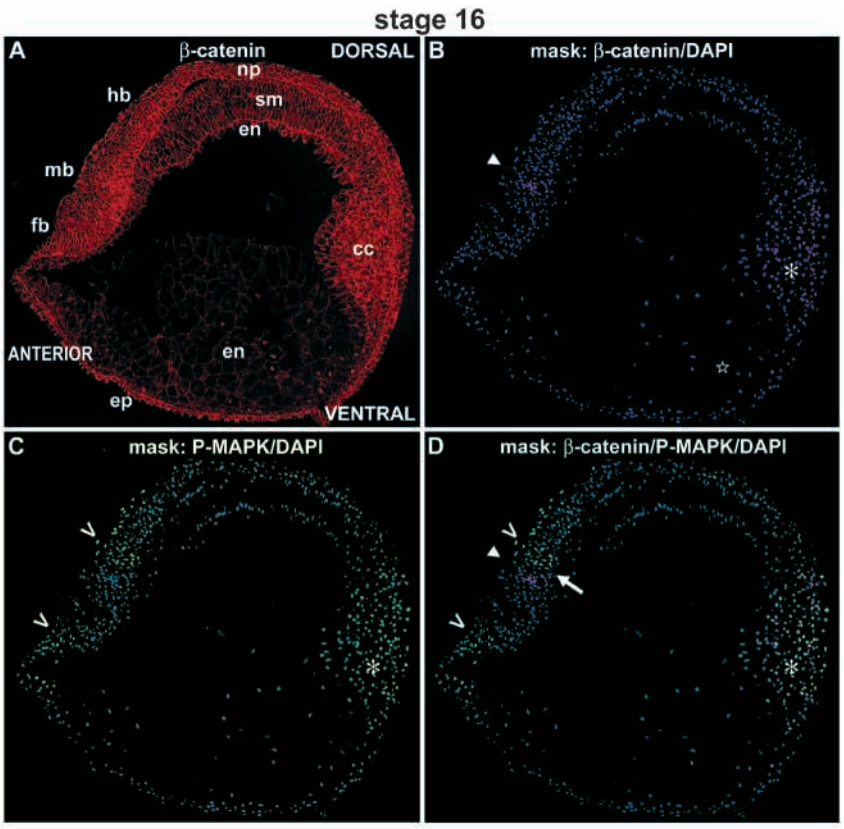

Fig. 7. β-catenin/P-MAPK staining of stage 16 neurula, parasagittal section. (A) Original β-catenin image; (B) β-catenin nuclear image; (C) P-MAPK nuclear image; (D) overlay of β-catenin and P-MAPK nuclear images. Note the overlapping staining (asterisk) in the posterior circumblastoporal collar (cc) and the complementary patterns in the brain (arrowhead and carets). The arrow indicates the midbrain-hindbrain boundary. Star, posterior endodermal β-catenin staining; en, endoderm; ep, epidermis; fb, forebrain; md, midbrain; hb, hindbrain; np, neural plate; sm, presomitic mesoderm.

Smad1

Smad1 staining at blastula stages (Fig. 2, Fig. 3, summary Fig. 12)

Low levels of P-Smad1 are detected ubiquitously in early blastulae (Fig. 2A‴,B‴). At stage 9, the pathway is globally activated, but remains weaker in the dorsal animal region (Fig. 2C‴,D‴ and 3A′, arrow). These patterns are generally consistent with the presence of maternal BMPs (Hemmati-Brivanlou and Thomsen, 1995), and with a transcription-independent activation detected biochemically (Faure et al., 2000). However, the pattern of lower activity in the dorsal animal quarter does not coincide with the Organizer, which is more vegetally centered, but partly prefigures the neural field. Recent data suggest that neural induction, classically thought to occur during gastrulation, may in fact start earlier (Baker et al., 1999; Streit et al., 2000), consistent with early dorsoventral differences observed in the ectoderm (London et al., 1988; Sokol and Melton, 1991).

Smad1 staining at gastrula and neurula stages (Fig. 5, Fig. 6, summary Fig. 12)

During gastrulation, P-Smad1 acquires a graded ventral to dorsal distribution (Fig. 5A′). The gradient appears at stage 10 by downregulation around the dorsal Organizer (summary Fig. 12). The polarity is then progressively sharpened by increased activity at the ventral side and by increased repression at the dorsal side (Fig. 6C′, summary Fig. 12). This process peaks at the end of gastrulation, when the embryo appears precisely divided into a ventral half filled with strong P-Smad1 signal, and a dorsal half devoid of signal (limit indicated by arrows in Fig. 6E″). From stage 14 on, the activity slowly decreases and has disappeared by stage 26 (summary Fig. 12, supplementary material). It persists longest in the most ventral endoderm.

BMPs can act as morphogens and induce lateral to ventral fates in a dose-dependent manner (Lemaire and Yasuo, 1998; Dale and Wardle, 1999). Although BMP expression itself is not graded, but is rather homogenous over the ventrolateral ectoderm mesoderm (Fainsod et al., 1994; Hemmati-Brivanlou and Thomsen, 1995), a graded BMP activity has been predicted to form in the gastrula embryo, controlled by the diffusion of the BMP antagonists from the dorsal side (Dale and Wardle, 1999; Lemaire and Yasuo, 1998). Our data demonstrate indeed the existence of a wide shallow gradient of BMP activity (Dale and Wardle, 1999). They provide a striking image of the dynamic antagonism between ventral BMPs and dorsal inhibitors, with the appearance of the gradient, its progressive sharpening and stabilization. A ventral/dorsal difference had been observed in previous P-Smad1 whole-mount staining, but the gradient had not been observed, probably due to the lower sensitivity of the method (Faure et al., 2000). The gradient spreads in fact in the three germ layers and is particularly intense in the ventral endoderm, suggesting that, unlike previously reported (Hemmati-Brivanlou and Thomsen, 1995; Fainsod et al., 1994), BMPs may be expressed in all layers. A

particularly remarkable feature of the P-Smad1 pattern is the perfect dorsoventral division observed at the end of gastrulation. A sharp dorsoventral boundary is for instance in agreement with the role of BMPs in determination of the cement gland (Gammill and Sive, 2000). Note also that two sources of BMPs, anterior and posterior, have been identified during neurulation (Hemmati-Brivanlou and Thomsen, 1995), yet Smad1 activation appears rather homogenous over the whole ventral side. This case exemplifies well the difficulty in predicting a pattern of activity from expression patterns, especially when the activity results from the integration of activating and inhibiting components. Note finally that ADMP, a BMP3 homologue, is strongly expressed in the notochord (Moos et al., 1995), yet no sign of Smad1 activation can be found in this structure. ADMP has been shown to function independently of the classical BMP receptors (Dosch and Niehrs, 2000).

Smad1 staining at late stages (summary Fig. 12, and supplementary material)

At late neurula stages, some P-Smad1 is also detected in the dorsal neuroderm/ectoderm, in agreement with the neural dorsalizing function of BMPs (Dale and Wardle, 1999). At later stages, P-Smad1 is found in many different structures, including the dorsal retina, head mesenchyme, dorsal fin, somites, notochord, branchial arches, ventral anterior ectoderm and mesoderm, heart anlage, around the proctodeum. All these sites coincide with known BMP expression patterns (Hemmati-Brivanlou and Thomsen, 1995).

Signaling patterns in manipulated embryos (Fig. 13 and supplementary Fig. S3)

Early dorsoventral asymmetry is established by cortical rotation, which activates maternal β-catenin signaling in the dorsal side (Darras et al., 1997; Harland and Gerhart, 1997; Marikawa et al., 1997). P-MAPK (Fig. 2A′-C′, Fig. 3B″) and P-Smad2 signals (Fig. 2C″, Fig. 3A″) also start on the dorsal side. In particular, the P-MAPK pattern strikingly overlaps with the β-catenin pattern at all blastula stages (Fig. 2). Thus, to test the influence of maternal β-catenin activity on other pathways, we compared the activation patterns in stage 9 blastulae after the following treatments: (1) UV irradiation, which prevents cortical rotation (Harland and Gerhart, 1997); (2) LiCl treatment, which activates β-catenin signaling ubiquitously (Schneider et al., 1996); (3) ventral injection of β-catenin mRNA.

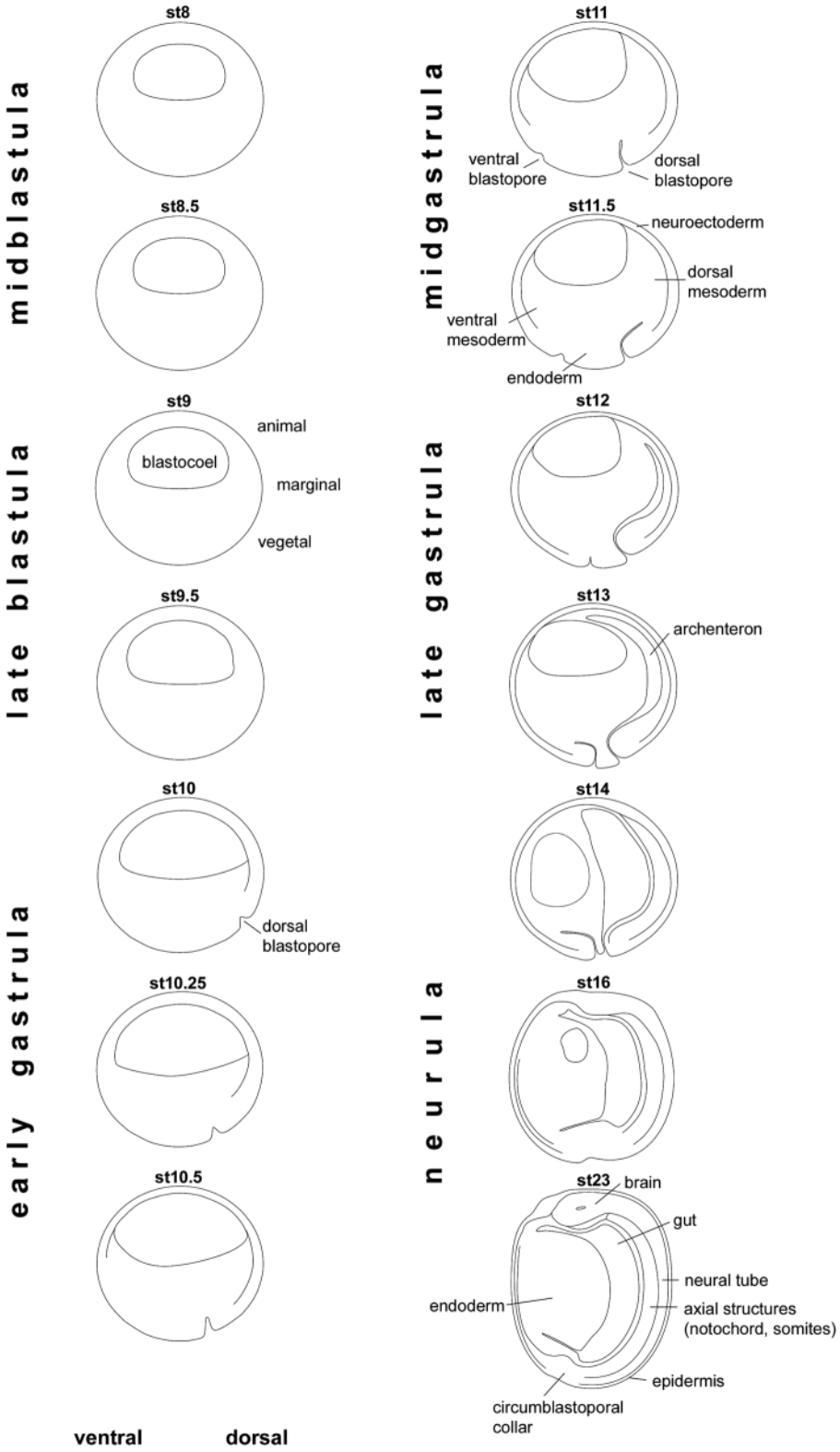

Fig. 8. Schematic drawings of the various stages and the main regions of the early *Xenopus* embryo.

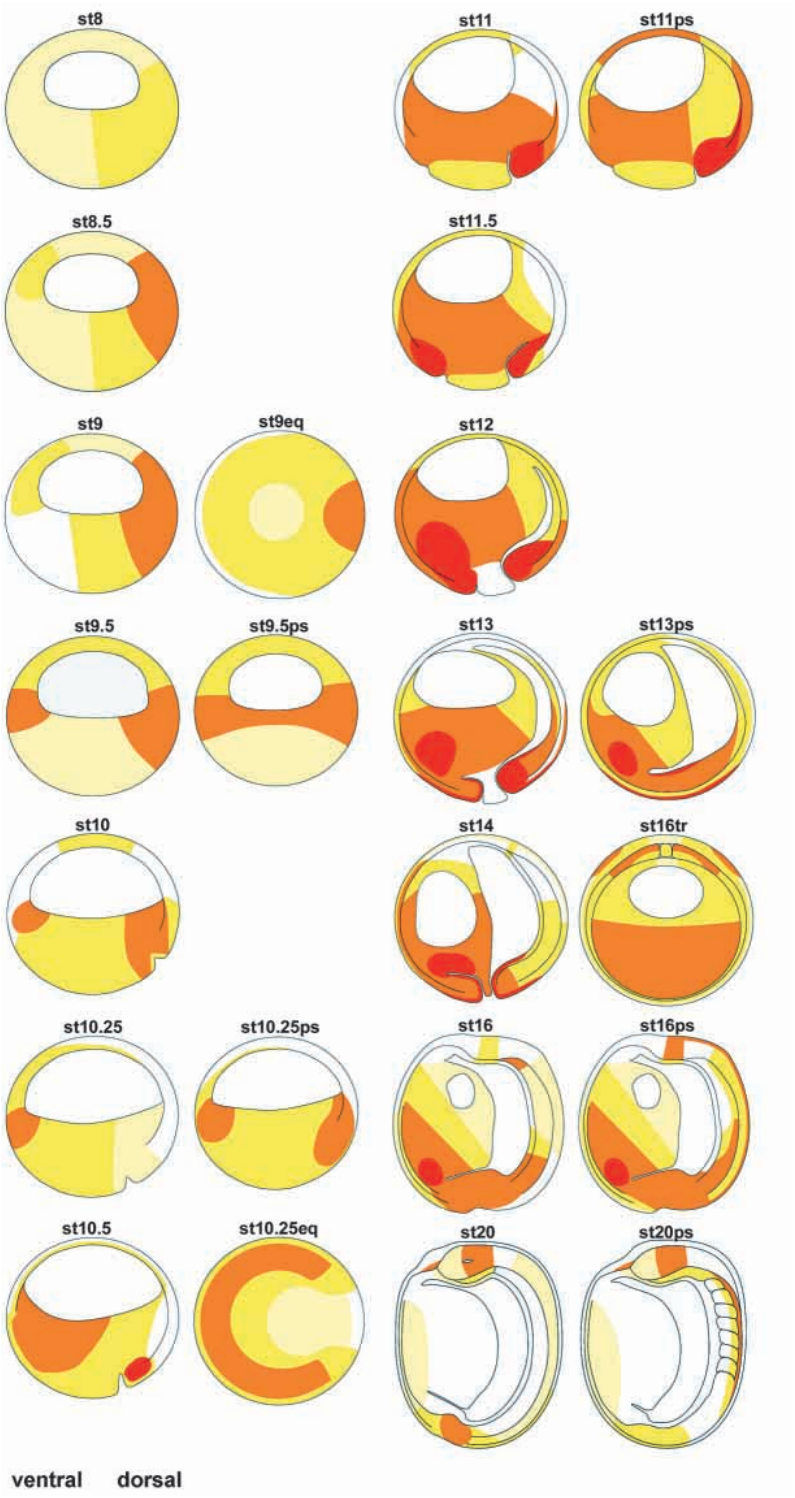

Fig. 9. Fig. 9, Fig. 10, Fig. 11, Fig. 12 are summary diagrams of β-catenin, P-MAPK, Smad2 and Smad1 pattern during early development, respectively. Each drawing represents an average pattern obtained by analysis of several sections. The relative intensities between various stages were compared using pseudocolors images (see Fig. 1). Red is strongest, pale yellow is very weak/inhomogeneous. The spotted pattern of Smad2 at stage 8 indicates a very heterogeneous signal. All sections are sagittal unless stated otherwise. eq, equatorial; ps, parasagittal; tr, transversal.

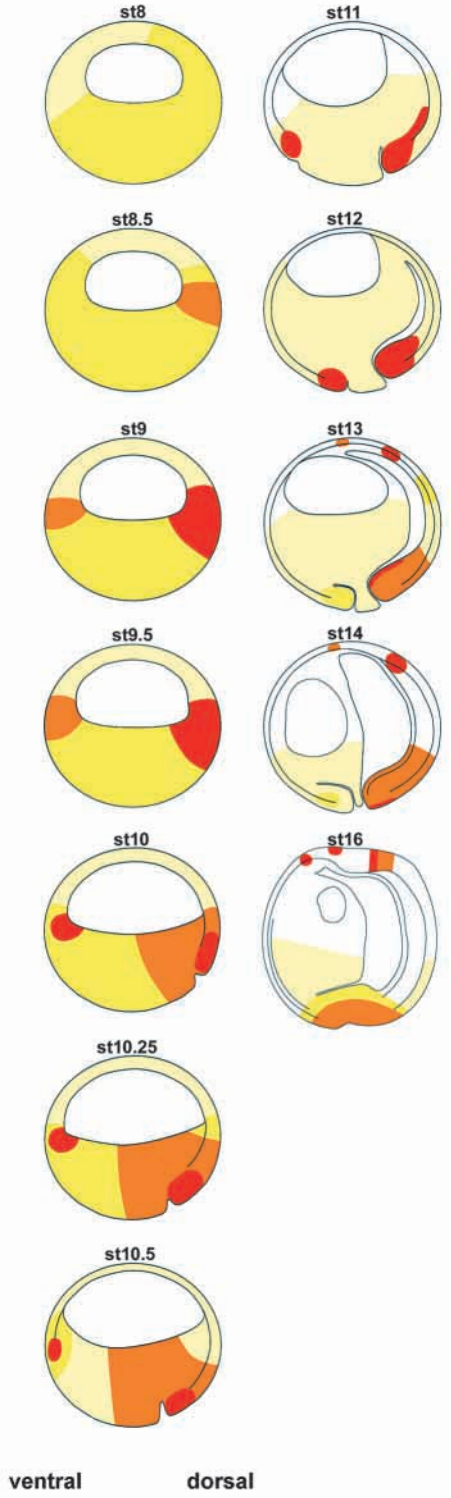

Fig. 10. MAPK signaling during early *Xenopus* development (see Fig. 9 legend).

We found that P-MAPK and P-Smad2 patterns were strongly dependent on β-catenin signaling at this stage (Fig. 13): their dorsal accumulation (Fig. 13A, double arrowheads) was absent in UV-irradiated embryos (Fig. 13B, arrows). The highest levels were then found symmetrically in the vegetal-equatorial region (asterisks), similar to β-catenin. Upon LiCl treatment, P-MAPK and P-Smad2 were strongly activated also in the ventral side (Fig. 13C, arrowheads). A similar activation was observed at the site of β-catenin overexpression (Fig. 13D, arrowheads). Despite extensive colocalization, P-MAPK and P-Smad2 activation appeared, nevertheless, spatially more restricted than β-catenin: in all conditions, high P-MAPK was limited to a broad equatorial ring, while P-Smad2 activation was most prominent in the vegetal hemisphere. These differences obviously reflect the differential distribution of other determinants, which limit activation of P-MAPK to the marginal zone and Smad2 to the vegetal pole. P-Smad1 has an opposite polarity, i.e. weakest in the dorsal animal region (Fig. 2C-C‴ and Fig. 3A′, supplementary Fig. S3A). In UV-irradiated embryos, P-Smad1 was also activated on the dorsal side (supplementary Fig. S3B). LiCl treatment or ventral β-catenin overexpression caused a significant decrease in the ventral side (supplementary Fig. S3C,D).

In conclusion, our data show that maternal β-catenin signaling is an important factor in controlling intensity and pattern of the other pathways at blastula stages. While other parameters regulate the latitude of the activation fields, β-catenin can entirely account for the dorsoventral polarity. Mechanistically, β-catenin probably contributes to Smad2 activation by stimulating Xnrs expression (Agius et al., 2000). How β-catenin controls MAPK and Smad1 remains to be investigated.

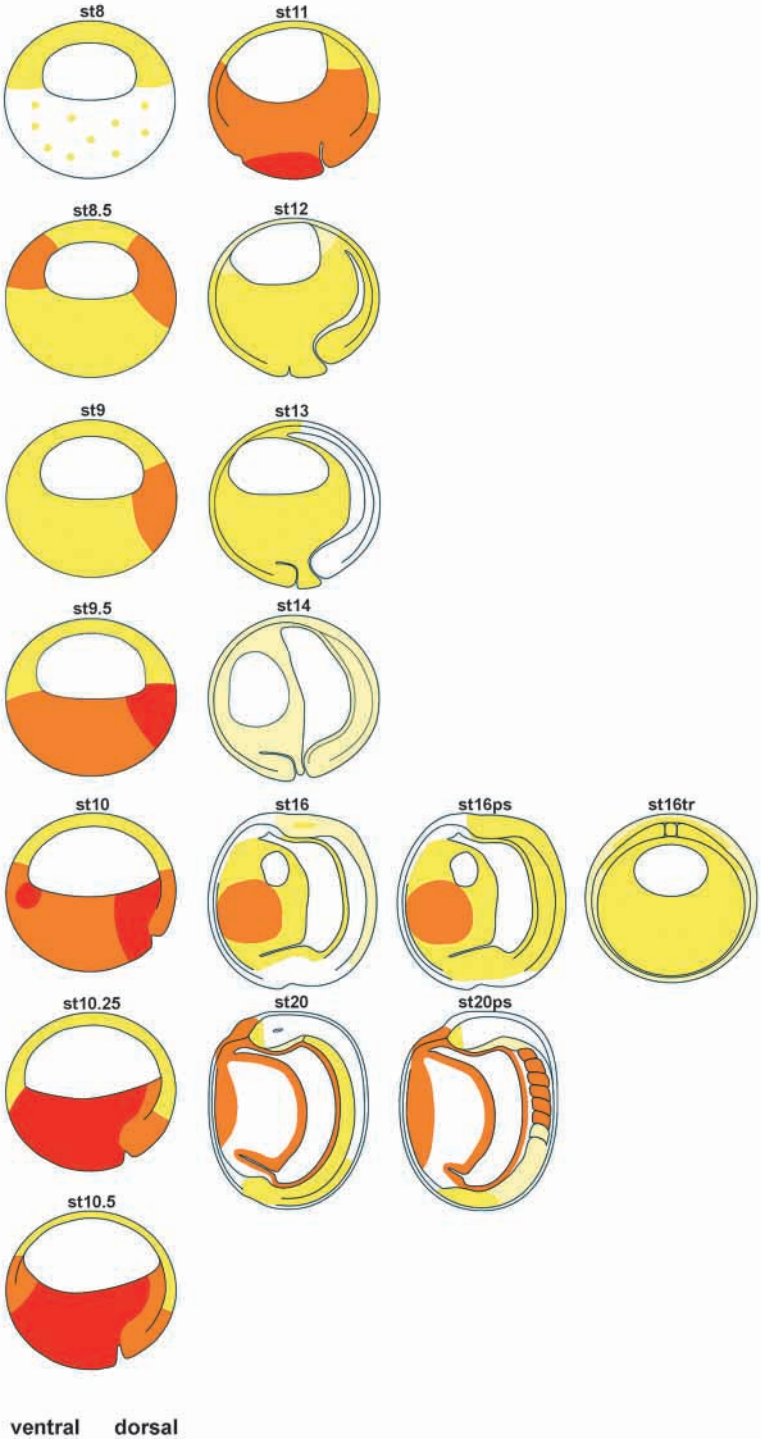

Fig. 11. Smad2 signaling during early *Xenopus* development (see Fig. 9 legend).

General observations and conclusions

We have generated a global view of signaling through four major pathways during early development of a vertebrate embryo. A glance at the various stages shows that the intensity of a signal is not sufficient to determine its significance. Indeed, one can find for each pathway well-defined fields of weak signal, which suggest that even the lowest intensities may be significant depending on the context. Signal activation is remarkably widespread, in particular in blastulae and gastrulae, with very few areas showing no signal. To what extent the weakest parts of these patterns are due to specific activation, or to 'sloppiness' of the pathways, remains unknown. However, one immediate inference from this observation is that gene activity must be as a rule controlled by thresholds rather than on/off switches. The regions completely devoid of signal during gastrulation are few, and clearly delimited. At least some of them are known to secrete inhibitors of the corresponding signals, such as the dorsal axial structures for Smad1 and the anterior dorsal structures for β-catenin (Harland and Gerhart, 1997; Niehrs, 1999). We hypothesize that in early development the absence of signal might be only achieved by active repression/inhibition. Note that patterning is certainly not the only role of these pathways. They have other well-established functions, in particular, control of cell proliferation, which may be important at late stages (Ikeya et al., 1997; Neumann and Cohen, 1996).

In many instances, changes in signaling patterns are very dynamic, and could only be followed by a systematic analysis of consecutive stages. In some cases, the patterns seem stable

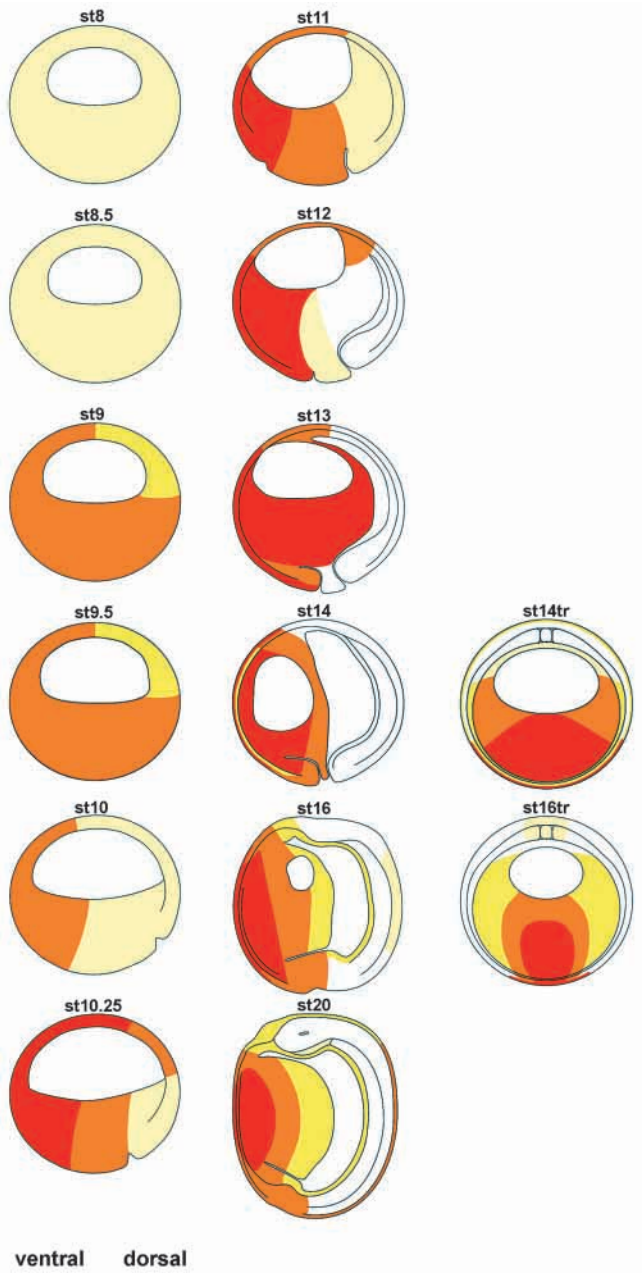

Fig. 12. Smad1 signaling during early *Xenopus* development (see Fig. 9 legend).

relative to particular regions of the embryo despite the extensive tissue remodeling occurring during gastrulation, but for the individual cells that migrate in and out of these regions, signaling is particularly transient. Examples include the blastopore lips for β-catenin and MAPK, and the ventral side for Smad1. Importantly, spreading of these signals is generally not limited to particular germ layers or tissues, but appears to freely cross boundaries. Recent work on gastrulation movements has demonstrated that the early embryo can be divided in well-defined domains characterized by specific cell behaviors, and that the limits of these domains do not coincide with germ layer boundaries (Wacker et al., 2000). We propose that the early embryo could also be subdivided into signaling domains, which do not necessarily depend on anatomical structures.

Comparison of the different pathways point in several instances to common or related patterns, which may suggest possible interplay. Such patterns include for instance the ring at blastula stages, the blastopore lips during gastrulation, the posterior region of neurulae. Known connections include the induction of Xnrs by β-catenin (Agius et al., 2000) and of Wnt11 by FGF-Xbra (Saka et al., 2000). Furthermore, potential direct intersections between intracellular pathways exist, for instance between β-catenin and MAPK pathways (Behrens, 2000) or MAPK and TFGβ (Heldin et al., 1997; Mulder, 2000). We have verified the occurrence of such crosstalk in the dorsoventral asymmetry observed for all four pathways at blastula stages, which appears to be controlled by β-catenin (Fig. 13 and Fig. S3).

Our data raise additional questions on how embryonic patterns are established. (1) As a rule, signaling fields consist of mosaics of single cells with widely variable intensities. What modulates the activity at the level of single cells, and what the consequences are on cell fate, are unknown. (2) The spatial patterns are unexpectedly refined, even at early stages. For instance, at stage 10, ventral β-catenin, P-MAPK and P-Smad2 are stronger inside, in a narrow area at the edge of the blastocoel floor (Fig. 8, Fig. 9, Fig. 10, Fig. 11). What determines these patterns? Is location (e.g. superficial) or cell type (e.g. epithelial) contributing to patterning? (3) Our images show, for each pathway, a variety of patterns, from large shallow gradients to localized 'hot' spots. This suggests that the range of the signals might vary greatly, and could be in some instances extremely restricted.

The signaling patterns obtained may be roughly divided in three phases. (1) An early phase, reflecting maternal and very early zygotic events; (2) a second phase of zygotic patterning, which from late blastula to neurula establishes the general plan of the embryo, and which is characterized by generally robust and widespread activities; and finally (3), the late phase of pattern refinement associated with the beginning of organogenesis. The transition from the first to the second phase could be set around stage 9.5, and correlates with a somewhat higher variability of staining patterns. Transition from the second to the third phase appears progressive, with small defined patterns appearing first in the anterior dorsal structures (β-catenin and MAPK), while the posterior region maintains for a longer time broad signaling fields, probably reflecting its prolonged organizer activity (Gont et al., 1993).

Surprisingly, novel patterns were observed in the first phase, and the emerging image is somewhat unfamiliar, suggesting that, with the exception of dorsal maternal β-catenin, early processes are still incompletely understood. We found that all four pathways are activated in the midblastula (stage 8.5), and thus could all potentially influence the earliest steps of gene regulation. The ring-shaped patterns observed for β-catenin, MAPK and Smad2 signals are consistent with a contribution of these early activities to mesoderm formation, in addition to the well-established role of VegT relayed by Xnrs [see discussion in Zhang et al., and Clements et al. (Zhang et al., 1998; Clements et al., 1999)]. How are these patterns established remains to be determined. In the case of Smad2, for instance, some Xnrs are expressed as early as stage 8-8.5. The distribution of all known Xnrs is however clearly vegetal (Takahashi et al., 2000), and this pattern is reflected in P-Smad2 activation only from stage 9 (Fig. 11), a lag likely due to the

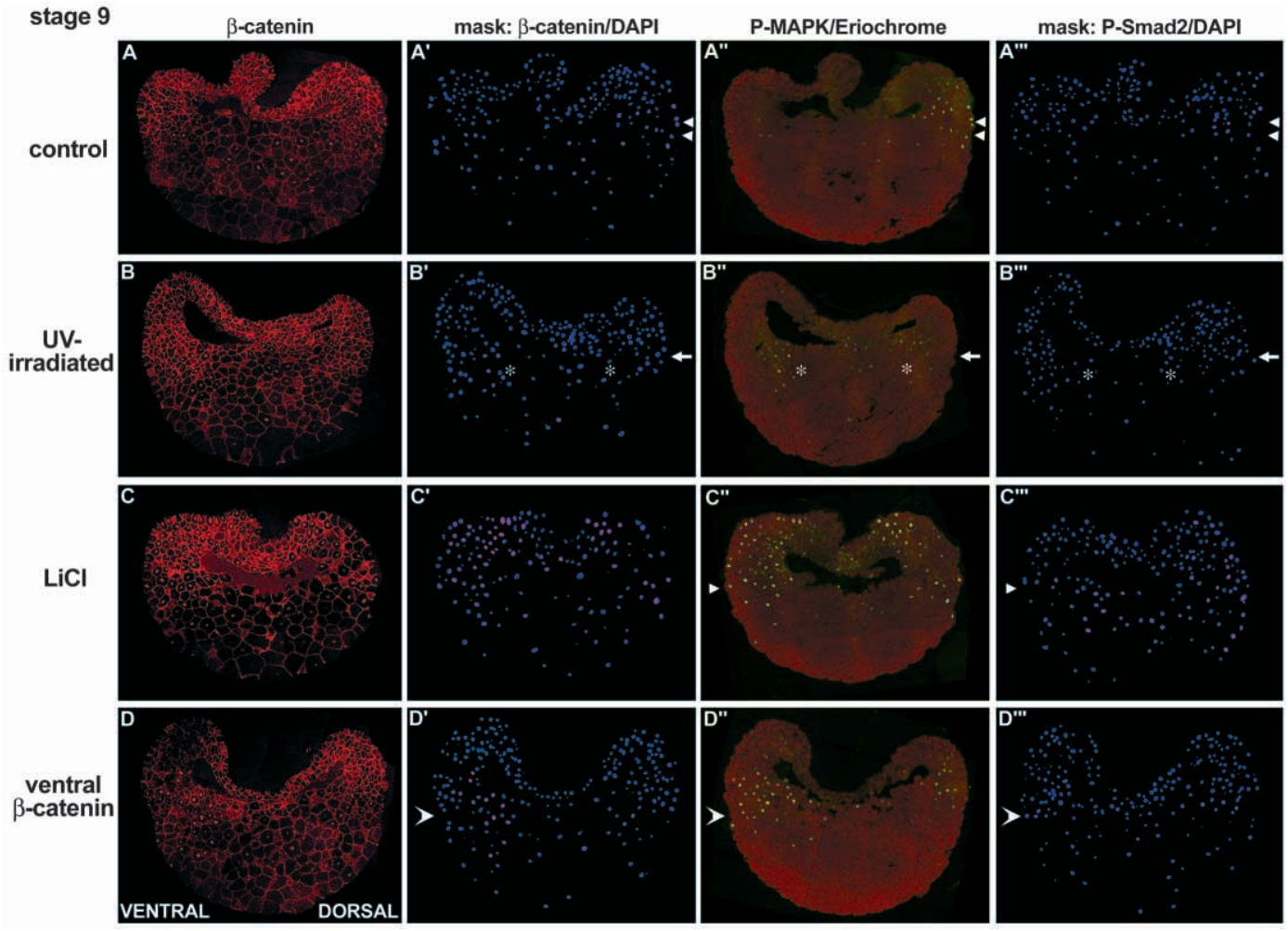

Fig. 13. Signaling patterns at blastula stage in manipulated embryos. (A-A‴) controls; (B-B‴) UV-irradiated embryos; (C-C‴) LiCl-treated embryos; (D-D‴) embryos ventrally injected with β-catenin mRNAs (large arrowhead). (A-D,A″-D″) original images; (A′-D′,A‴-D‴) nuclear images. A-A″, B-B″ and C-C″ are from double stained sections. All other images are from contiguous sections from the same embryos. Arrows, arrowheads and asterisks: see explanations in the text.

time required for protein synthesis and secretion. The stage 8.5 ring-shaped pattern suggests the existence of additional signals. Possible candidates could be maternal activin (Oda et al., 1995) and Vg1. Although Vg1 mRNAs accumulates vegetally in the oocyte (Weeks and Melton, 1987), distribution of active Vg1 protein is not known. In fact, there is evidence both for very early mesoderm inductive activities in the cleaving embryo (Jones and Woodland, 1987), and for pre-localized, cell-autonomous properties of the marginal zone (Nakamura et al., 1970; Gurdon et al., 1985; Lemaire and Gurdon, 1994).

Early signals are difficult to study, and their importance might have been underestimated because of technical limitations. There are still few early markers and levels are often below detection by most localization methods. The role of the Smad1, Smad2 and MAPK pathways has been mostly addressed using dominant negative receptors [see Harland and Gerhart, and Heasman for reviews (Harland and Gerhart, 1997, and Heasman, 1997)]. These constructs generate severe phenotypes at later stages, but, in our hands, they have only marginal effects on stage 9 signals (not shown), perhaps because sufficient expression levels are not reachable and/or maternal signals might arise very early and be somehow stabilized even in the absence of ligand input.

While the first phase of early signaling is somewhat puzzling, patterns that are more familiar appear at late blastula or early gastrula, which are largely consistent with current models. Stage 10.25 in fact fulfils all predictions, with vegetal Smad2, marginal MAPK, ventrolateral β-catenin, and a ventral to dorsal gradient of Smad1. Nevertheless, even at gastrula stages important aspects remain to be characterized. Our images reveal in particular striking β-catenin signals (e.g. at the blastopore lip), which await identification of sources and functions. The detection of dynamic patterns in the vegetal cells, including intense β-catenin and Smad1 activities, further emphasizes our incomplete understanding of early endoderm development (Clements et al., 1999; Yasuo and Lemaire, 1999; Grapin-Botton and Melton, 2000).

We now know with reasonable precision when and where, and to what extend, four signaling pathways are active. This systematic description of signaling patterns should provide a basis for future investigation/re-investigation of patterning processes during development. It will be now possible to test

the specific contribution of the various inducing factors, determine the function of each individual activity detected in these patterns, and identify possible interconnections between the pathways. Our results on the role of β-catenin in patterning the other pathways in the late blastula illustrate such immediate applications.

This work is dedicated to Prof. Peter Hausen. We thank Peter ten Dijke for kindly providing the anti-P-Smads antibodies and Thomas Kurth for the β-catenin antibody. We thank Jürgen Löschinger for help in setting the optical and electronic equipment, and Wolfgang Reintsch, Metta Riebesell, Ralph Rupp, Herbert Steinbeisser and Rudi Winklbauer, as well as the anonymous reviewers, for their helpful comments.

REFERENCES

Agius, E., Oelgeschlager, M., Wessely, O., Kemp, C. and De Robertis, E. M. (2000). Endodermal Nodal-related signals and mesoderm induction in *Xenopus*. *Development* **127**, 1173-1183.

Amaya, E., Musci, T. J. and Kirschner, M. W. (1991). Expression of a dominant negative mutant of the FGF receptor disrupts mesoderm formation in Xenopus embryos. *Cell* **66**, 257-270.

Ataliotis, P., Symes, K., Chou, M. M., Ho, L. and Mercola, M. (1995). PDGF signalling is required for gastrulation of *Xenopus laevis*. *Development* **121**, 3099-3110.

Baker, J. C., Beddington, R. S. and Harland, R. M. (1999). Wnt signaling in Xenopus embryos inhibits bmp4 expression and activates neural development. *Genes Dev.* **13**, 3149-3159.

Behrens, J. (2000). Cross-regulation of the Wnt signalling pathway: a role of MAP kinases. *J. Cell Sci.* **113**, 911-919.

Cadigan, K. and Nusse, R. (1997). Wnt signaling: a common theme in animal development. *Genes Dev.* **11**, 3286-3305.

Christen, B. and Slack, J. (1999). Spatial response to fibroblast growth factor signalling in Xenopus embryos. *Development* **126**, 119-125.

Christian, J. L. and Moon, R. T. (1993). Interactions between Xwnt-8 and Spemann organizer signaling pathways generate dorsoventral pattern in the embryonic mesoderm of Xenopus. *Genes Dev.* **7**, 13-28.

Clements, D., Friday, R. V. and Woodland, H. R. (1999). Mode of action of VegT in mesoderm and endoderm formation. *Development* **126**, 4903-4911.

Cobb, M. H. and Goldsmith, E. J. (2000). Dimerization in MAP-kinase signaling. *Trends Biochem. Sci.* **25**, 7-9.

Cornell, R. A., Musci, T. J. and Kimelman, D. (1995). FGF is a prospective competence factor for early activin-type signals in *Xenopus* mesoderm induction. *Development* **121**, 2429-2437.

Cox, W. G. and Hemmati-Brivanlou, A. (1995). Caudalization of neural fate by tissue recombination and bFGF. *Development* **121**, 4349-4358.

Cui, Y., Brown, J. D., Moon, R. T. and Christian, J. L. (1995). Xwnt-8b: a maternally expressed *Xenopus* Wnt gene with a potential role in establishing the dorsoventral axis. *Development* **121**, 2177-2186.

Curran, K. L. and Grainger, R. M. (2000). Expression of activated MAP kinase in Xenopus laevis embryos: evaluating the roles of FGF and other signaling pathways in early induction and patterning. *Dev. Biol.* **228**, 41-56.

Dale, L. and Wardle, F. C. (1999). A gradient of BMP activity specifies dorsal-ventral fates in early Xenopus embryos. *Semin. Cell Dev. Biol.* **10**, 319-326.

Darras, S., Marikawa, Y., Elinson, R. P. and Lemaire, P. (1997). Animal and vegetal pole cells of early Xenopus embryos respond differently to maternal dorsal determinants: implications for the patterning of the organiser. *Development* **124**, 4275-4286.

Dorsky, R. I., Moon, R. T. and Raible, D. W. (2000). Environmental signals and cell fate specification in premigratory neural crest. *BioEssays* **22**, 708-716.

Dosch, R. and Niehrs, C. (2000). Requirement for anti-dorsalizing morphogenetic protein in organizer patterning. *Mech. Dev.* **90**, 195-203.

Fagotto, F. and Gumbiner, B. M. (1994). β-catenin localization during *Xenopus* embryogenesis: accumulation at tissue and somite boundaries. *Development* **120**, 3667-3679.

Fagotto, F. (1999). The Wnt pathway in Xenopus development. In *Signaling Through Cell Adhesion* (ed. J.-L. Guan), pp. 303-356: CRC Press.

Fainsod, A., Steinbeisser, H. and De Robertis, E. M. (1994). On the function of BMP-4 in patterning the marginal zone of the Xenopus embryo. *EMBO J.* **13**, 5015-5025.

Fan, C. M., Lee, C. S. and Tessier-Lavigne, M. (1997). A role for Wnt proteins in induction of dermomyotome. *Dev. Biol.* **191**, 160-165.

Faure, S., Lee, M. A., Keller, T., ten Dijke, P. and Whitman, M. (2000). Endogenous patterns of TGFβ superfamily signaling during early *Xenopus* development. *Development* **127**, 2917-2931.

Gammill, L. S. and Sive, H. (2000). Coincidence of otx2 and BMP4 signaling correlates with Xenopus cement gland formation. *Mech. Dev.* **92**, 217-226.

Gont, L. K., Steinbeisser, H., Blumberg, B. and De Robertis, E. M. (1993). Tail formation as a continuation of gastrulation: the multiple cell populations of the *Xenopus* tailbid derive from the late blastopore lip. *Development* **119**, 991-1004.

Grapin-Botton, A. and Melton, D. A. (2000). Endoderm development: from patterning to organogenesis. *Trends Genet.* **16**, 124-130.

Green, J. B., New, H. V. and Smith, J. C. (1992). Responses of embryonic Xenopus cells to activin and FGF are separated by multiple dose thresholds and correspond to distinct axes of the mesoderm. *Cell* **71**, 731-739.

Gurdon, J. B., Mohun, T. J., Fairman, S. and Brennan, S. (1985). All components required for the eventual activation of muscle-specific actin genes are localized in the subequatorial region of the uncleaved amphibian egg. *Proc. Natl. Acad. Sci. USA* **82**, 139-143.

Gurdon, J. B., Harger, P., Mitchell, A. and Lemaire, P. (1994). Activin signalling and response to a morphogen gradient [see comments]. *Nature* **371**, 487-492.

Harland, R. and Gerhart, J. (1997). Formation and function of Spemann's organizer. *Ann. Rev. Cell Dev. Biol.* **13**, 611-667.

Heasman, J., Crawford, A., Goldstone, K., Garner-Hamrick, P., Gumbiner, B., McCrea, P., Kintner, C., Noro, C. Y. and Wylie, C. (1994). Overexpression of cadherins and underexpression of β-catenin inhibit dorsal mesoderm induction in early Xenopus embryos. *Cell* **79**, 791-803.

Heasman, J. (1997). Patterning the *Xenopus* blastula. *Development* **124**, 4179-4191.

Heisenberg, C. P., Tada, M., Rauch, G. J., Saude, L., Concha, M. L., Geisler, R., Stemple, D. L., Smith, J. C. and Wilson, S. W. (2000). Silberblick/Wnt11 mediates convergent extension movements during zebrafish gastrulation. *Nature* **405**, 76-81.

Heldin, C. H., Miyazono, K. and ten Dijke, P. (1997). TGF-beta signalling from cell membrane to nucleus through SMAD proteins. *Nature* **390**, 465-471.

Hemmati-Brivanlou, A. and Melton, D. A. (1992). A truncated activin receptor inhibits mesoderm induction and formation of axial structures in Xenopus embryos. *Nature* **359**, 609-614.

Hemmati-Brivanlou, A. and Thomsen, G. H. (1995). Ventral mesodermal patterning in Xenopus embryos: expression patterns and activities of BMP-2 and BMP-4. *Dev. Genet.* **17**, 78-89.

Hoppler, S., Brown, J. D. and Moon, R. T. (1996). Expression of a dominant-negative Wnt blocks induction of MyoD in Xenopus embryos. *Genes Dev.* **10**, 2805-2817.

Hudson, C., Clements, D., Friday, R. V., Stott, D. and Woodland, H. R. (1997). Xsox17alpha and -beta mediate endoderm formation in Xenopus. *Cell* **91**, 397-405.

Hyde, C. E. and Old, R. W. (2000). Regulation of the early expression of the *Xenopus* nodal-related 1 gene, *Xnr1*. *Development* **127**, 1221-1229.

Ikeya, M., Lee, S. M., Jonhson, J. E., McMahon, A. P. and Takada, S. (1997). Wnt signaling required for expansion of neural crest and CNS progenitors. *Nature* **389**, 966-970.

Isaacs, H. V., Pownall, M. E. and Slack, J. M. (1994). eFgf regulates Xbra expression during Xenopus gastrulation. *EMBO J.* **13**, 4469-4481.

Isaacs, H. V., Pownall, M. E. and Slack, J. M. W. (1998). Regulation of Hox gene expression and posterior development by the caudal homologue Xcad3. *EMBO J.* **17**, 3413-3427.

Jones, C. M., Kuehn, M. R., Hogan, B. L., Smith, J. C. and Wright, C. V. (1995). Nodal-related signals induce axial mesoderm and dorsalize mesoderm during gastrulation. *Development* **121**, 3651-3662.

Jones, E. A. and Woodland, H. R. (1987). The development of animal cap cells in *Xenopus*. A measure of start of animal cap competence to form mesoderm. *Development* **101**, 557-563.

Joseph, E. M. and Melton, D. A. (1997). Xnr4: a Xenopus nodal-related gene expressed in the Spemann organizer. *Dev. Biol.* **184**, 367-372.

Joyner, A. L. (1996). Engrailed, Wnt and Pax genes regulate midbrain-hindbrain development. *Trends Genet.* **12**, 15-20.

Joyner, A. L., Liu, A. and Millet, S. (2000). Otx2, Gbx2 and Fgf8 interact to position and maintain a mid-hindbrain organizer. *Curr. Opin. Cell Biol*. **12**, 736-741.

Kao, K. R. and Elinson, R. P. (1988). The entire mesodermal mantle behaves as Spemann's organizer in dorsoanterior enhanced Xenopus laevis embryos. *Dev. Biol*. **127**, 64-77.

Kimelman, D., Christian, J. L. and Moon, R. T. (1992). Synergistic principles of development: overlapping patterning systems in *Xenopus* mesoderm induction. *Development* **116**, 1-9.

Kofron, M., Deel, T., Xanthos, J., Lohr, J., Sun, B., Sive, H., Osada, S., Wright, C., Wylie, C. and Heasman, J. (1999). Mesoderm inudction in Xenopus is a zygotic event regulated by maternal VegT via TGFβ growth factors. *Development* **126**, 5759-5770.

Ku, M. and Melton, D. A. (1993). Xwnt-11: a maternally expressed Xenopus wnt gene. *Development* **119**, 1161-1173.

LaBonne, C. and Whitman, M. (1997). Localization of MAP kinase activity in early Xenopus embryos: implications for endogenous FGF signaling. *Dev. Biol*. **183**, 9-20.

Lamb, T. M. and Harland, R. M. (1995). Fibroblast growth factor is a direct neural inducer, which combined with noggin generates anterior-posterior neural pattern. *Development* **121**, 3627-3636.

Lemaire, P. and Gurdon, J. B. (1994). A role for cytoplasmic determinants in mesoderm patterning: cell- autonomous activation of the goosecoid and Xwnt-8 genes along the dorsoventral axis of early *Xenopus* embryos. *Development* **120**, 1191-1199.

Lemaire, P. and Yasuo, H. (1998). Developmental signalling: a careful balancing act. *Curr. Biol*. **8**, R228-231.

Leyns, L., Bouwmeester, T., Kim, S. H., Piccolo, S. and De Robertis, E. M. (1997). Frzb-1 is a secreted antagonist of Wnt signaling expressed in the Spemann organizer. *Cell* **88**, 747-756.

London, C., Akers, R. and Phillips, C. (1988). Expression of Epi 1, an epidermis-specific marker in Xenopus laevis embryos, is specified prior to gastrulation. *Dev. Biol*. **129**, 380-389.

Lowe, L. A., Supp, D. M., Sampath, K., Yokoyama, T., Wright, C. V. E., Potter, S. S., Overbeek, P. and Kuehn, M. R. (1996). Conserved left-right asymmetry of nodal expression and alterations in murine situs inversus. *Nature* **381**, 158-161.

Lustig, K. D., Kroll, K., Sun, E., Ramos, R., Elmrndorf, H. and Kirschner, M. W. (1996). A Xenopus nodal-related gene that acts in synergy with noggin to induce complete axis and notochord formation. *Development* **122**, 3275-3282.

Marikawa, Y., Li, Y. and Elinson, R. P. (1997). Dorsal determinants in the Xenopus egg are firmly associated with the vegetal cortex and behave like activators of the Wnt pathway. *Dev. Biol.* **191**, 69-79.

Massague, J. (1998). TGF-beta signal transduction. *Ann. Rev. Biochem.* **67**, 753-791.

Moos, M., Jr, Wang, S. and Krinks, M. (1995). Anti-dorsalizing morphogenetic protein is a novel TGF-beta homolog expressed in the Spemann organizer. *Development* **121**, 4293-4301.

Mulder, K. M. (2000). Role of Ras and MAPKs in TGFβ signaling. *Cytokine and Growth Factor Rev.* **11**, 23-35.

Nakamura, O., Takasaki, H. and Mizohata, T. (1970). Differentiation during cleavage in Xenopus leavis: Acquisition of self-differentiation capacity of the dorsl marginal zone. *Proc. Japan Acad.* **46**, 694-699.

Neumann, C. J. and Cohen, S. M. (1996). Distinct mitogenic and cell fate specification functions of wingless in different regions of the wing. *Development* **122**, 1781-1789.

Niehrs, C. (1999). Head in the Wnt. The molecular nature of Spemann's head organizer. *Trends Genet.* **15**, 314-319.

Oda, S., Nishimatsu, S., Murakami, K. and Ueno, N. (1995). Molecular cloning and functional amalysis of a new activitn beta subunit: a dorsal mesoderm-inducing activity in Xenopus. *Biochem. Biophys. Res. Commun.* **210**, 581-588.

Saka, Y., Tada, M. and Smith, J. C. (2000). A screen for targets of the Xenopus T-box gene Xbra. *Mech. Dev.* **93**, 27-39.

Sasai, Y. and De Robertis, E. M. (1997). Ectodermal patterning in vertebrate embryos. *Dev. Biol*. **182**, 5-20.

Schmidt, J. E., Suzuki, A., Ueno, N. and Kimelman, D. (1995). Localized BMP-4 mediates dorsal/ventral patterning in the early Xenopus embryo. *Dev. Biol*. **169**, 37-50.

Schneider, S., Steinbeisser, H., Warga, R. M. and Hausen, P. (1996). β-catenin translocation into nuclei demarcates the dorsalizing centers in frog and fish embryos. *Mech. Dev.* **57**, 191-198.

Schulte-Merker, S., Smith, J. C. and Dale, L. (1994). Effects of truncated activin and FGF receptors and of follistatin on the inducing activities of BVg1 and activin: does activin play a role in mesoderm induction? *EMBO J.* **13**, 3533-3541.

Schulte-Merker, S. and Smith, J. C. (1995). Mesoderm formation in response to Brachyury requires FGF signalling. *Curr. Biol.* **5**, 62-67.

Shanmugalingam, S., Houart, C., Picker, A., Reifers, F., Macdonald, R., Barth, A., Griffin, K., Brand, M. and Wilson, S. W. (2000). Ace/Fgf8 is required for forebrain commissure formation and patterning of the telencephalon. *Development* **127**, 2549-2561.

Sokol, S. and Melton, D. A. (1991). Pre-existent pattern in Xenopus animal pole cells revealed by induction with activin. *Nature* **351**, 409-411.

Streit, A., Berliner, A. J., Papanayotou, C., Sirunilk, A. and Stern, C. D. (2000). Initiation of neural induction by FGF signalling before gastrulation. *Nature* **406**, 74-78.

Sun, B. I., Bush, S. M., Collins-Racie, L. A., LaVallie, E. R., DiBlasio-Smith, E. A., Wolfman, N. M., McCoy, J. M. and Sive, H. L. (1999). derrière: a TGF-β family member required for posterior development in Xenopus. *Development* **126**, 1467-1482.

Takahashi, S., Yokota, C., Takano, K., Tanegashima, K., Onuma, Y., Goto, J. I. and Asashima, M. (2000). Two novel nodal-related genes initiate early inductive events in *Xenopus* nieuwkoop center. *Development* **127**, 5319-5329.

Wacker, S., Grimm, K., Joos, T. and Winklbauer, R. (2000). Development and control of tissue separation at gastrulation in Xenopus. *Dev. Biol.* **224**, 428-439.

Wang, S., Krinks, M. and Moos, M., Jr (1997). Frzb-1, an antagonist of Wnt-1 and Wnt-8, does not block signaling by Wnts-3A, -5A, or -11. *Biochem. Biophys. Res. Commun.* **236**, 502-504.

Weeks, D. L. and Melton, D. A. (1987). A maternal mRNA localized to the vegetal hemisphere in Xenopus eggs codes for a growth factor related to TGF-beta. *Cell* **51**, 861-867.

Yasuo, H. and Lemaire, P. (1999). A two-step model for the fate determination of presumptive endodermal blastomeres in Xenopus embryos. *Curr. Biol.* **9**, 869-879.

Zhang, J., Houston, D. W., King, M. L., Payne, C., Wylie, C. and Heasman, J. (1998). The role of maternal VegT in establishing the primary germ layers in Xenopus embryos. *Cell* **94**, 515-524.

Zorn, A. M., Barish, G. D., Williams, B. O., Lavender, P., Klymkowsky, M. W. and Varmus, H. E. (1999). Regulation of Wnt signaling by Sox proteins: XSox17 alpha/beta and XSox3 physically interact with beta-catenin. *Mol. Cell* **4**, 487-498.

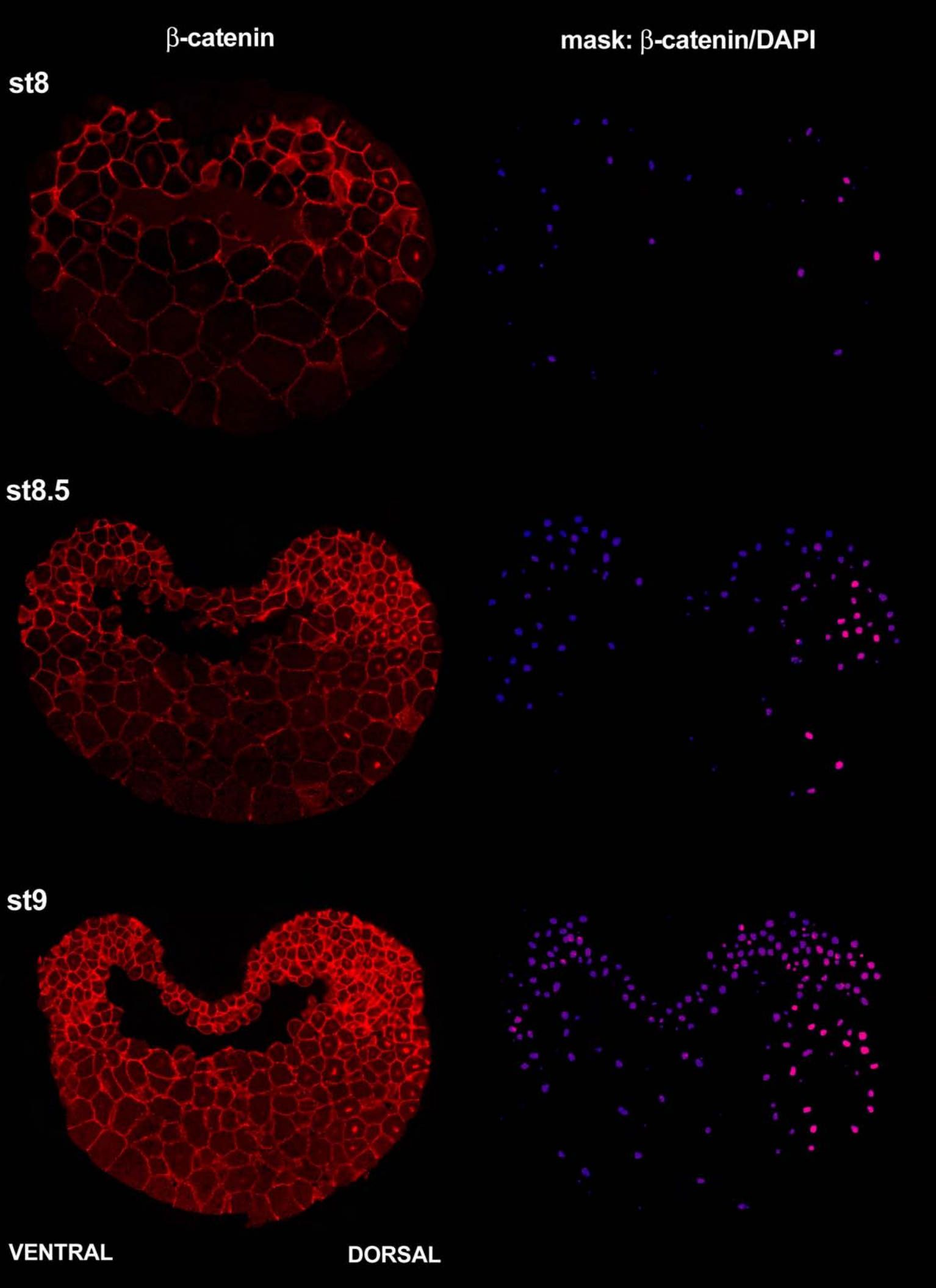
β-catenin
mask: β-catenin/DAPI
st8
st8.5
st9
VENTRAL
DORSAL

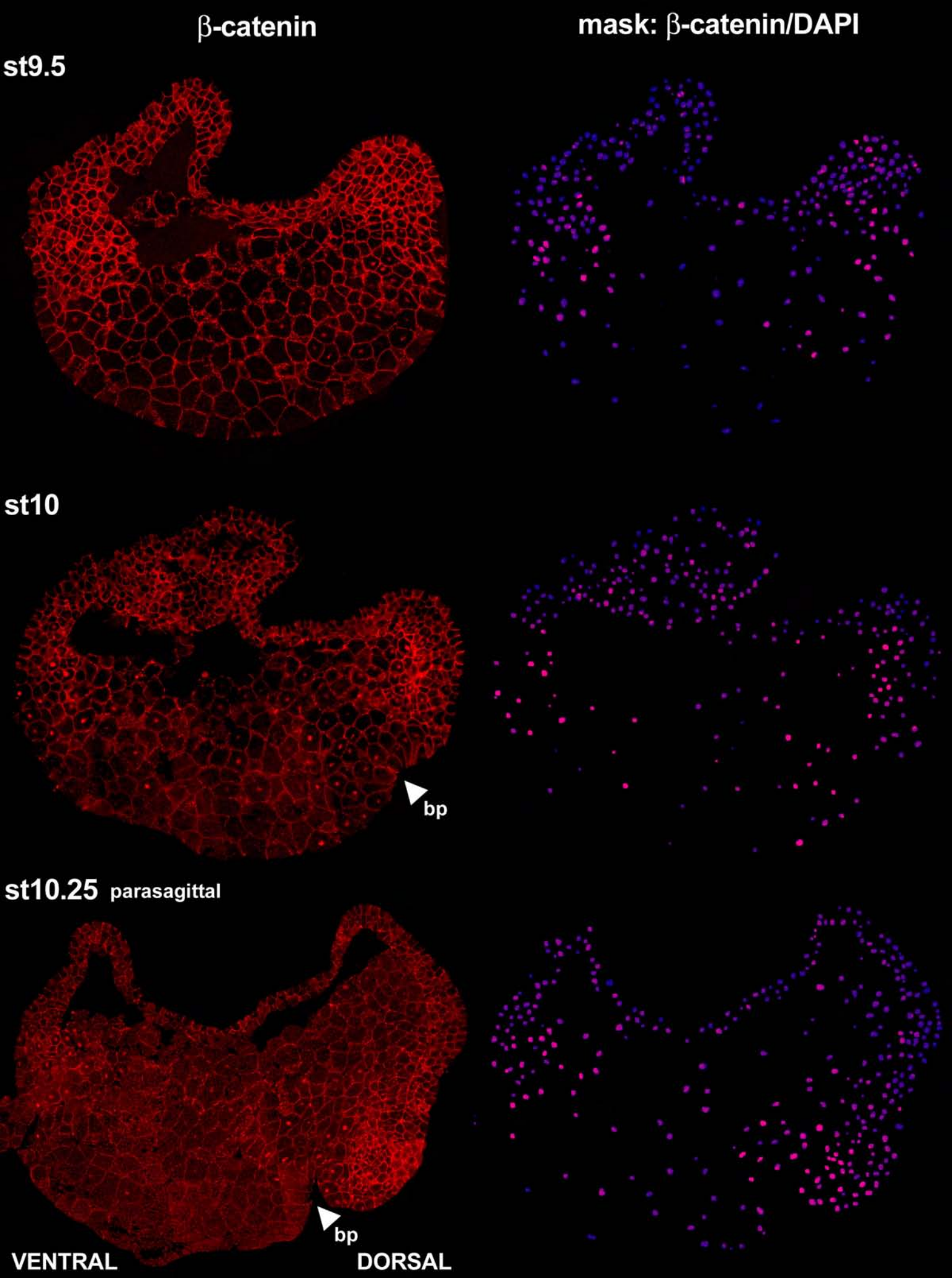
β-catenin
mask: β-catenin/DAPI
st9.5
st10
bp
st10.25 parasagittal
bp
VENTRAL
DORSAL

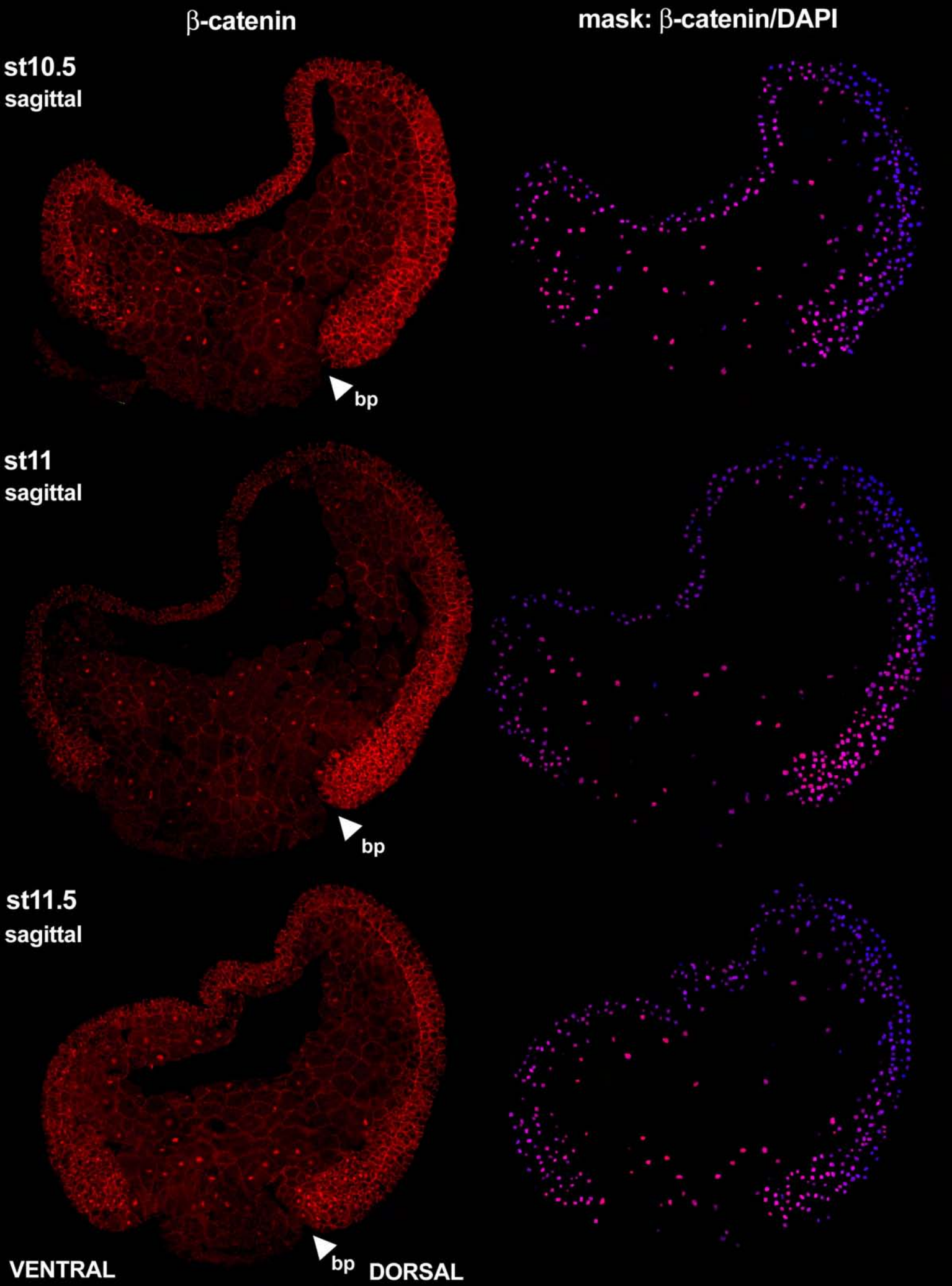
β-catenin
mask: β-catenin/DAPI
st10.5
sagittal
bp
st11
sagittal
bp
st11.5
sagittal
bp
VENTRAL
DORSAL

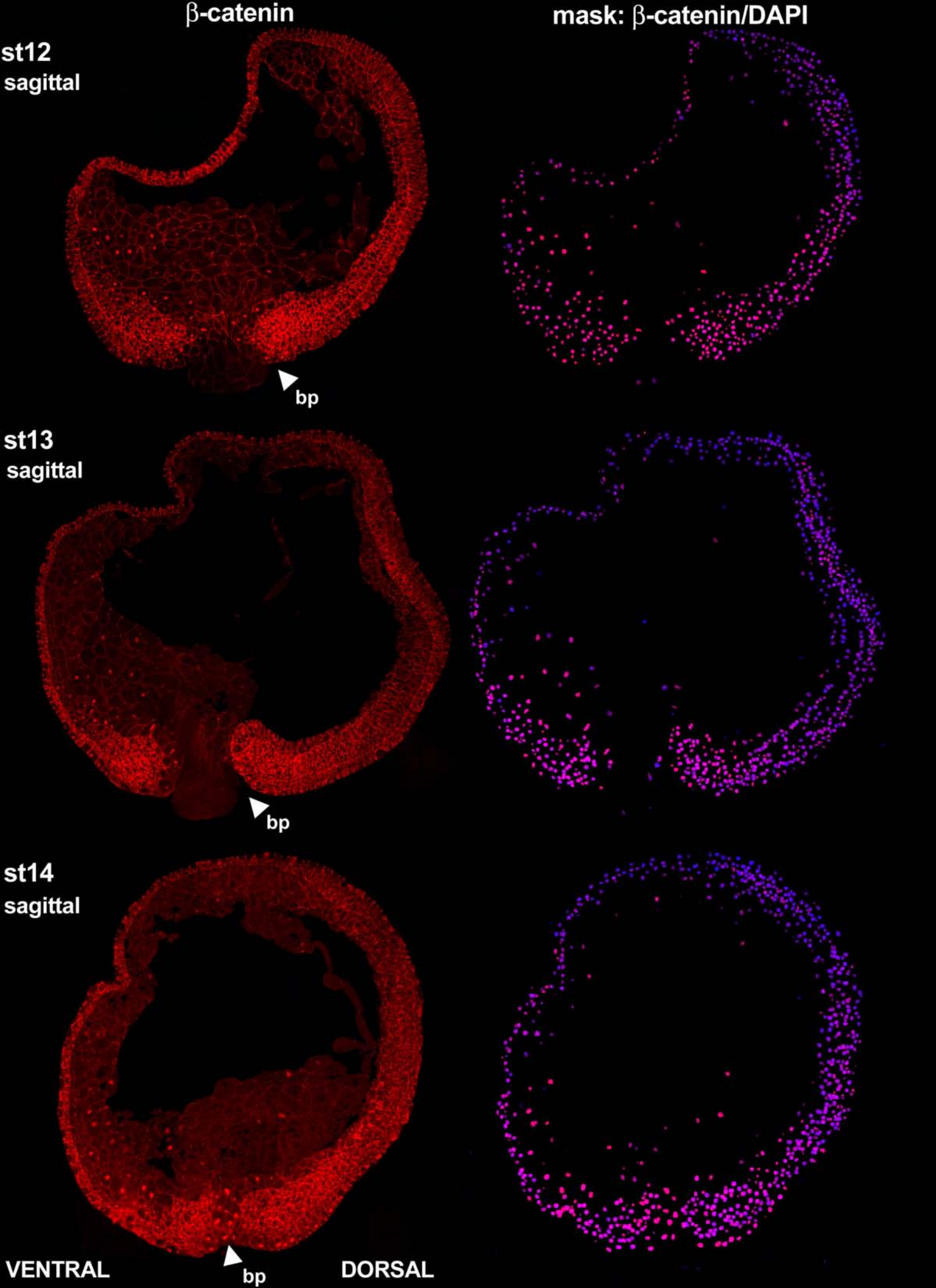
β-catenin
mask: β-catenin/DAPI
st12
sagittal
bp
st13
sagittal
bp
st14
sagittal
bp
VENTRAL
DORSAL

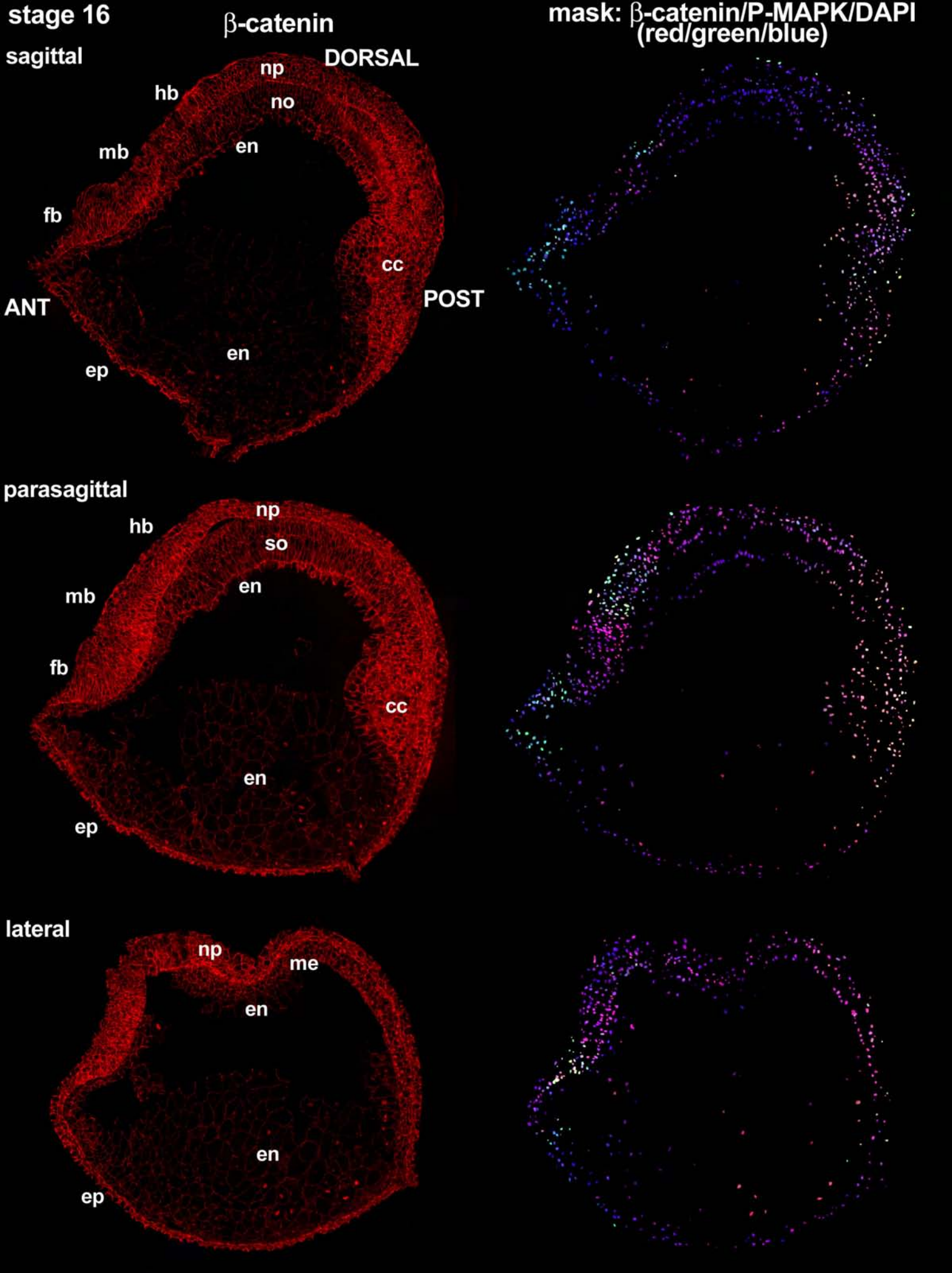
stage 16
β-catenin
mask: β-catenin/P-MAPK/DAPI
(red/green/blue)
sagittal
DORSAL
np
hb
no
mb
en
fb
cc
ANT
POST
en
ep
parasagittal
np
hb
so
en
mb
fb
cc
en
ep
lateral
np
me
en
en
ep

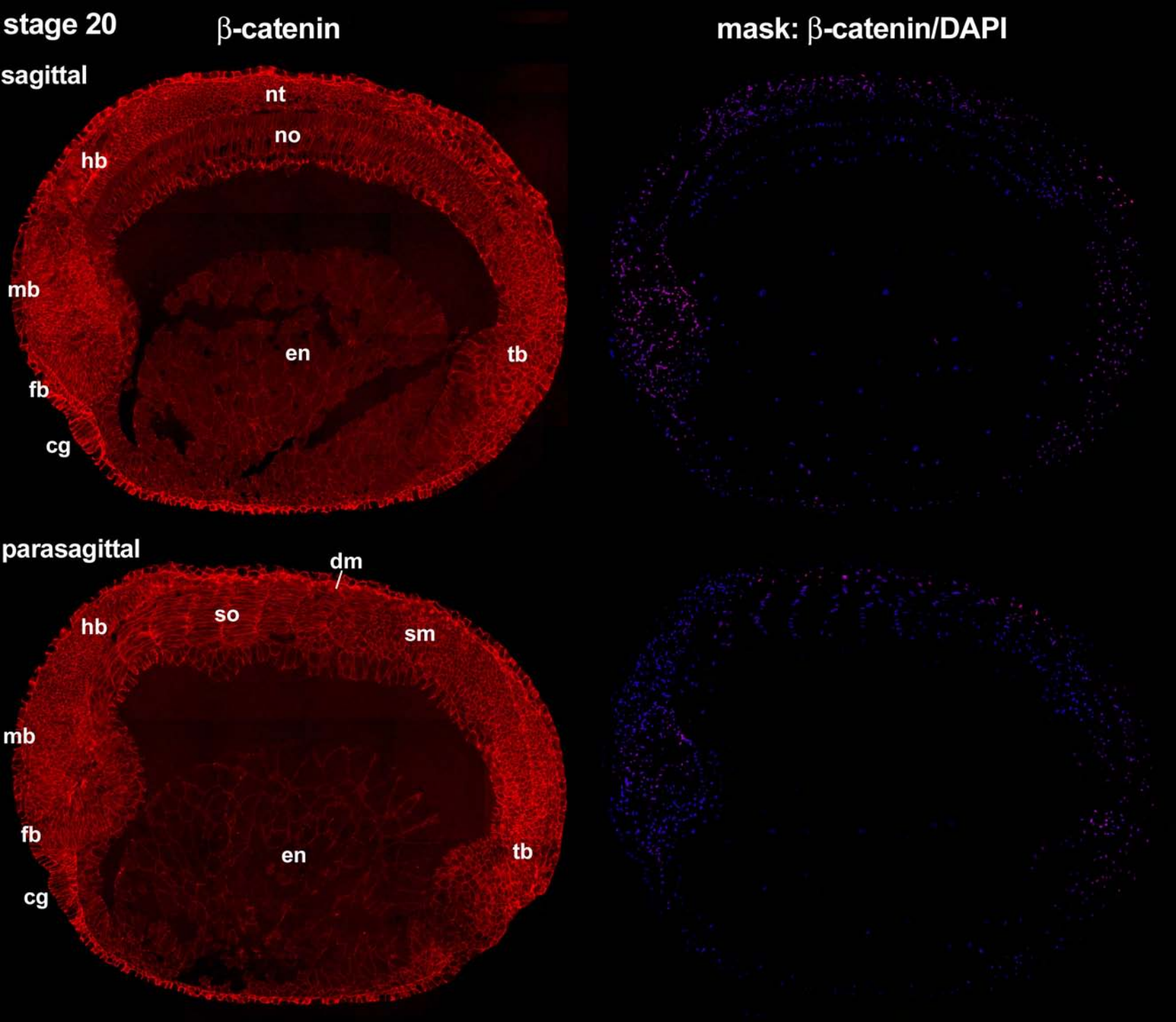
stage 20
β-catenin
mask: β-catenin/DAPI
sagittal
nt
no
hb
mb
en
tb
fb
cg
parasagittal
dm
hb
so
sm
mb
fb
en
tb
cg

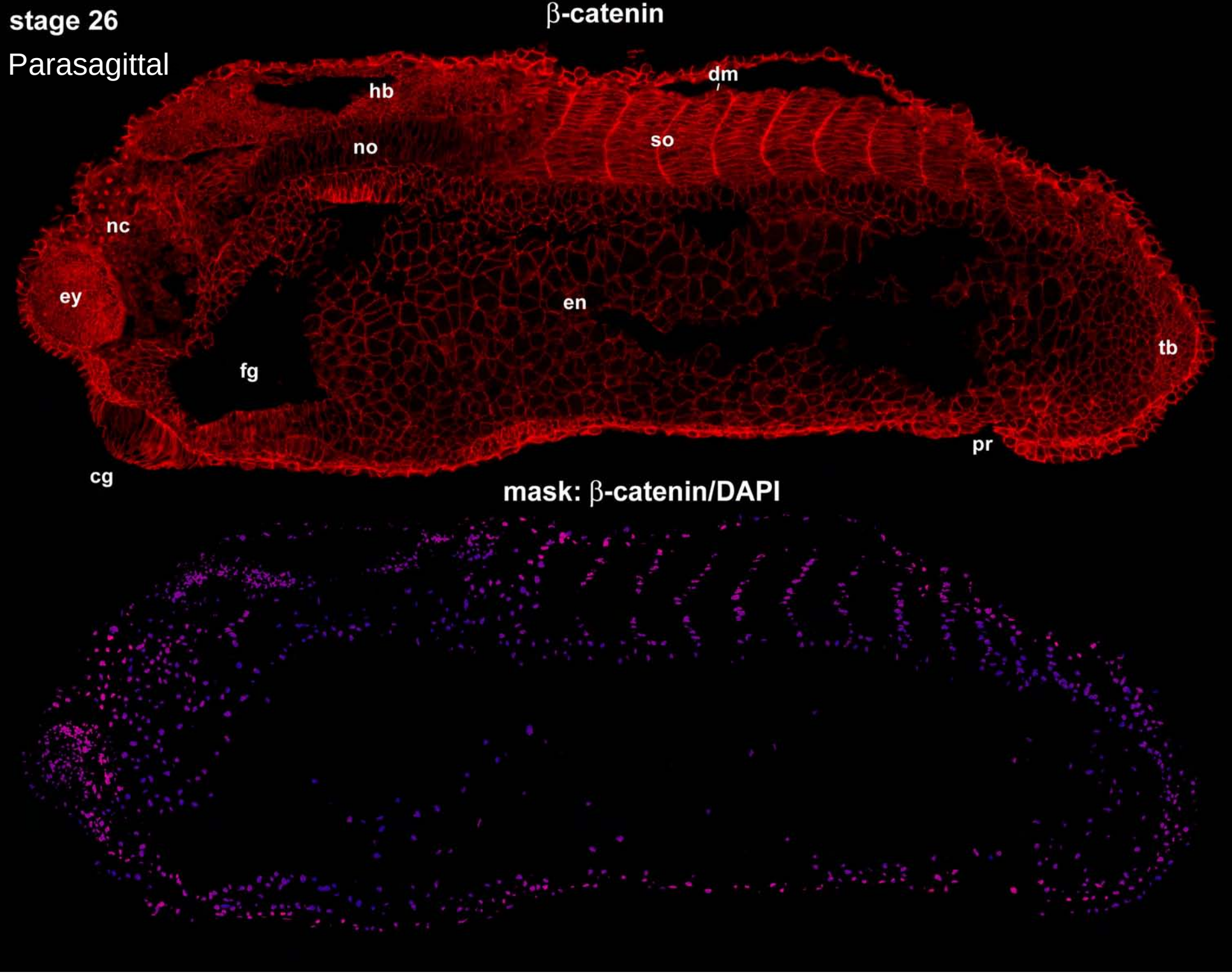
stage 26
Parasagittal
β-catenin
dm
hb
no
so
nc
ey
en
tb
fg
pr
cg
mask: β-catenin/DAPI

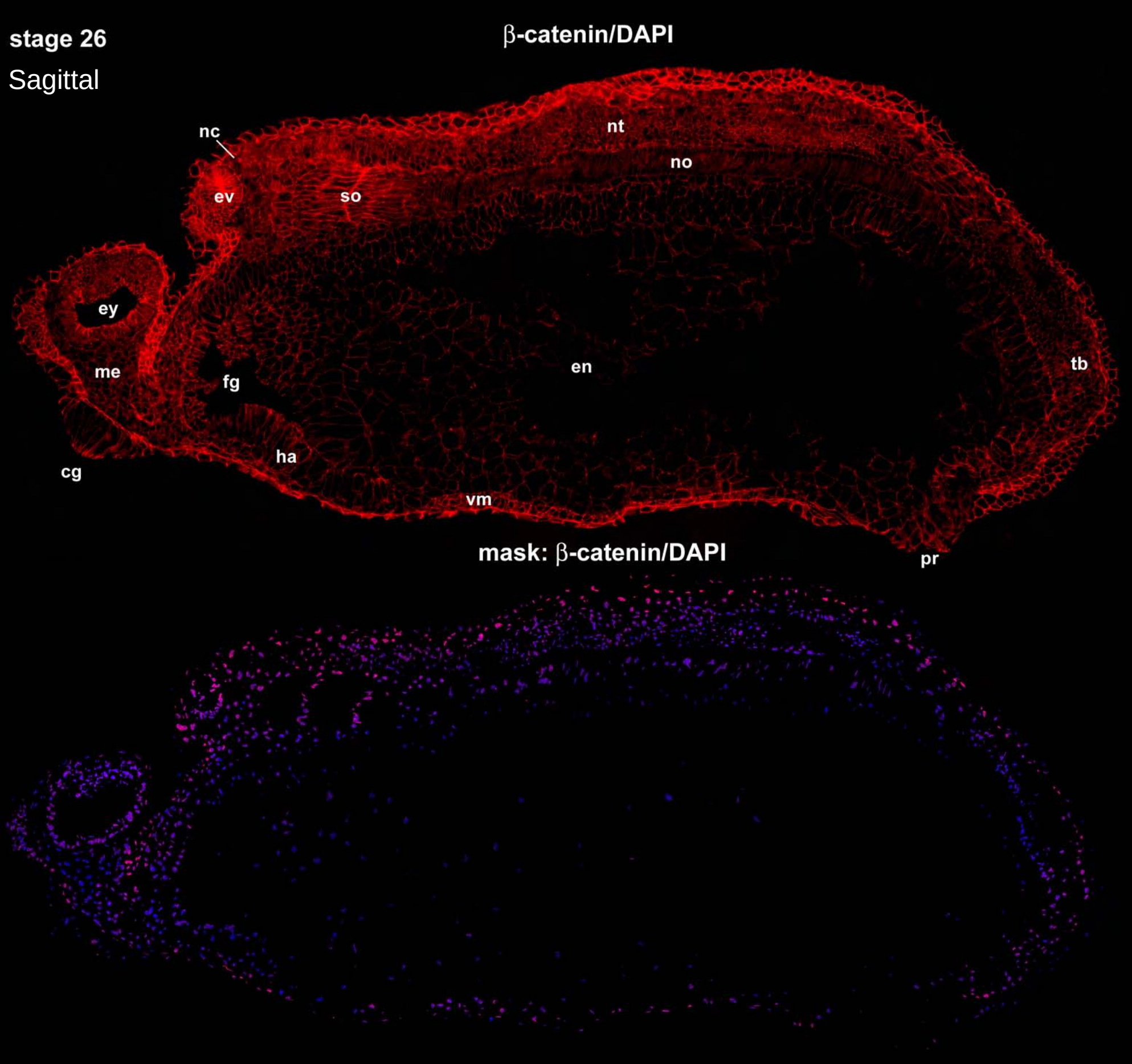
stage 26
Sagittal
β-catenin/DAPI
nc
nt
no
ev
so
ey
me
fg
en
tb
ha
cg
vm
pr
mask: β-catenin/DAPI

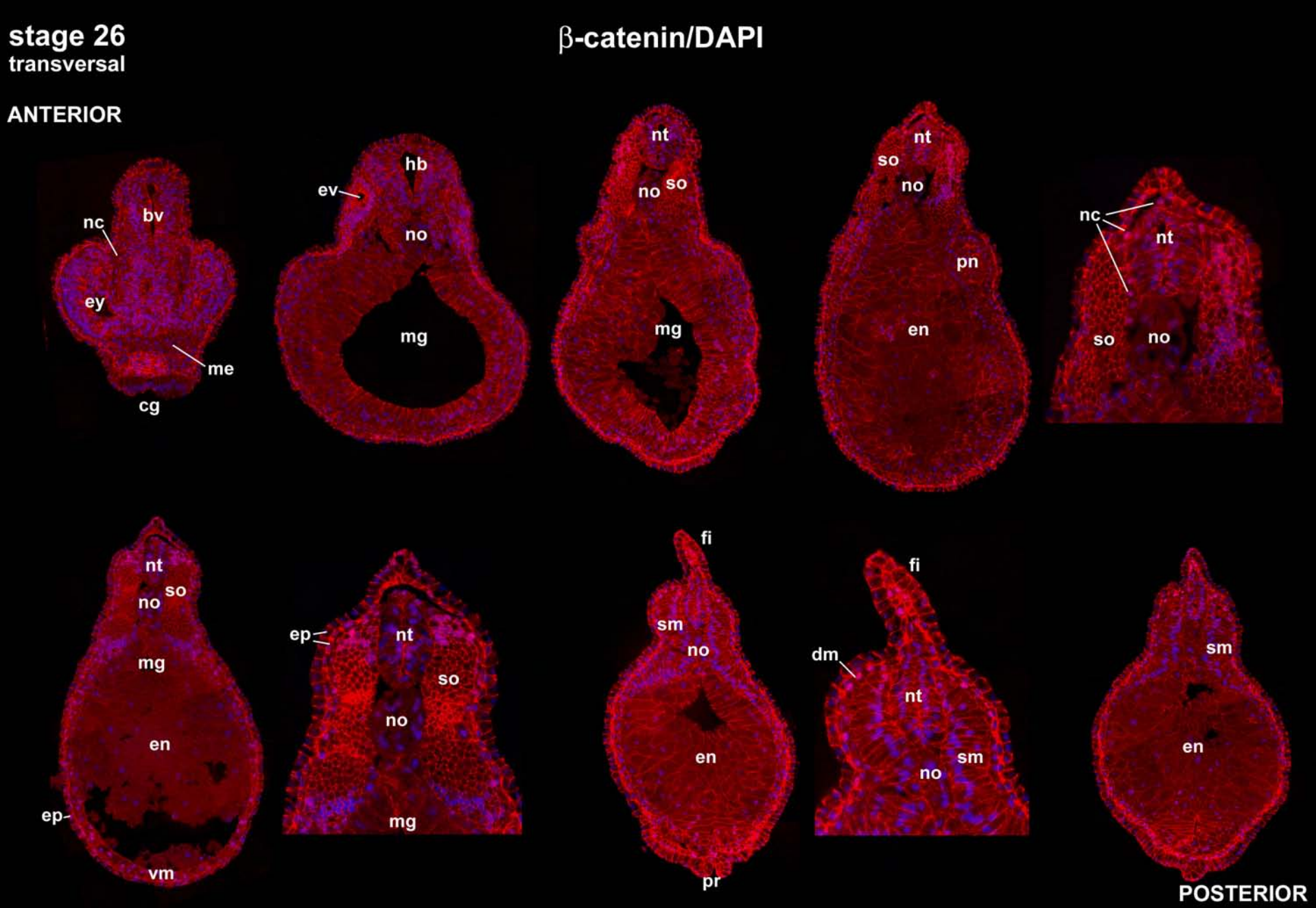
stage 26
transversal
β-catenin/DAPI
ANTERIOR
nc
bv
ey
me
cg
ev
hb
no
mg
nt
no
so
mg
nt
so
no
pn
en
nc
nt
so
no
nt
no
so
mg
ep
ep
nt
so
no
mg
fi
sm
no
en
pr
fi
dm
nt
sm
no
sm
en
POSTERIOR
vm

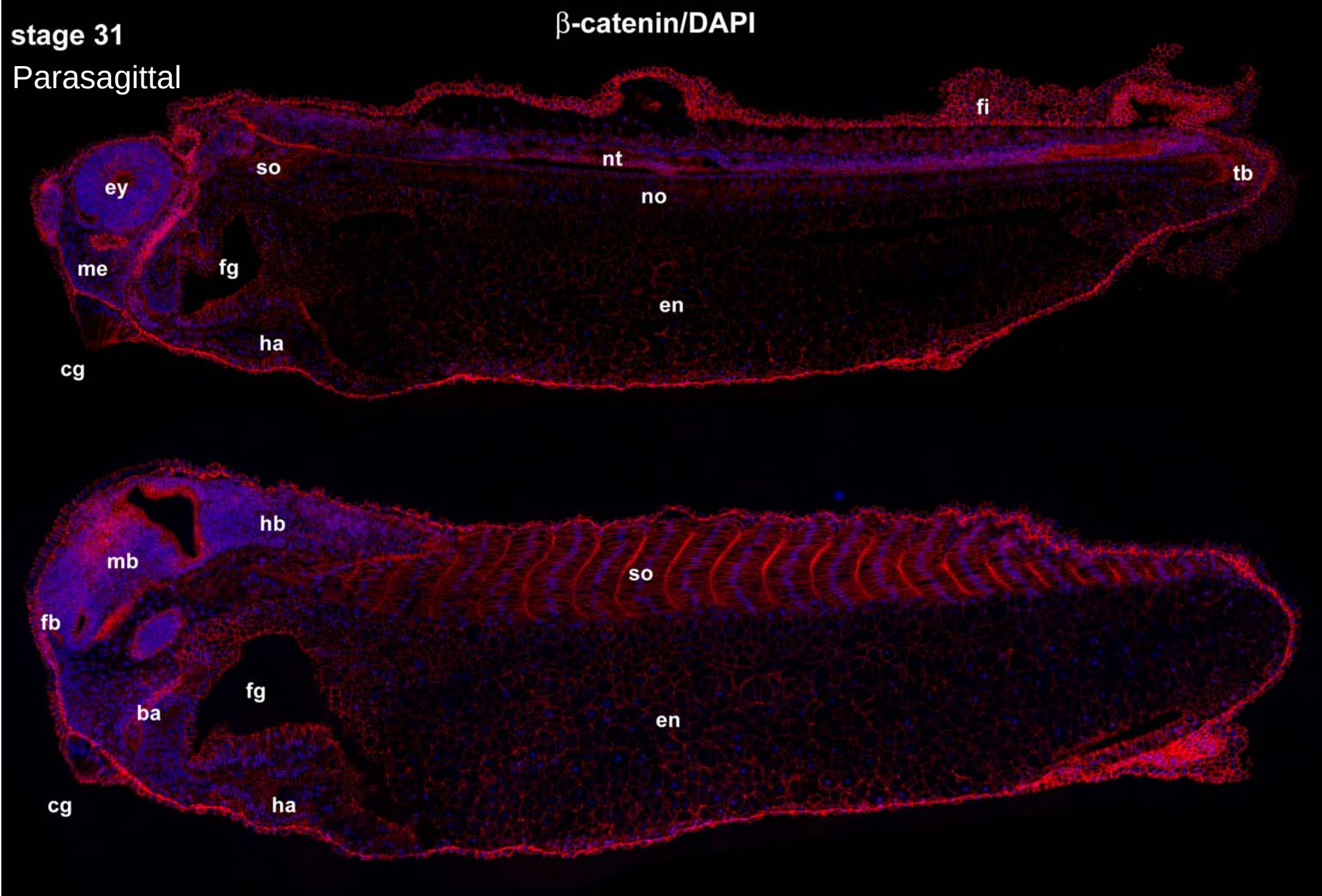
stage 31
Parasagittal
β-catenin/DAPI
fi
nt
so
tb
ey
no
me
fg
en
ha
cg
hb
mb
so
fb
fg
ba
en
cg
ha

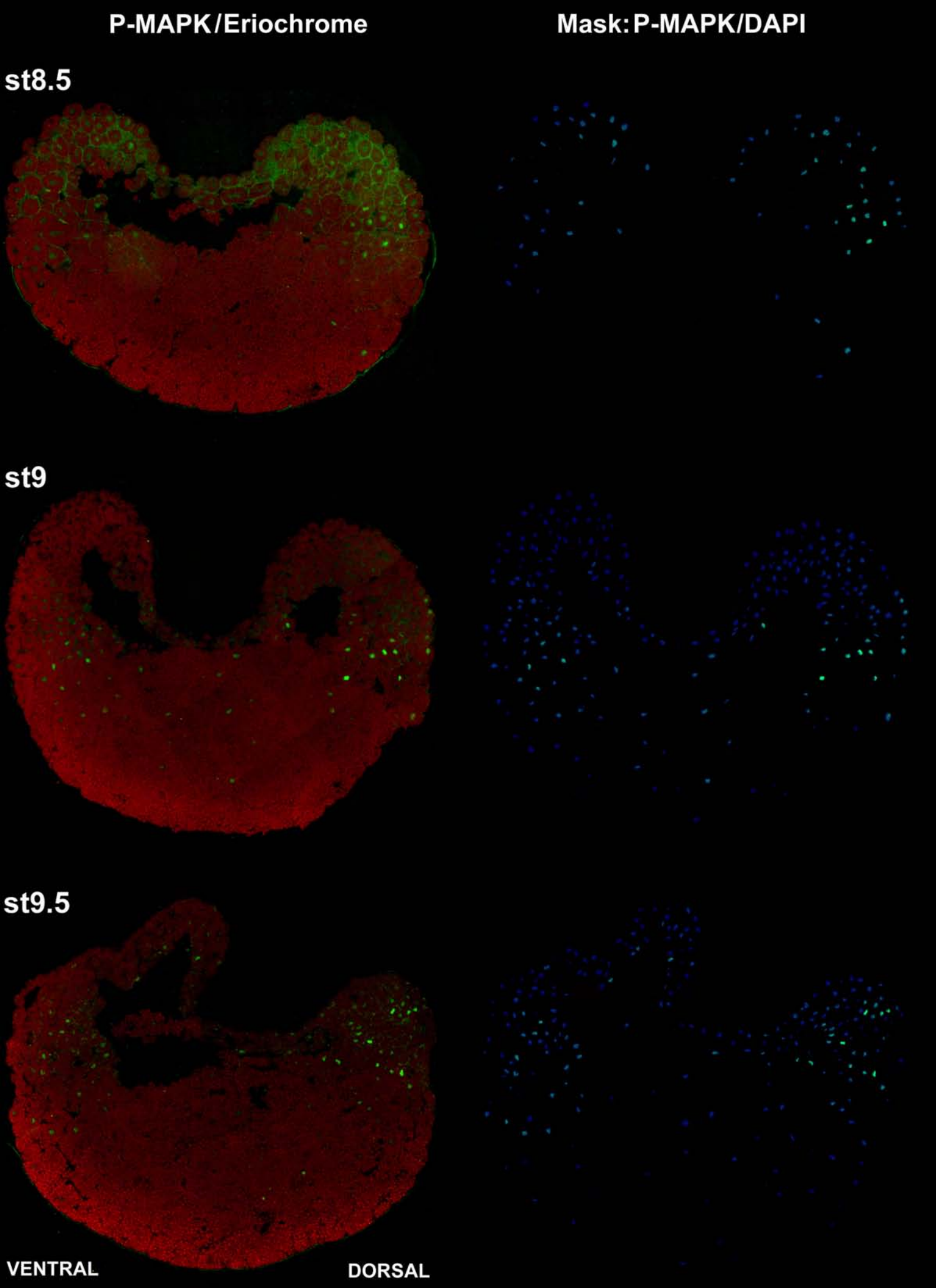
P-MAPK/Eriochrome
Mask: P-MAPK/DAPI
st8.5
st9
st9.5
VENTRAL
DORSAL

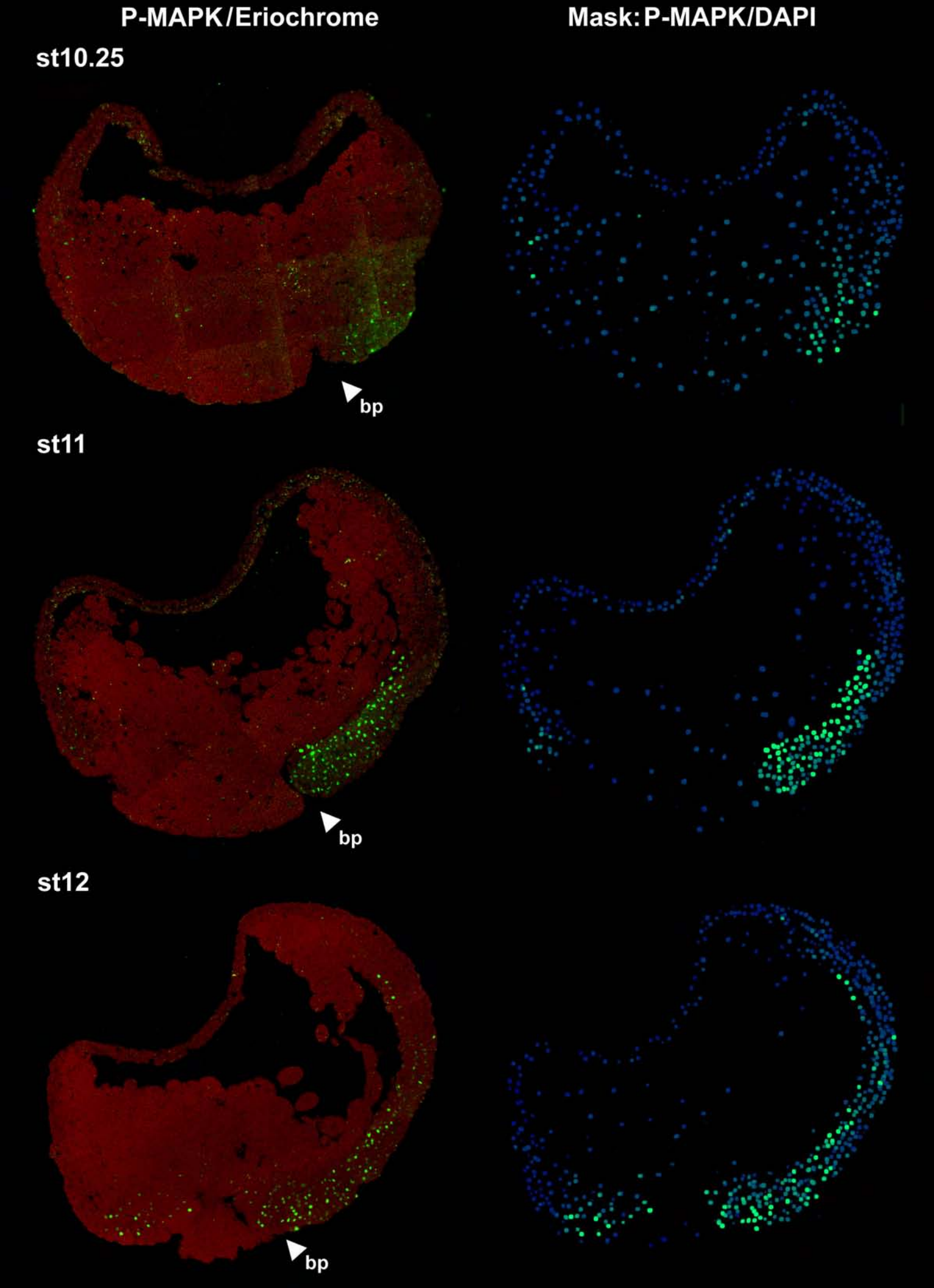
P-MAPK/Eriochrome
Mask: P-MAPK/DAPI
st10.25
bp
st11
bp
st12
bp

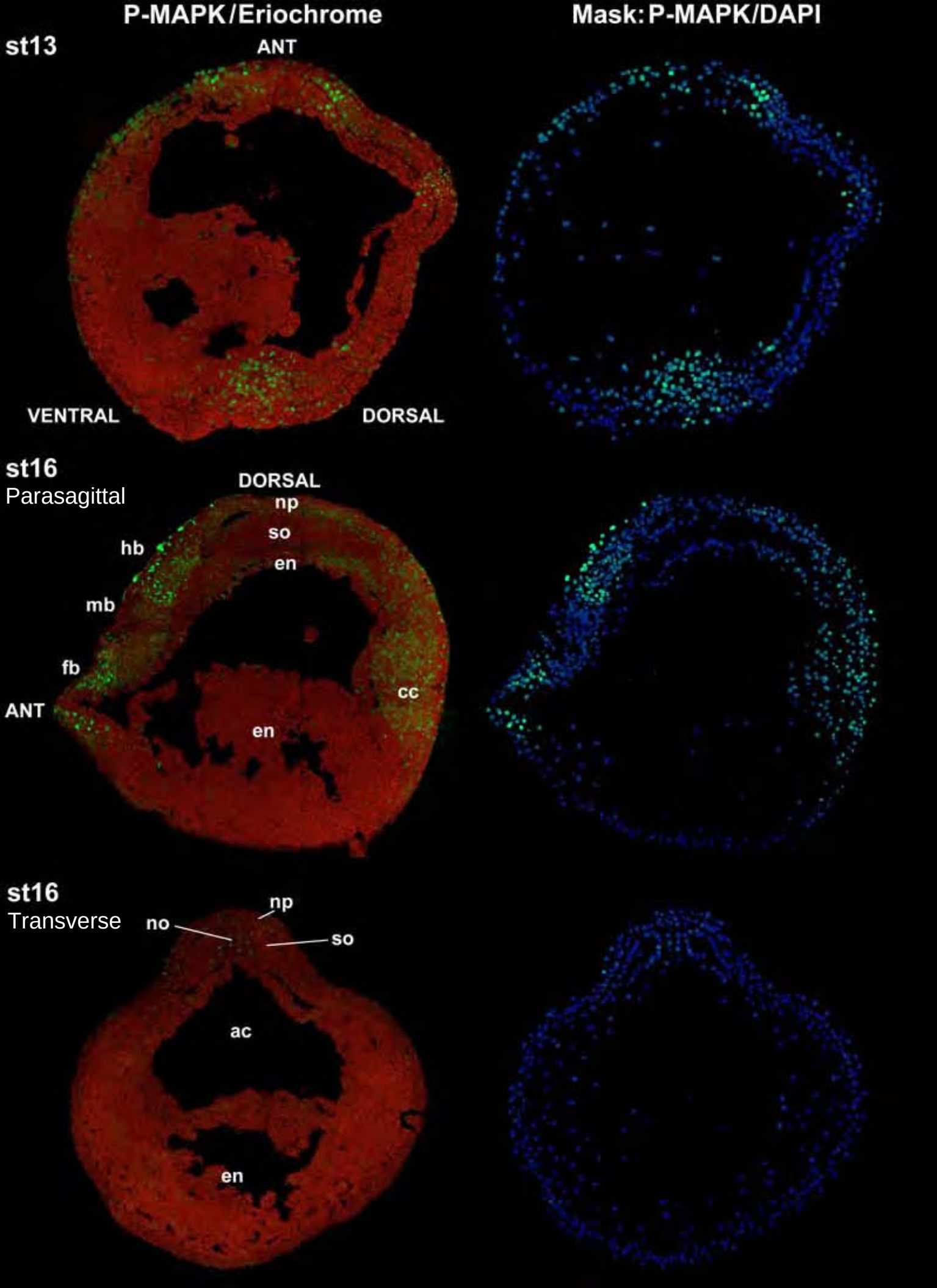
P-MAPK/Eriochrome
Mask: P-MAPK/DAPI
st13
ANT
VENTRAL
DORSAL
st16
Parasagittal
DORSAL
np
so
hb
en
mb
fb
cc
ANT
en
st16
Transverse
np
no
so
ac
en

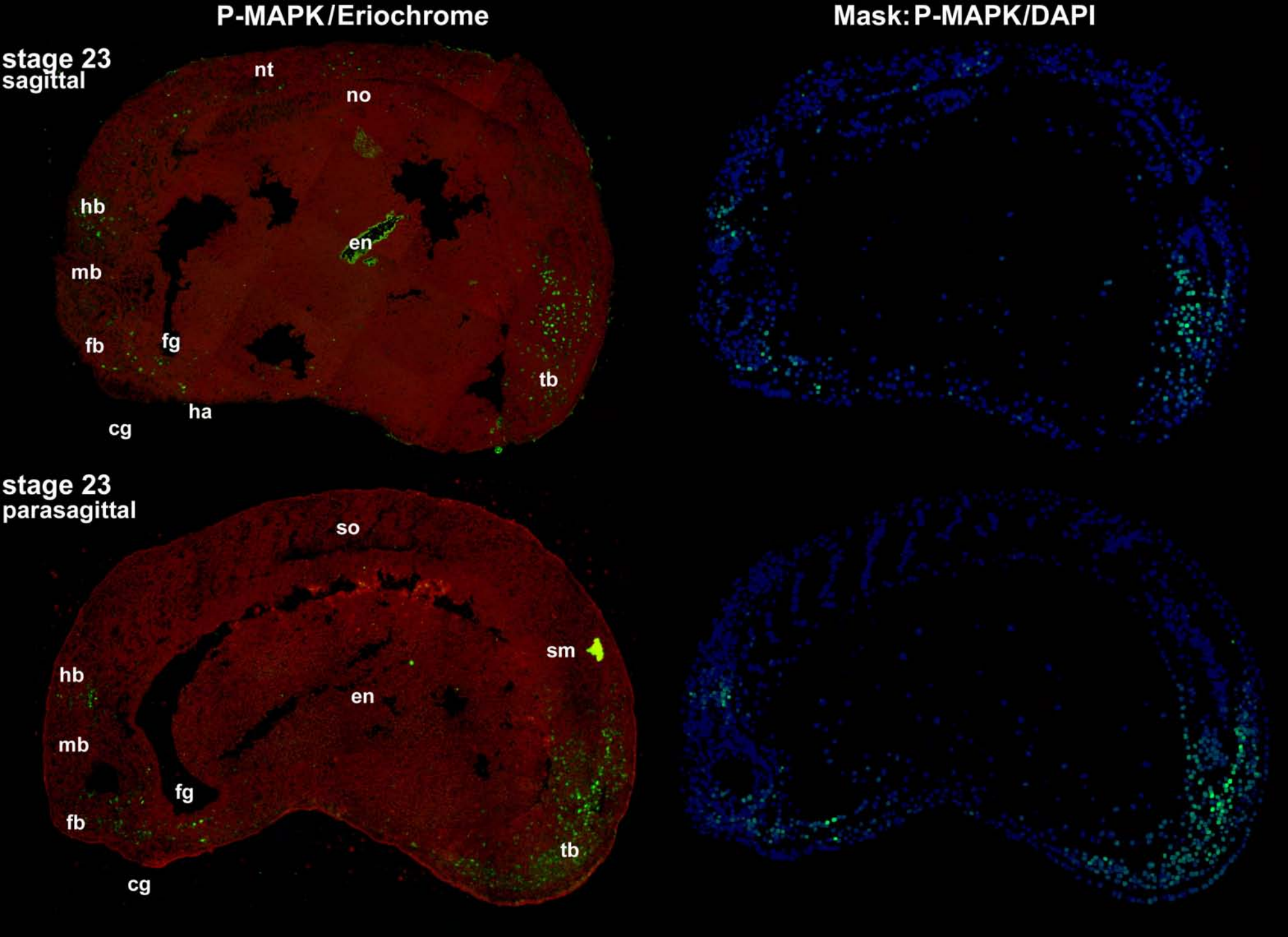
P-MAPK/Eriochrome
Mask: P-MAPK/DAPI
stage 23
sagittal
nt
no
hb
en
mb
fb
fg
tb
ha
cg
stage 23
parasagittal
so
sm
hb
en
mb
fg
fb
tb
cg

Sagittal

stage 26, notochord

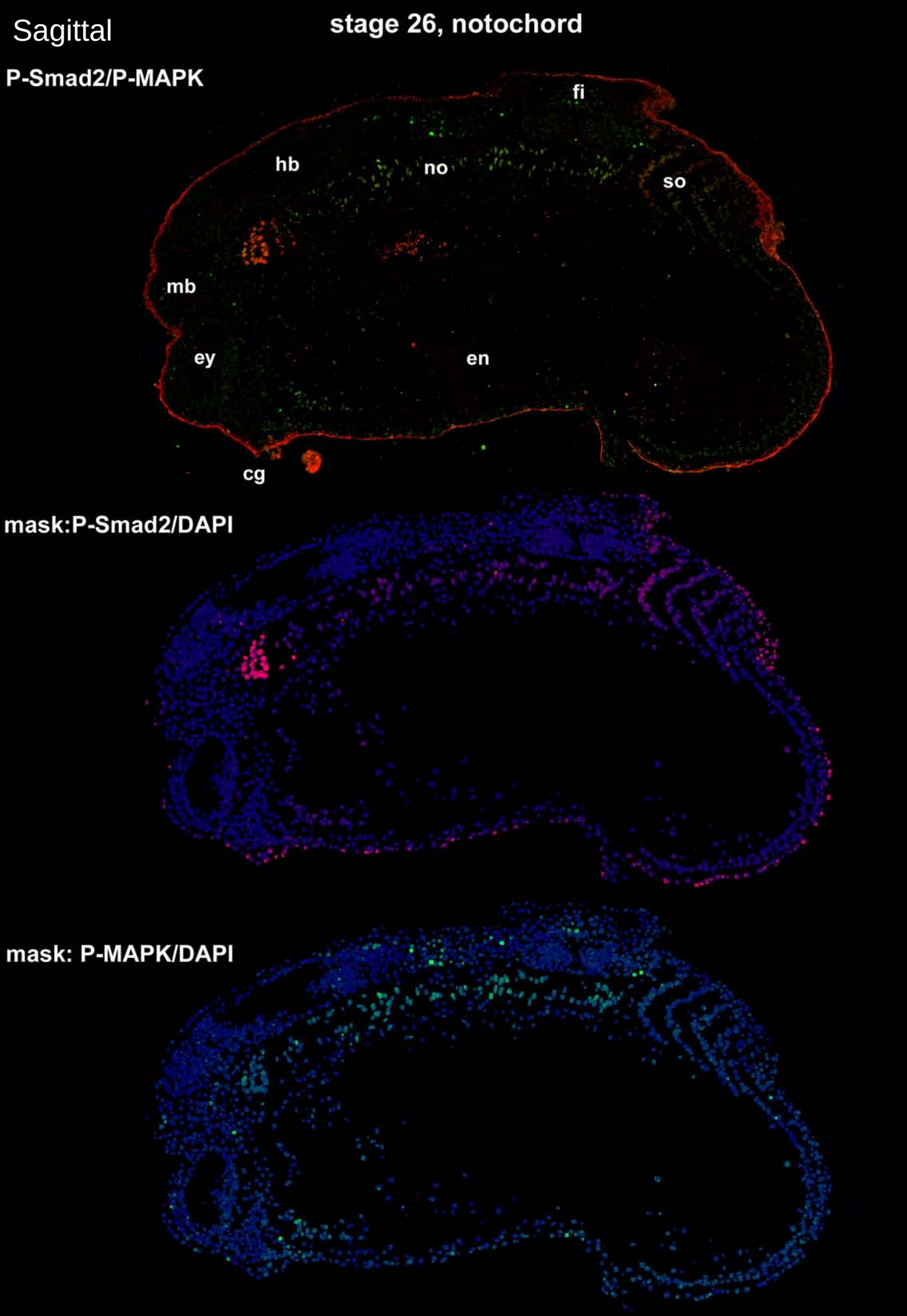

Parasagittal

stage 26, somites

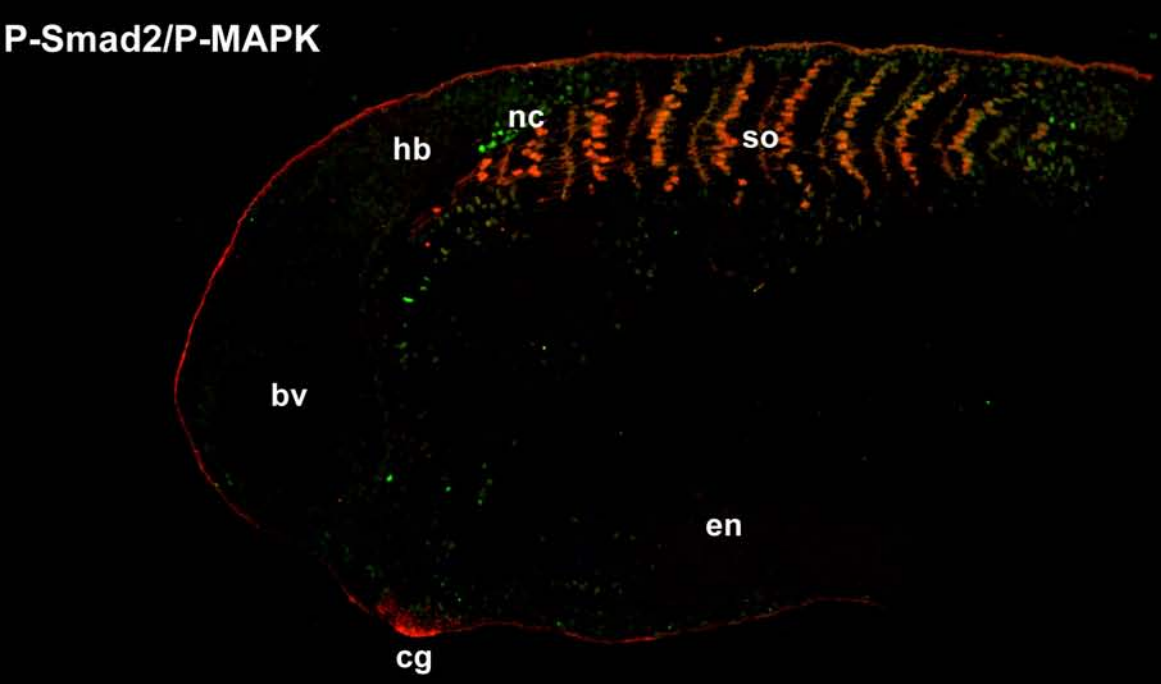

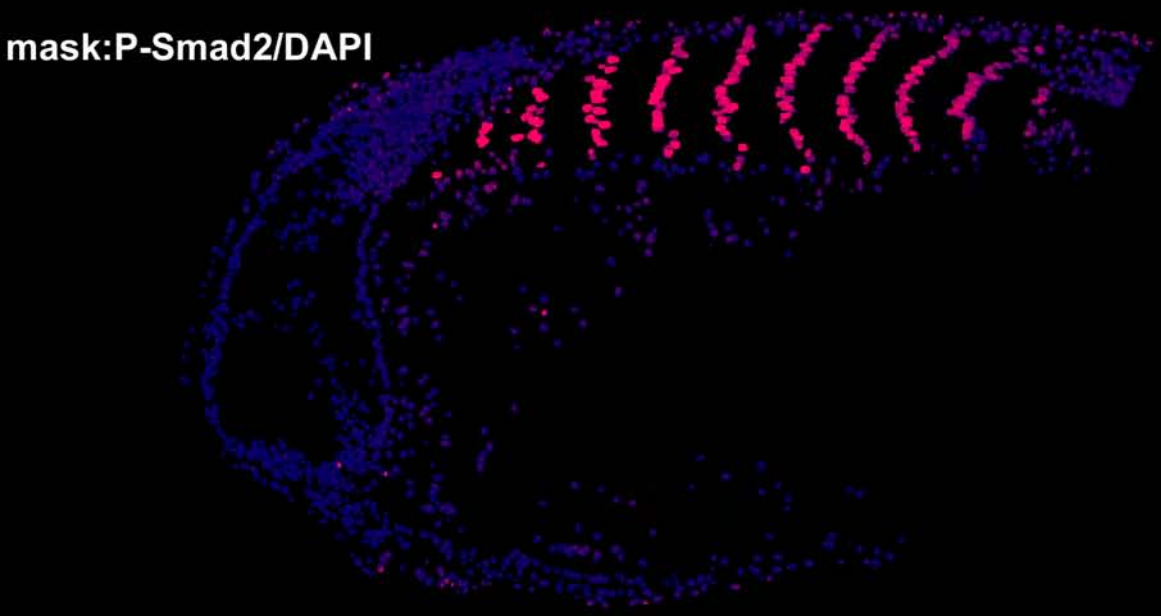

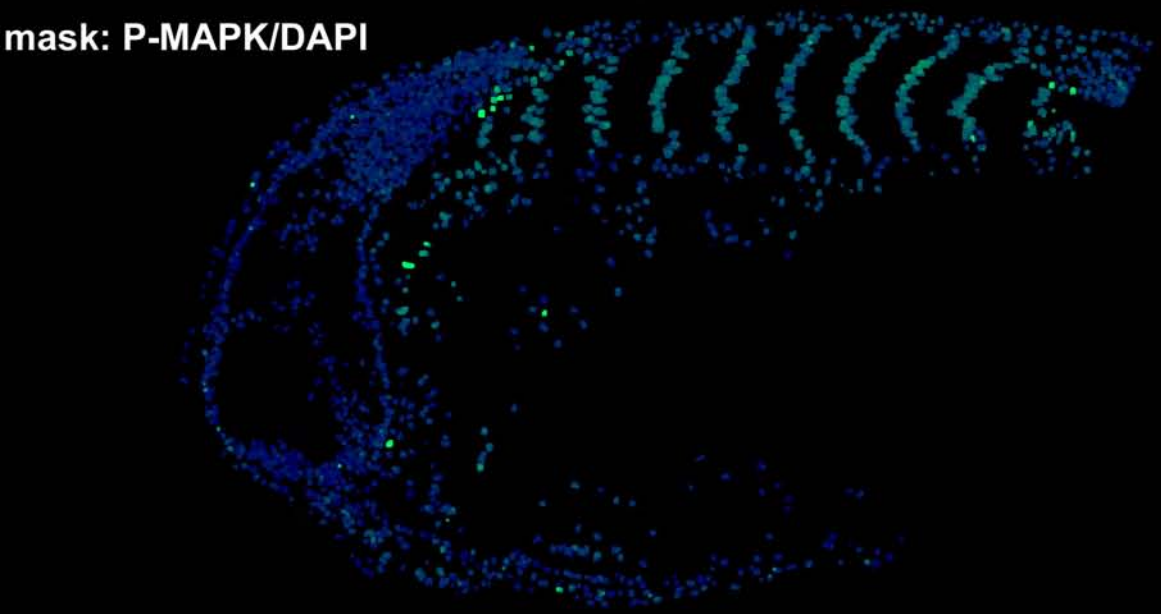

Sagittal

stage 31, notochord

P-Smad2/P-MAPK

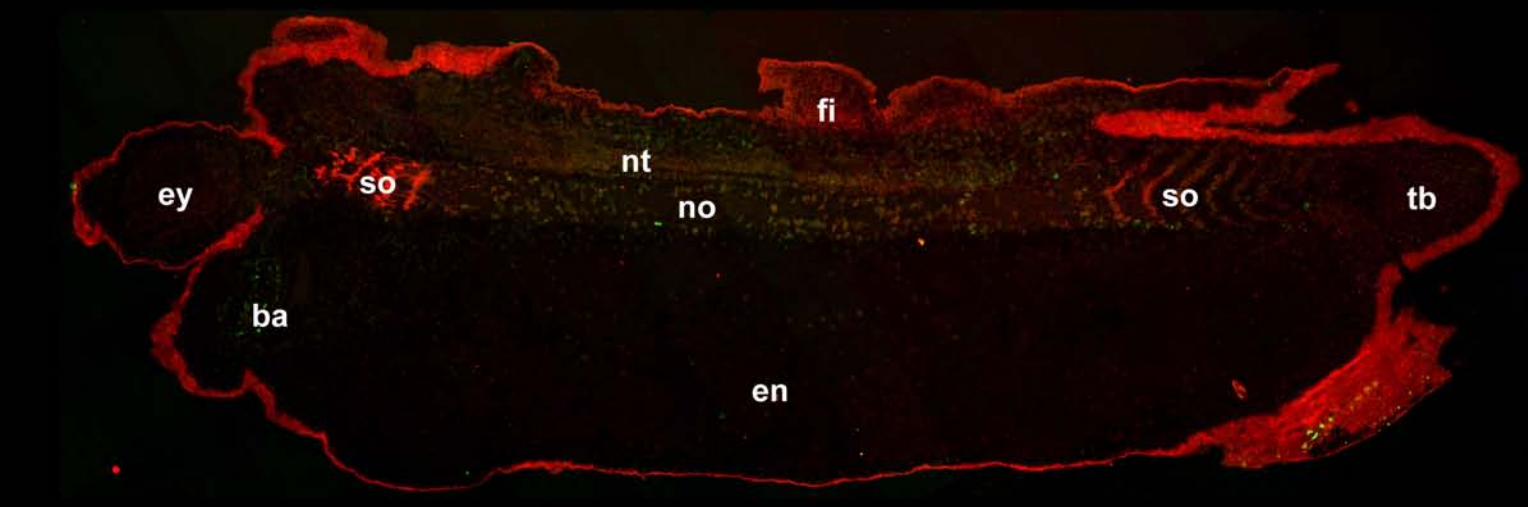

mask: P-Samd2/DAPI

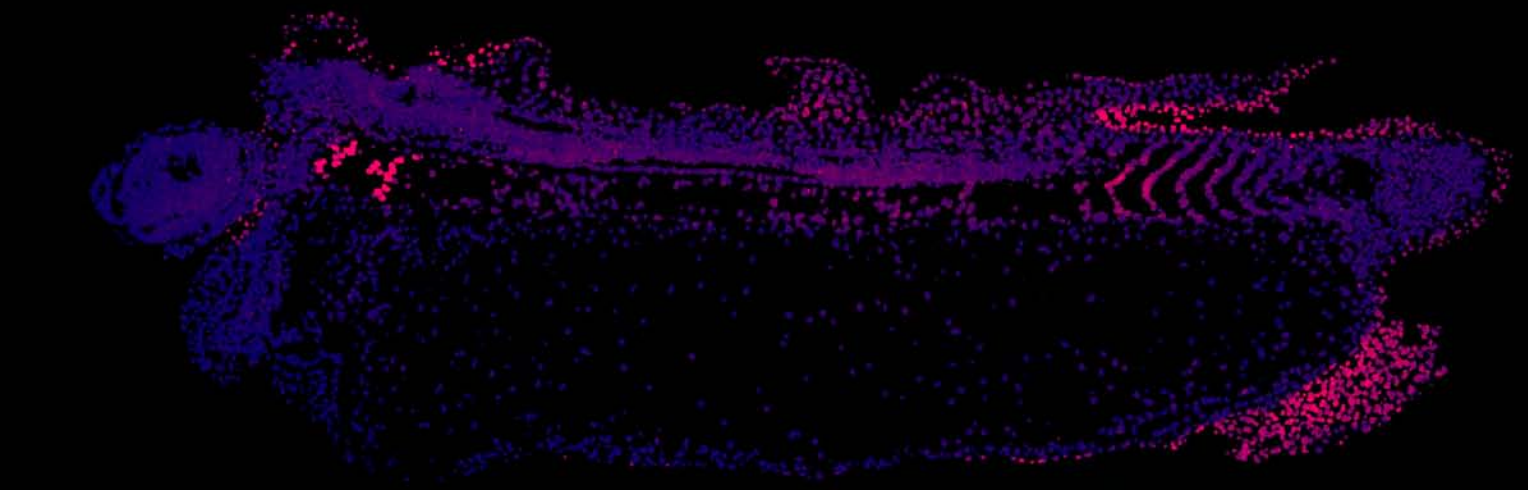

mask: P-MAPK/DAPI

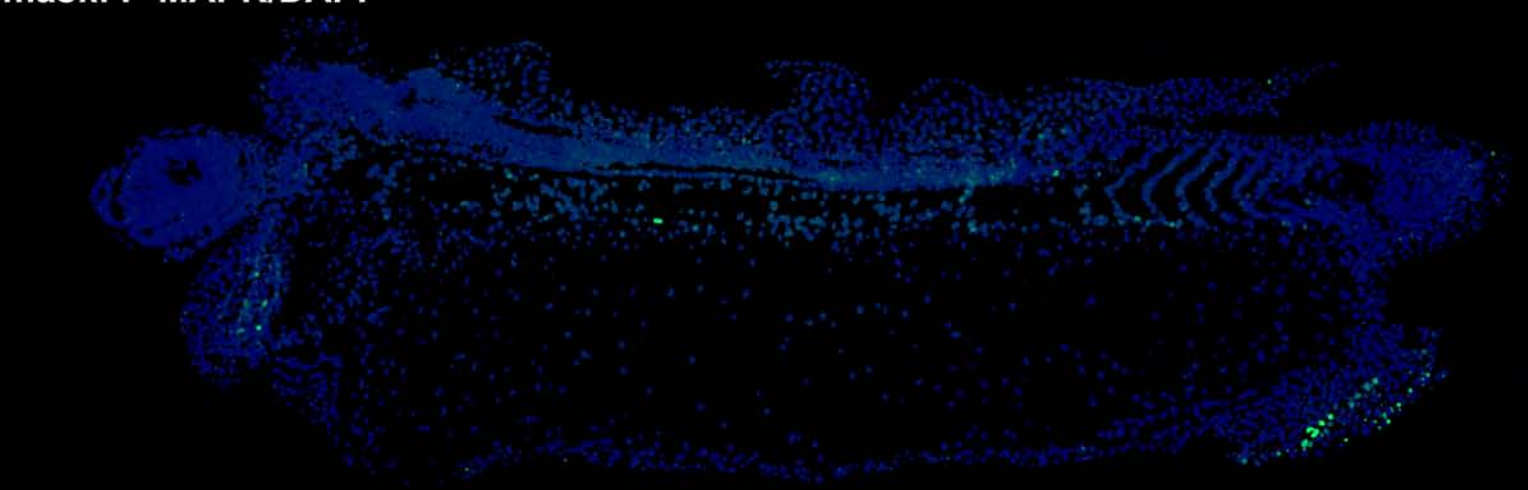

Parasagittal

stage 31, somites

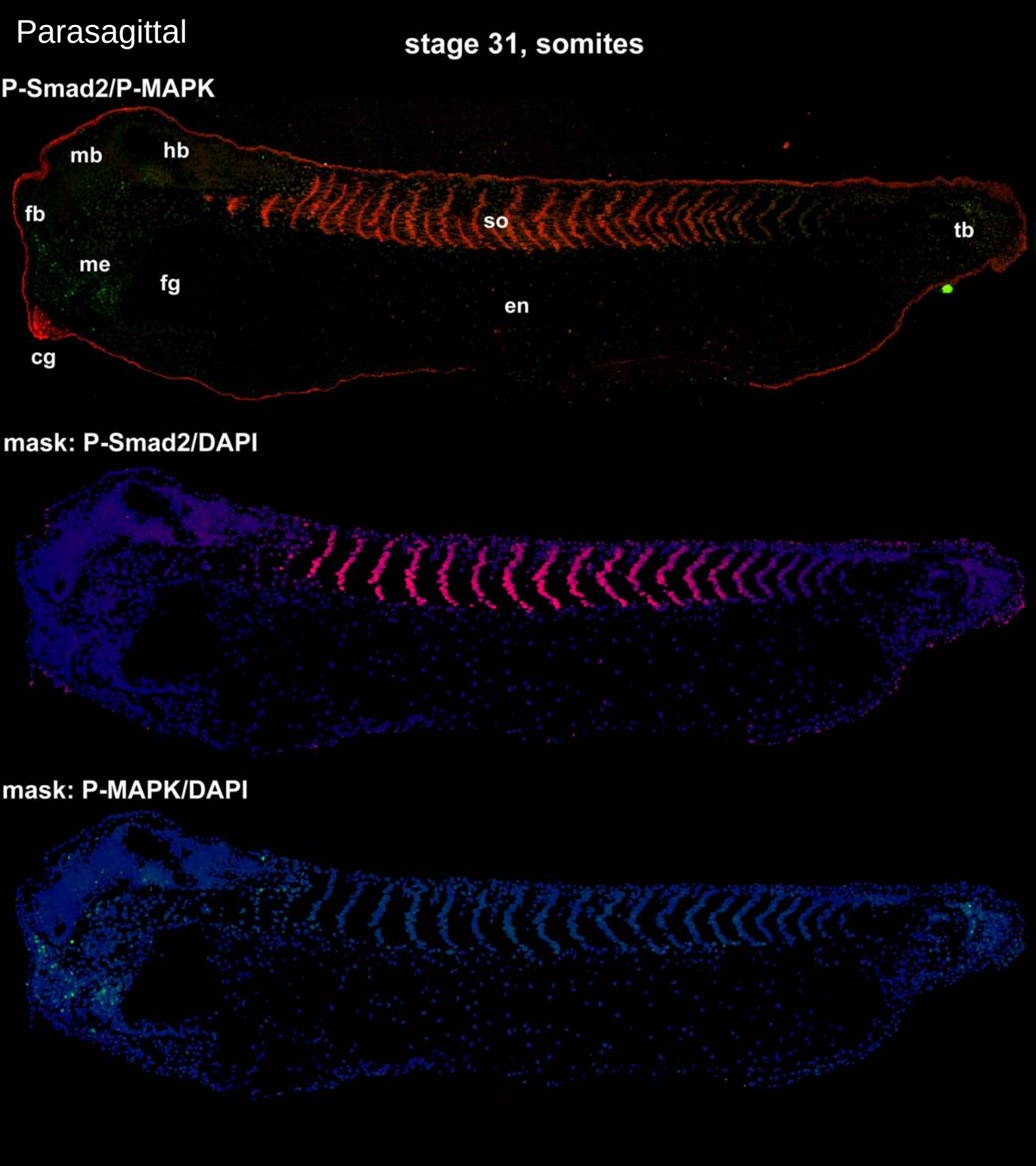

Parasagittal **stage 31**

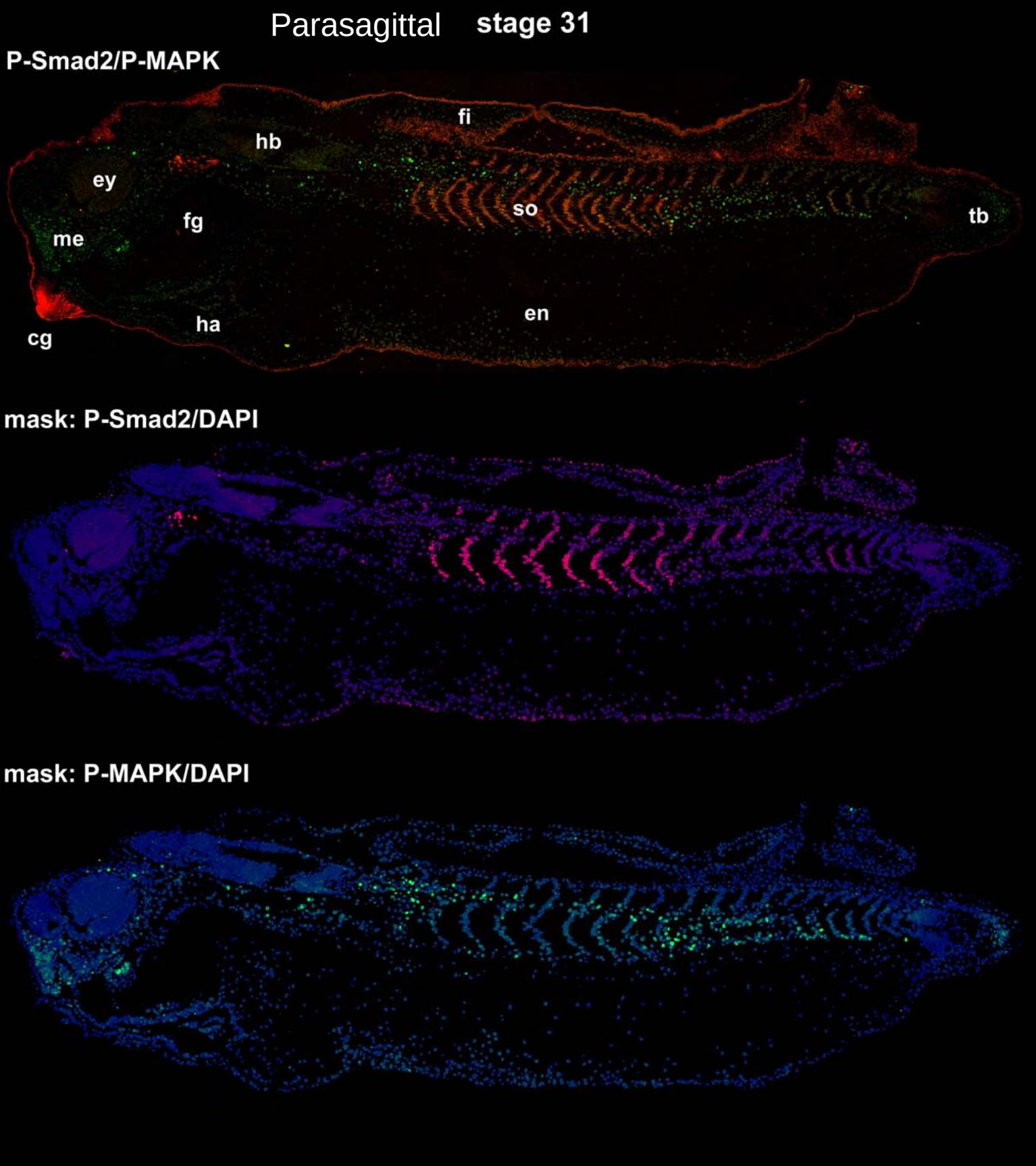

stage 31, head

P-Smad2/P-MAPK

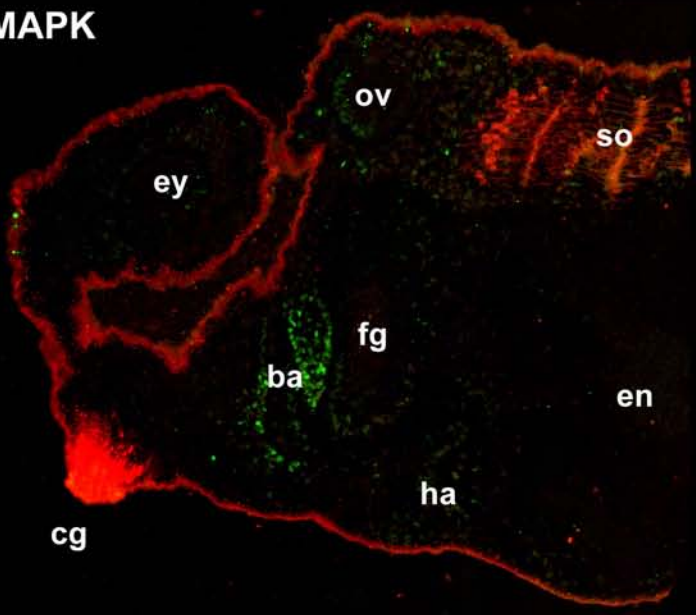

mask: P-Smad2/DAPI

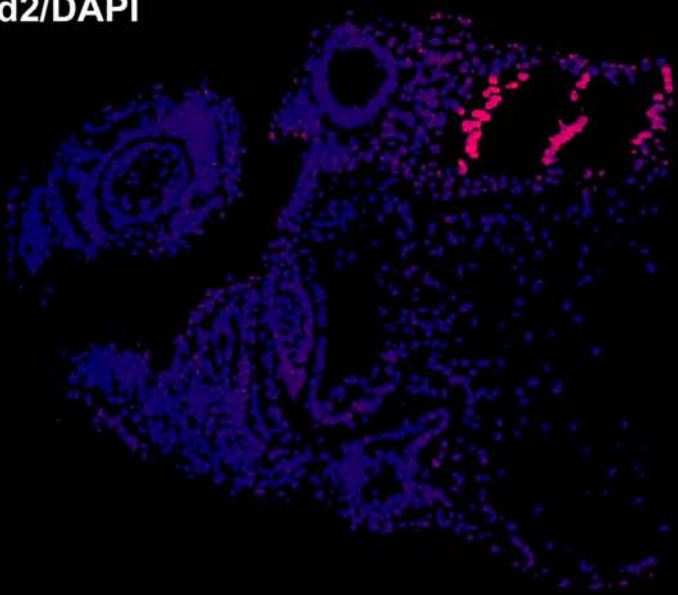

mask: P-MAPK/DAPI

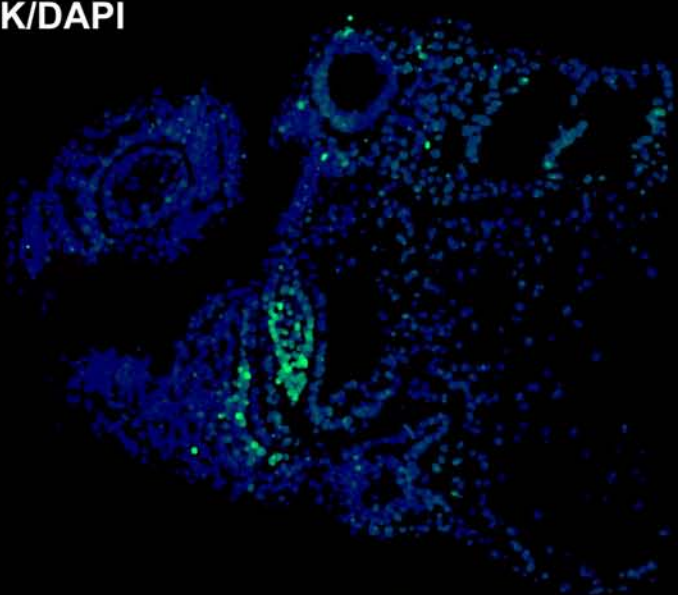

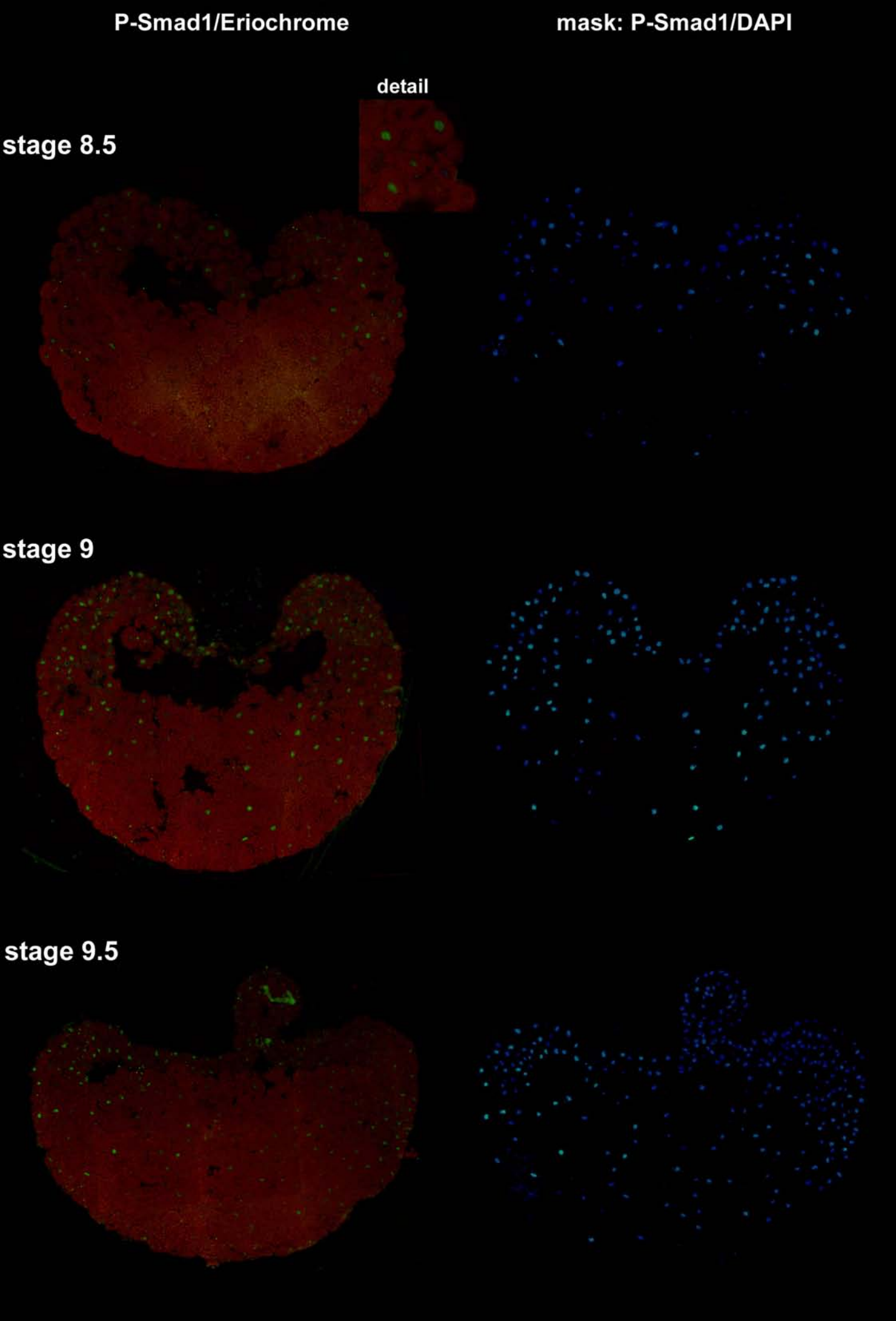
P-Smad1/Eriochrome
mask: P-Smad1/DAPI
detail
stage 8.5
stage 9
stage 9.5

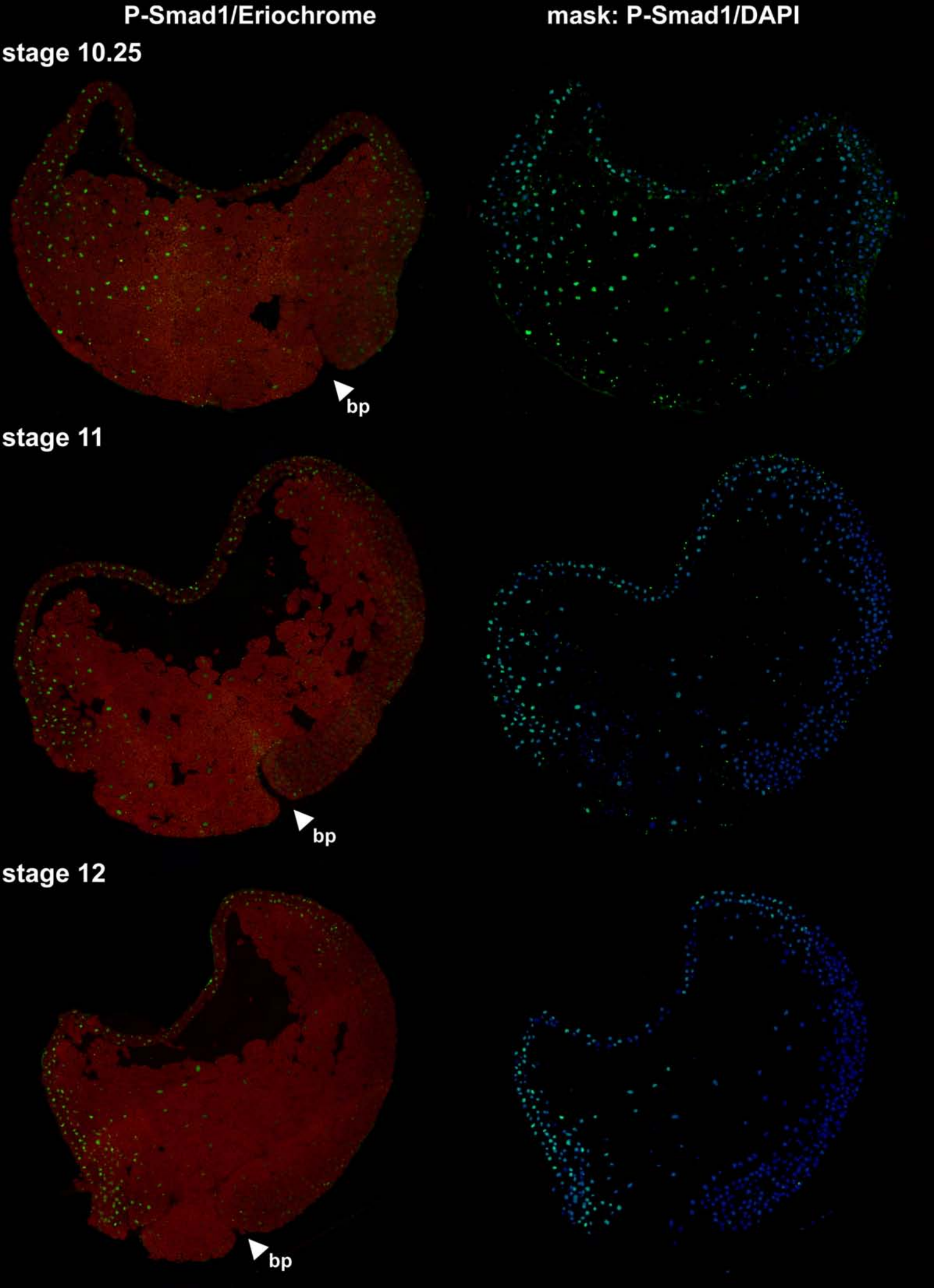
P-Smad1/Eriochrome
mask: P-Smad1/DAPI
stage 10.25
bp
stage 11
bp
stage 12
bp

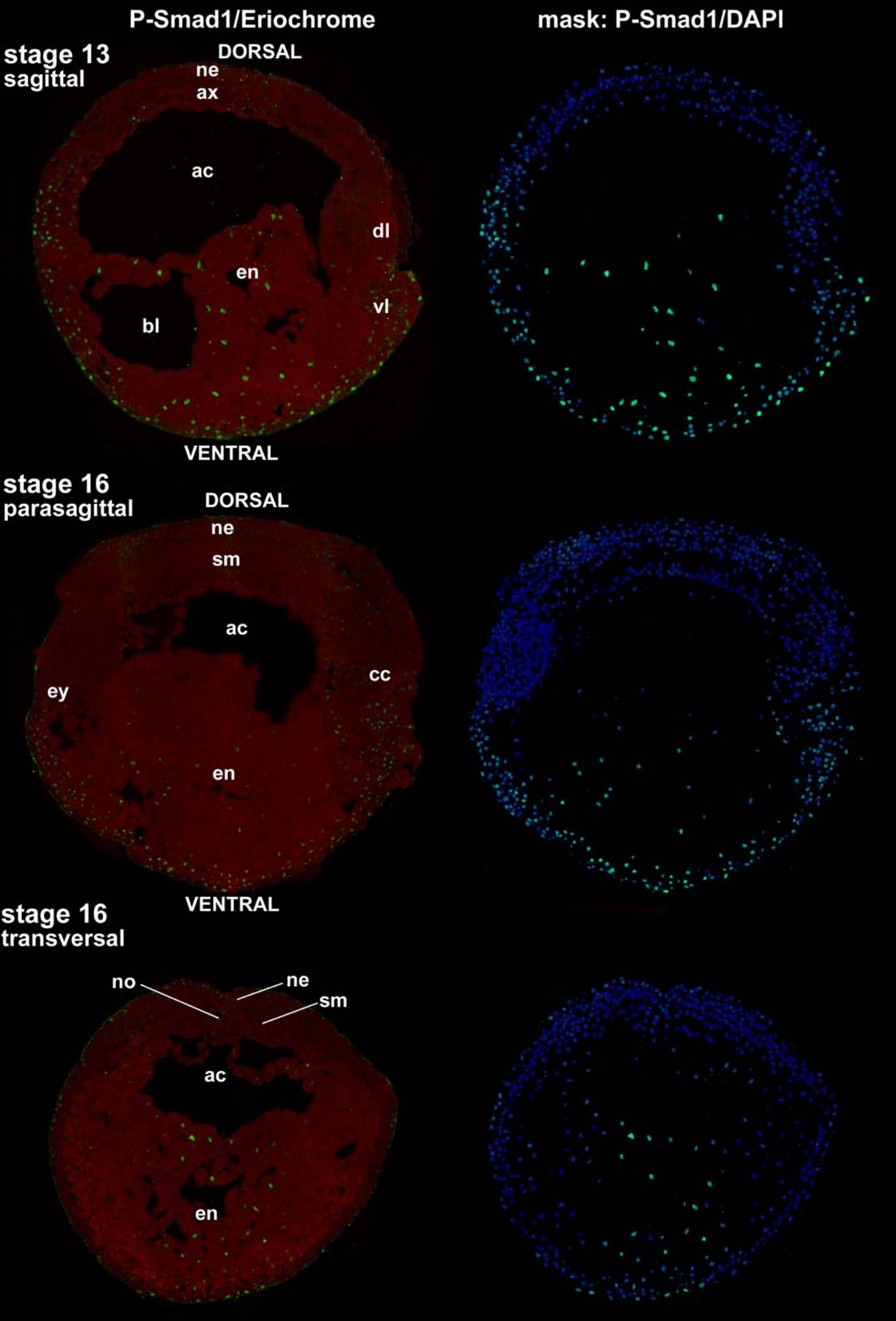
P-Smad1/Eriochrome
mask: P-Smad1/DAPI
stage 13
sagittal
DORSAL
ne
ax
ac
dl
en
vl
bl
VENTRAL
stage 16
parasagittal
DORSAL
ne
sm
ac
cc
ey
en
VENTRAL
stage 16
transversal
no
ne
sm
ac
en

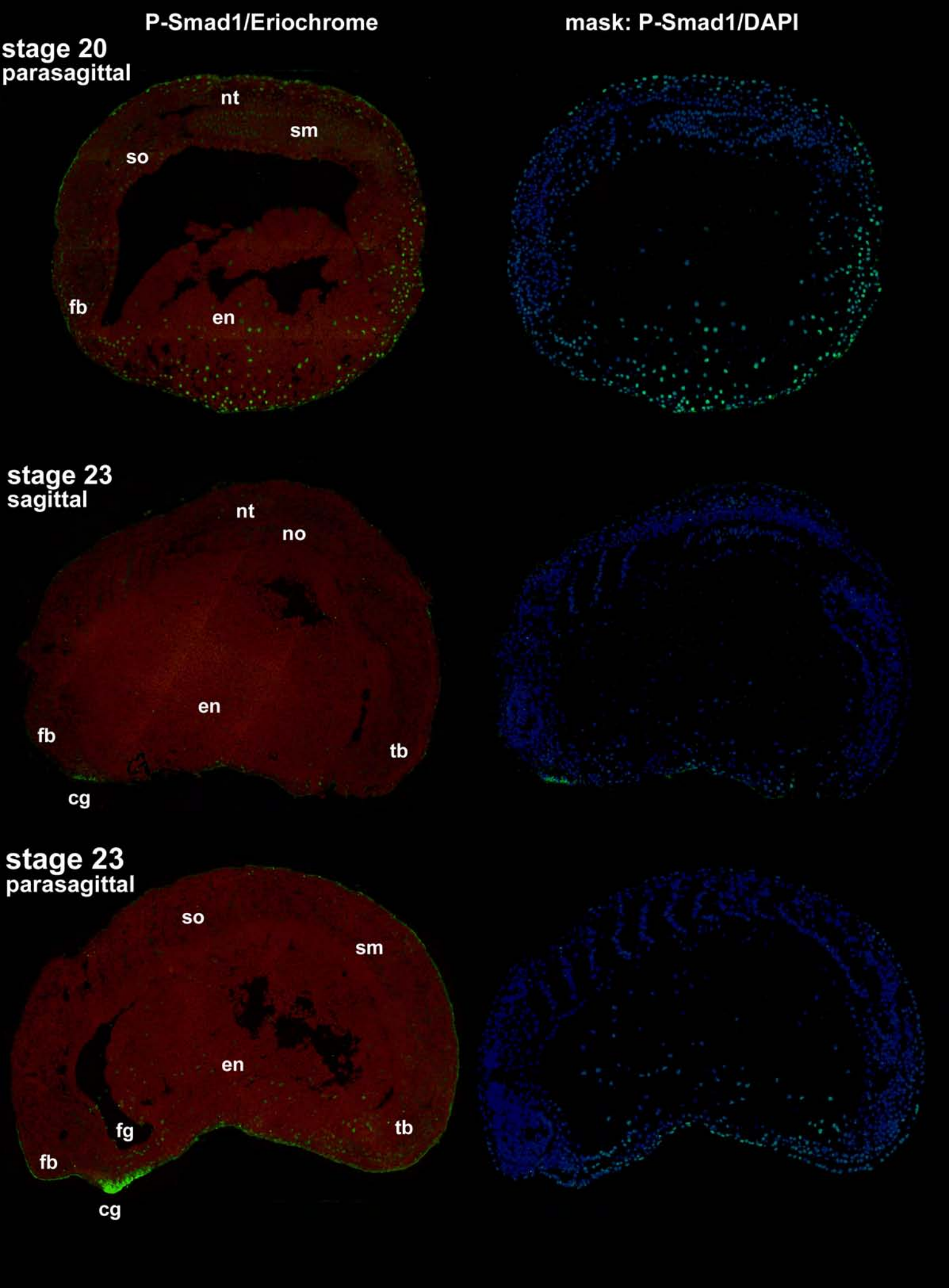
P-Smad1/Eriochrome
mask: P-Smad1/DAPI
stage 20
parasagittal
nt
sm
so
fb
en
stage 23
sagittal
nt
no
en
fb
tb
cg
stage 23
parasagittal
so
sm
en
fg
tb
fb
cg

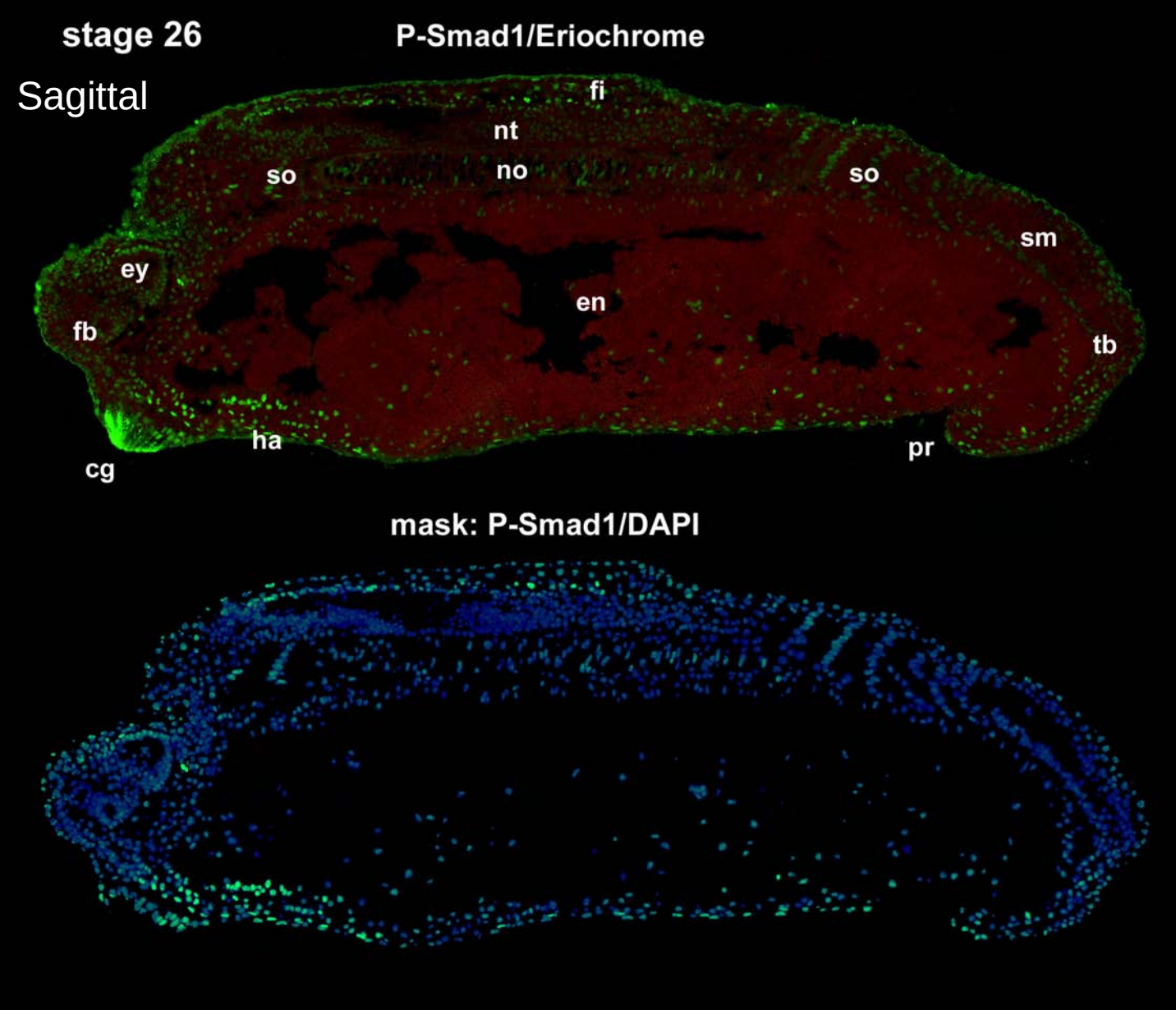
stage 26
P-Smad1/Eriochrome
Sagittal
fi
nt
no
so
so
sm
ey
en
fb
tb
ha
pr
cg
mask: P-Smad1/DAPI

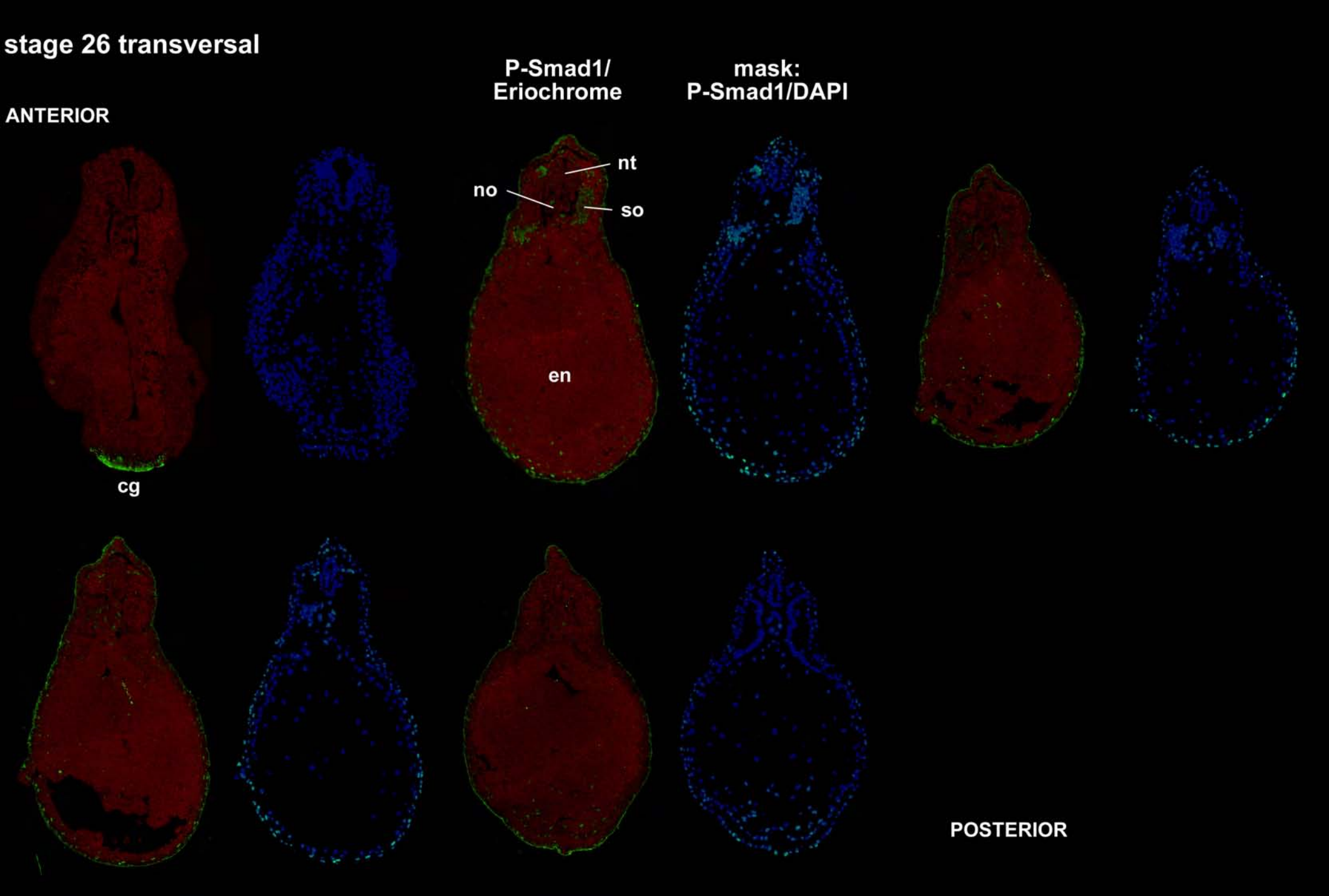
stage 26 transversal
P-Smad1/
Eriochrome
mask:
P-Smad1/DAPI
ANTERIOR
nt
no
so
en
cg
POSTERIOR

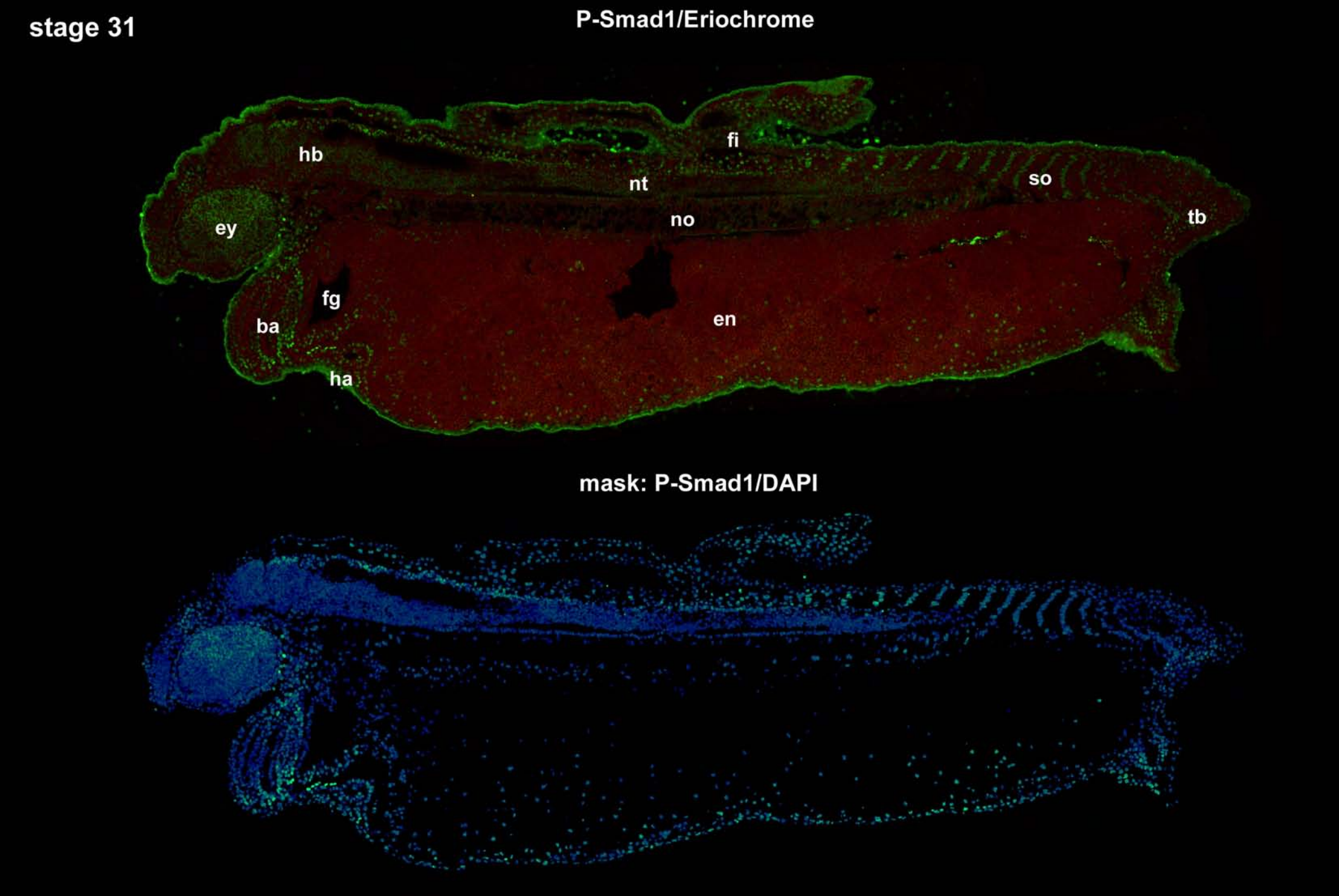
stage 31
P-Smad1/Eriochrome
hb
fi
nt
so
ey
no
tb
fg
ba
en
ha
mask: P-Smad1/DAPI

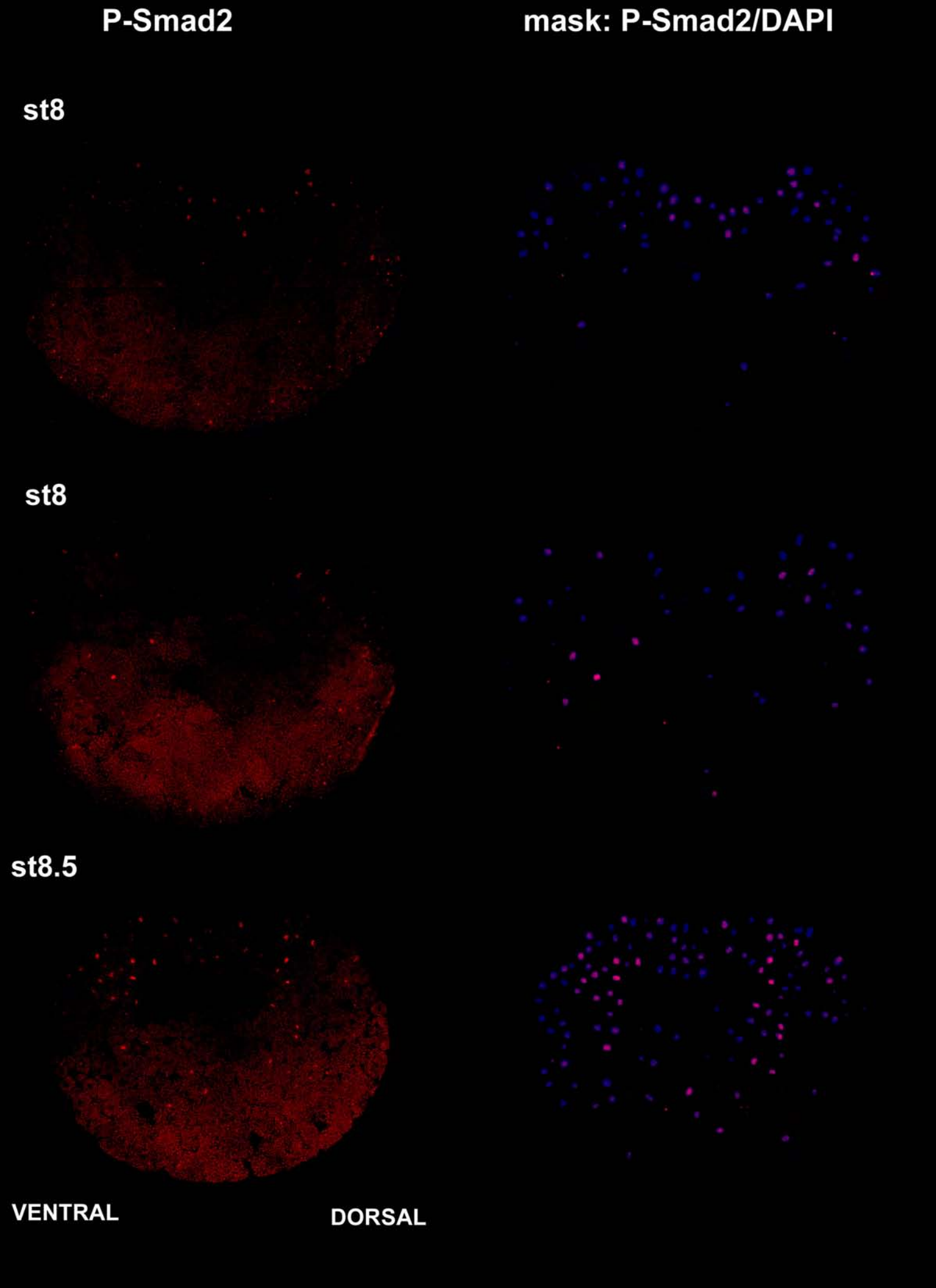
P-Smad2
mask: P-Smad2/DAPI
st8
st8
st8.5
VENTRAL
DORSAL

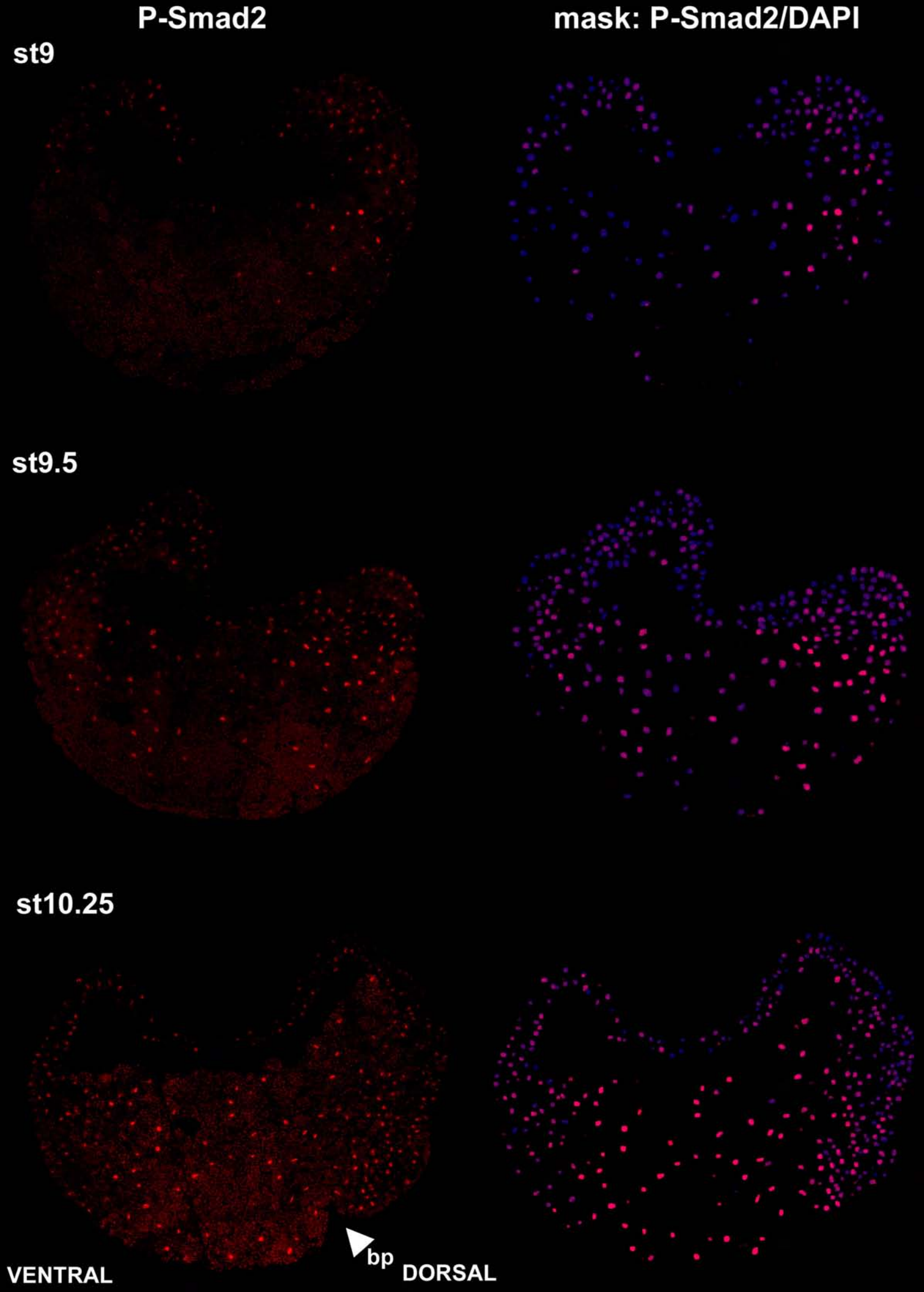
P-Smad2
mask: P-Smad2/DAPI
st9
st9.5
st10.25
bp
VENTRAL
DORSAL

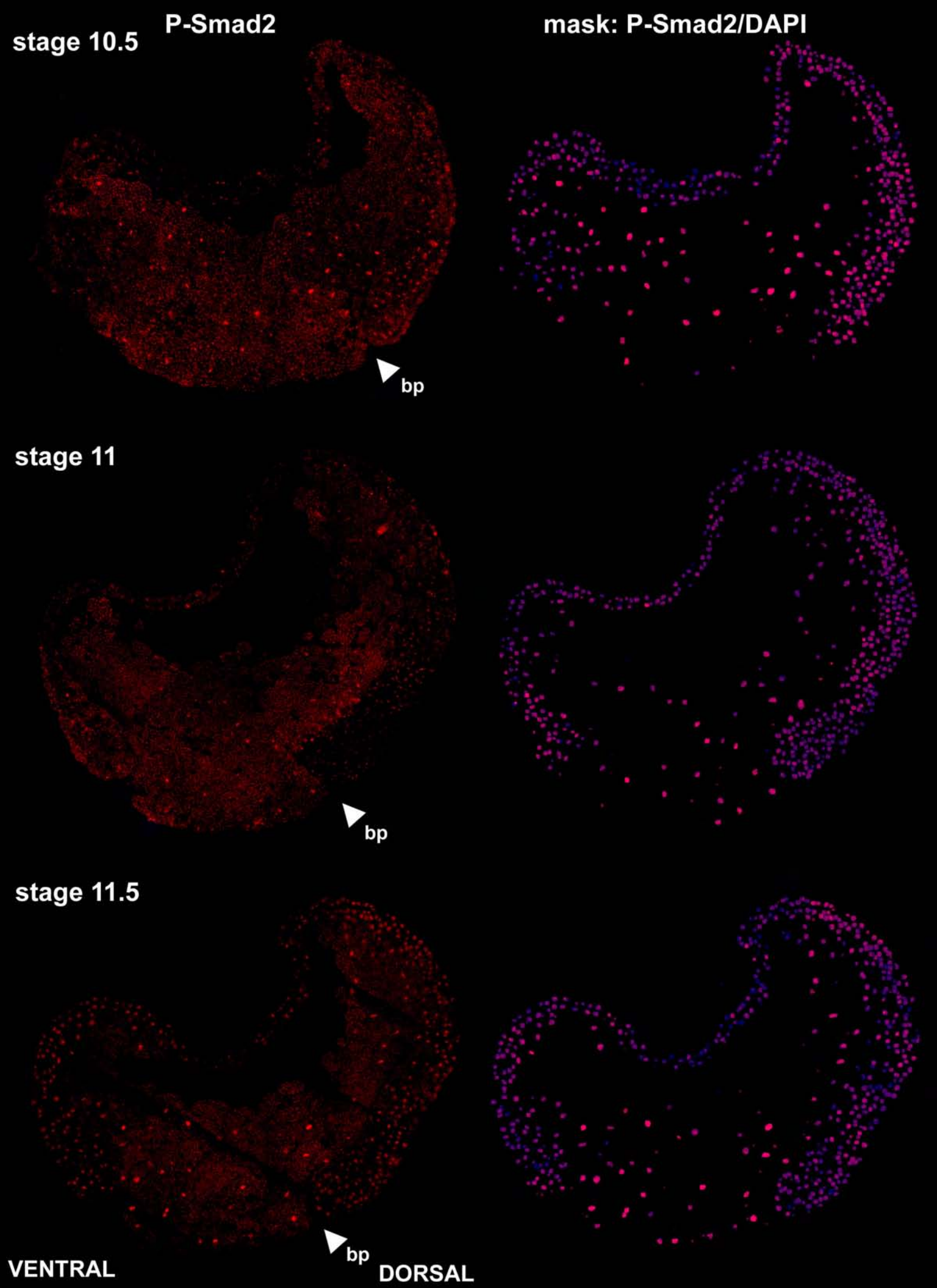
P-Smad2
mask: P-Smad2/DAPI
stage 10.5
bp
stage 11
bp
stage 11.5
bp
VENTRAL
DORSAL

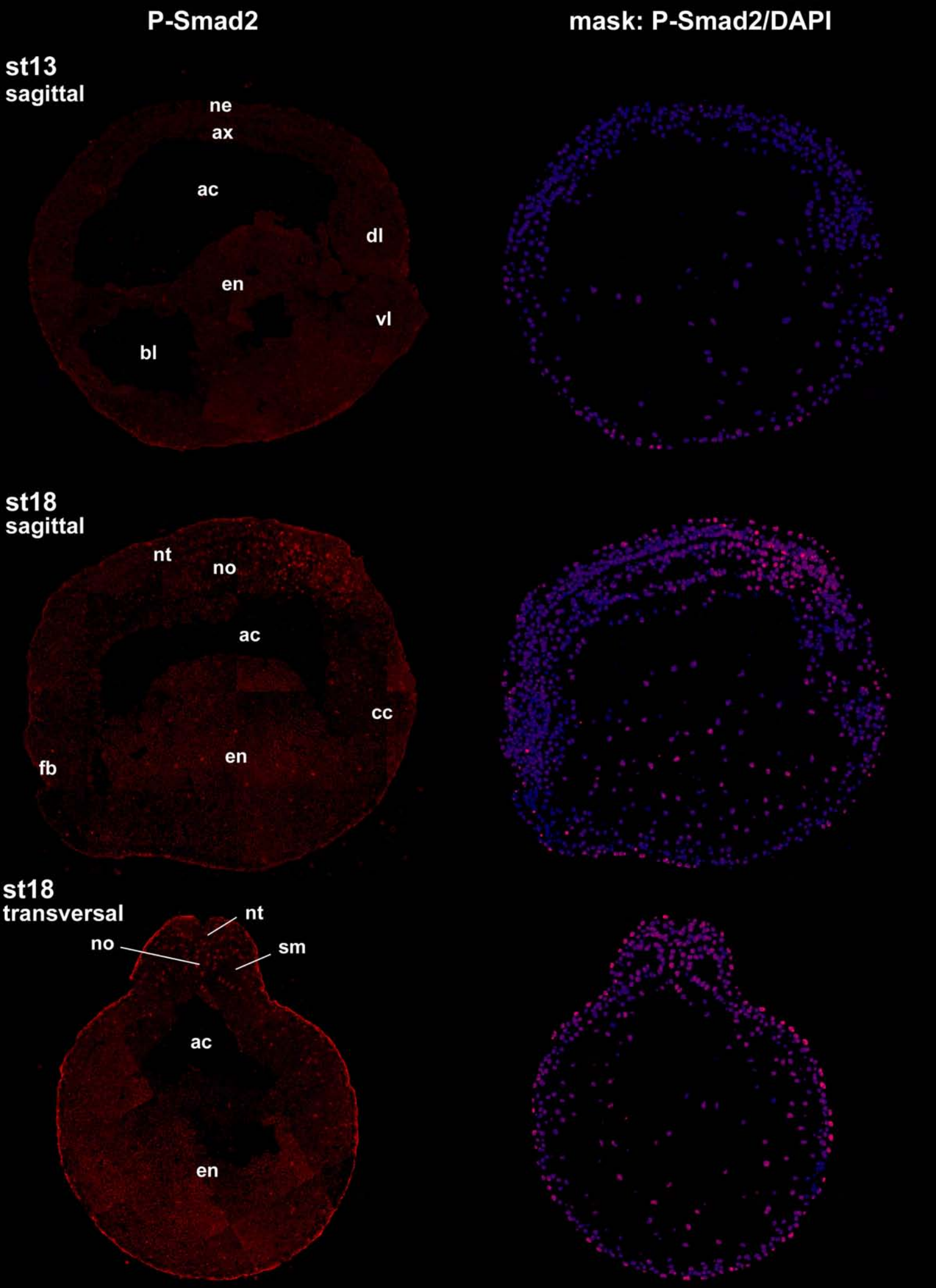
P-Smad2
mask: P-Smad2/DAPI
st13
sagittal
ne
ax
ac
dl
en
vl
bl
st18
sagittal
nt
no
ac
cc
en
fb
st18
transversal
nt
no
sm
ac
en

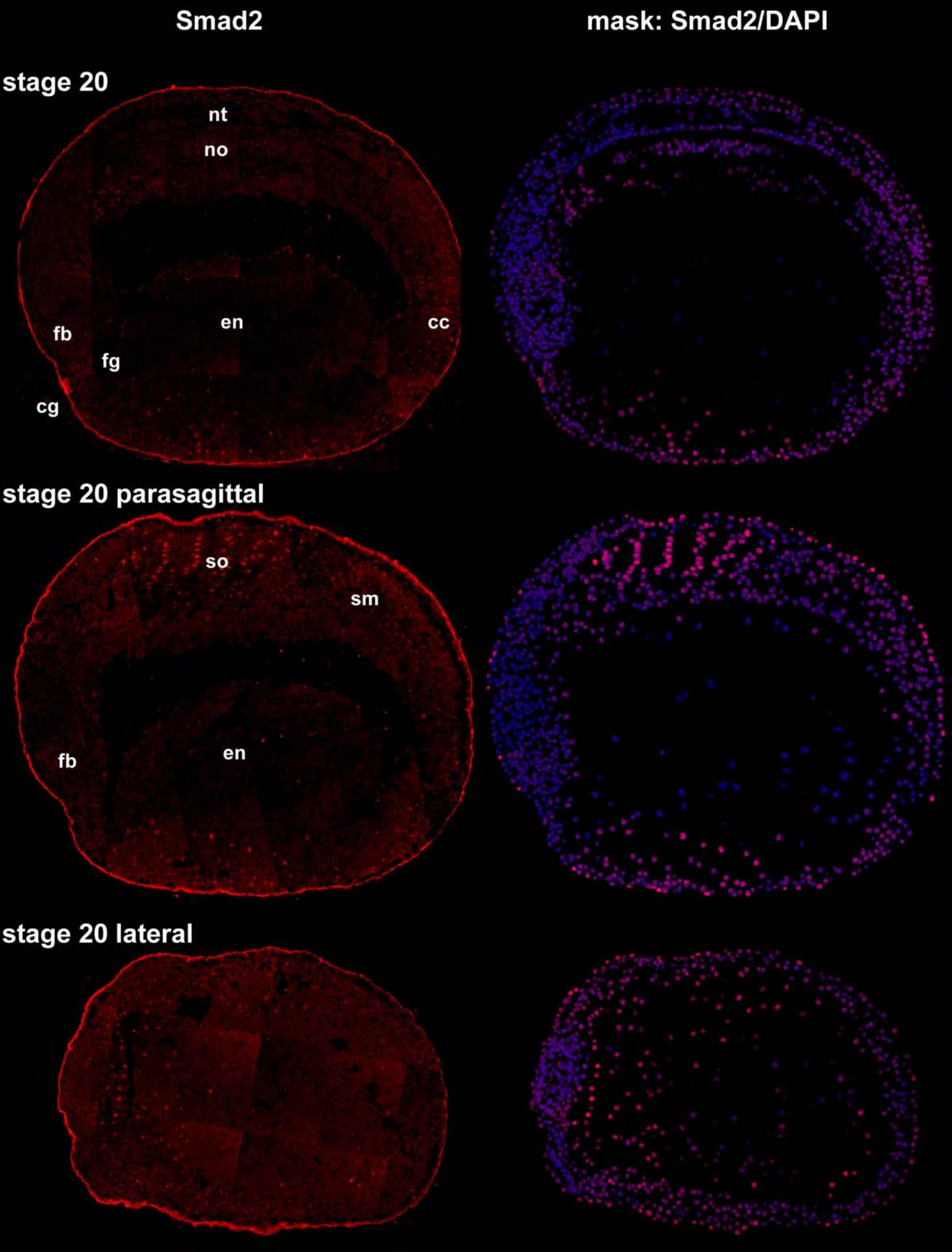
Smad2
mask: Smad2/DAPI
stage 20
nt
no
en
cc
fb
fg
cg
stage 20 parasagittal
so
sm
fb
en
stage 20 lateral

Sagittal

stage 26, notochord

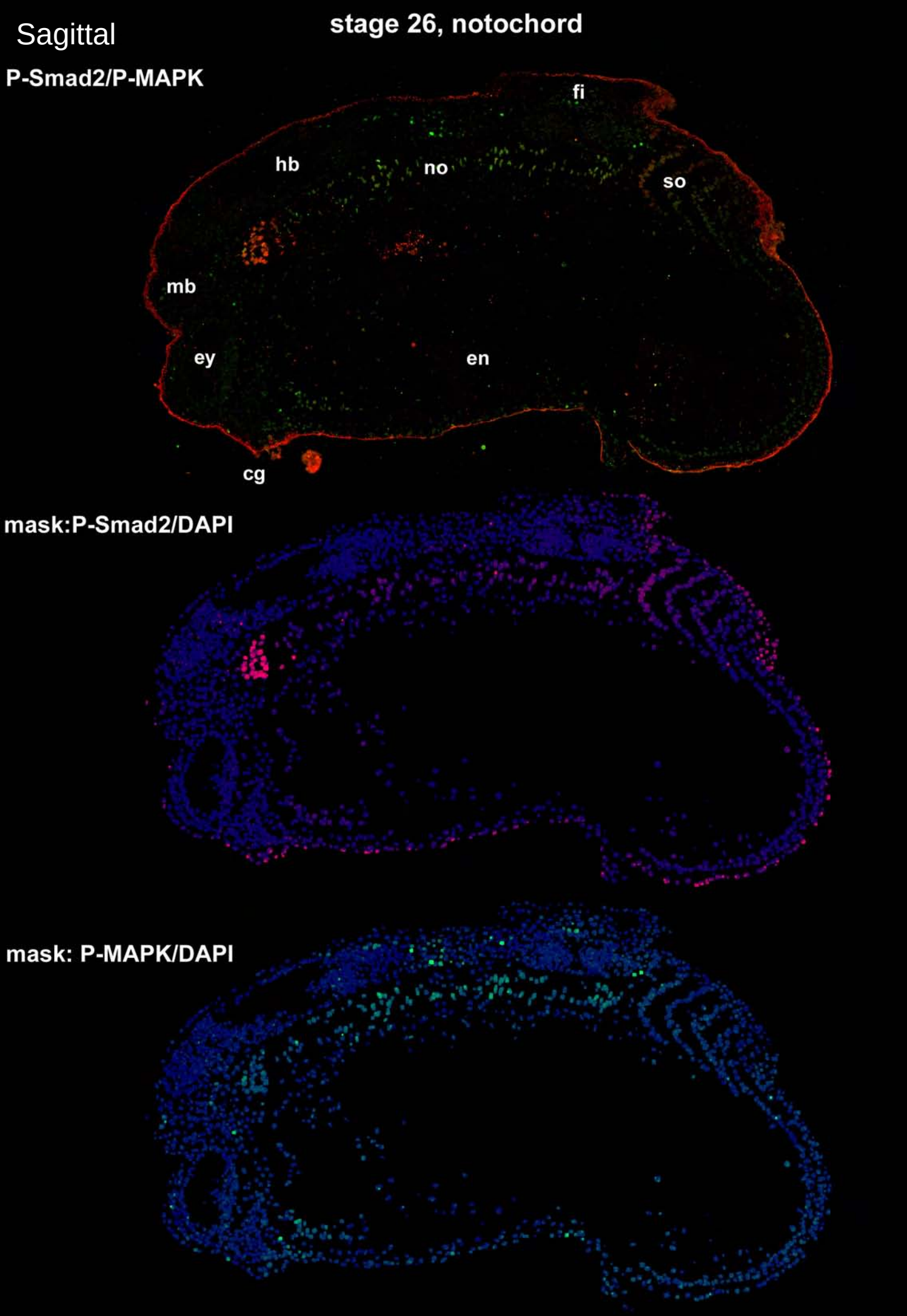

Parasagittal

stage 26, somites

P-Smad2/P-MAPK

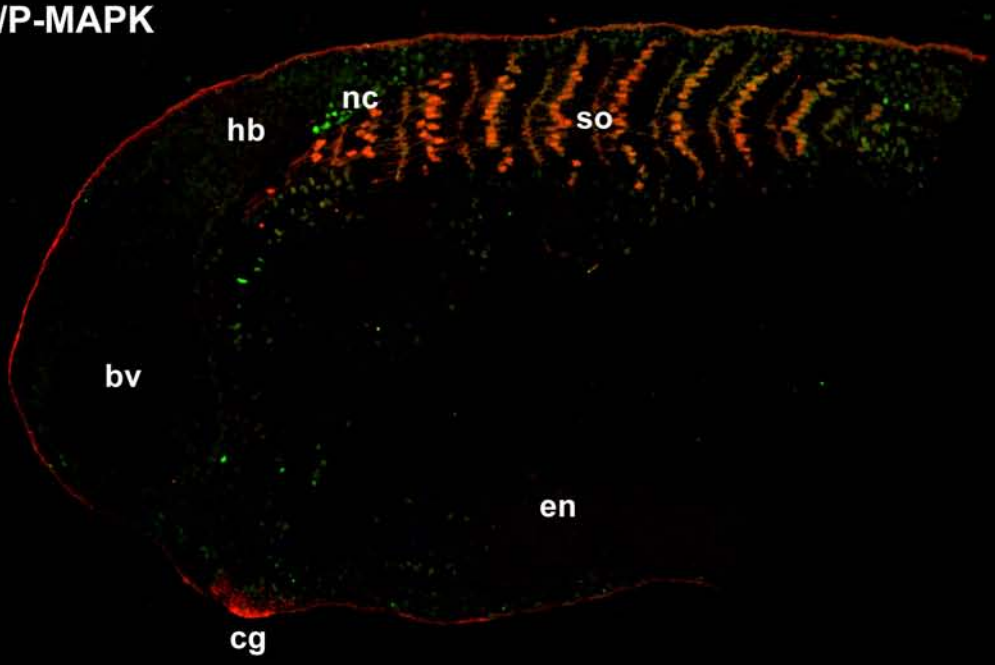

mask:P-Smad2/DAPI

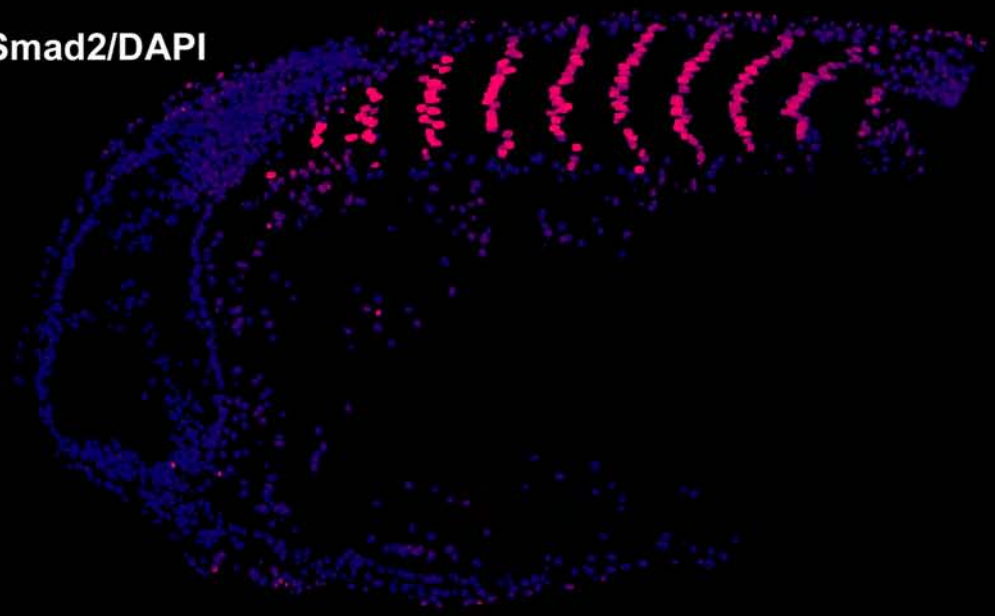

mask: P-MAPK/DAPI

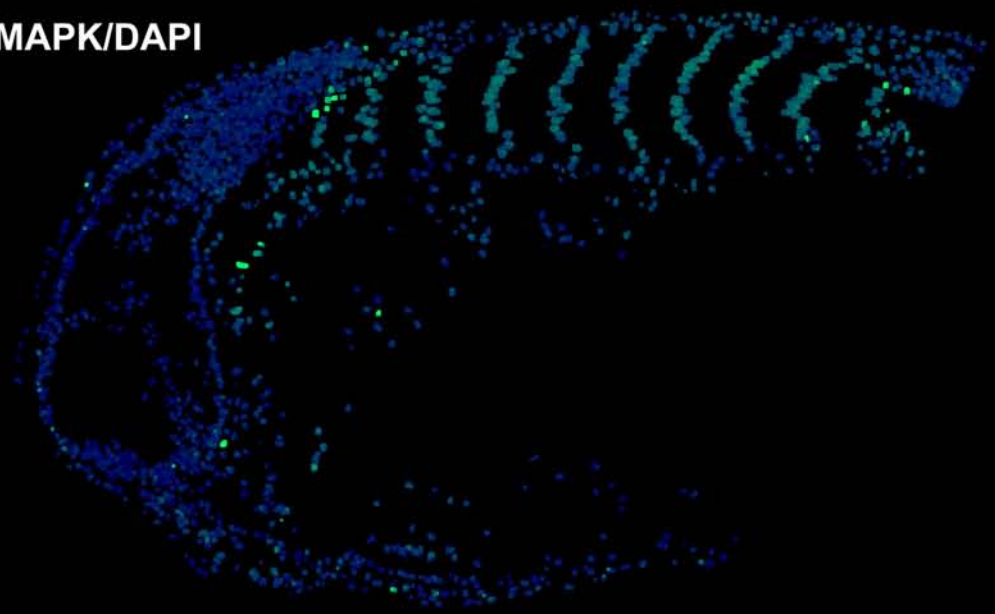

Sagittal

stage 31, notochord

P-Smad2/P-MAPK

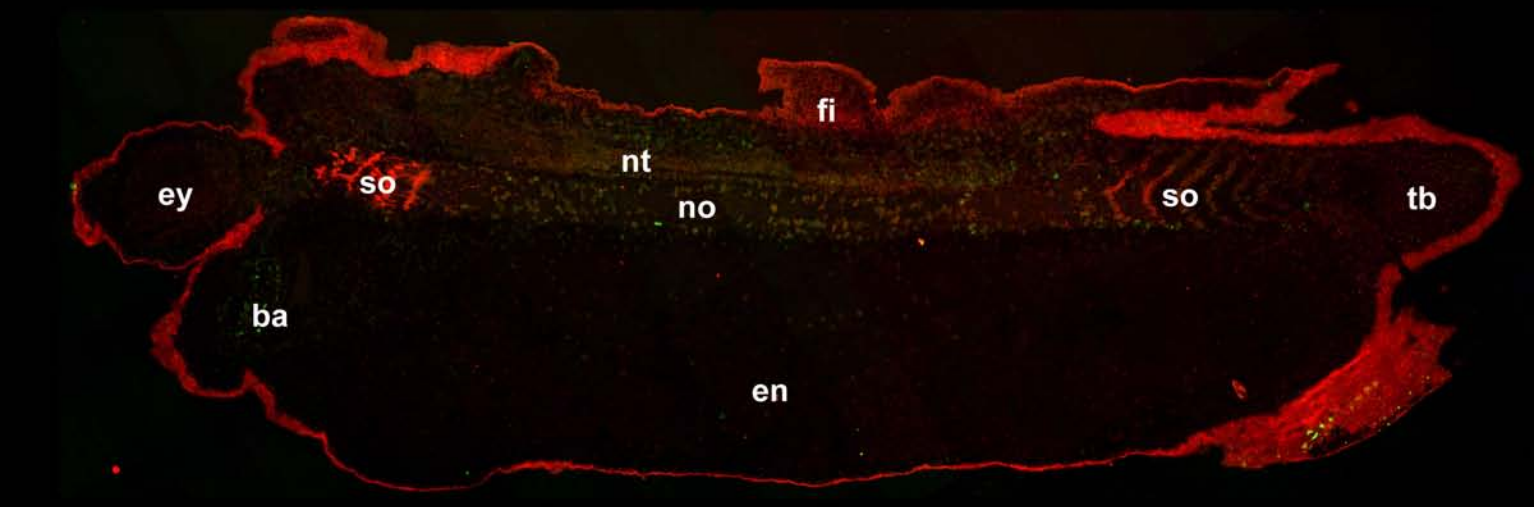

mask: P-Samd2/DAPI

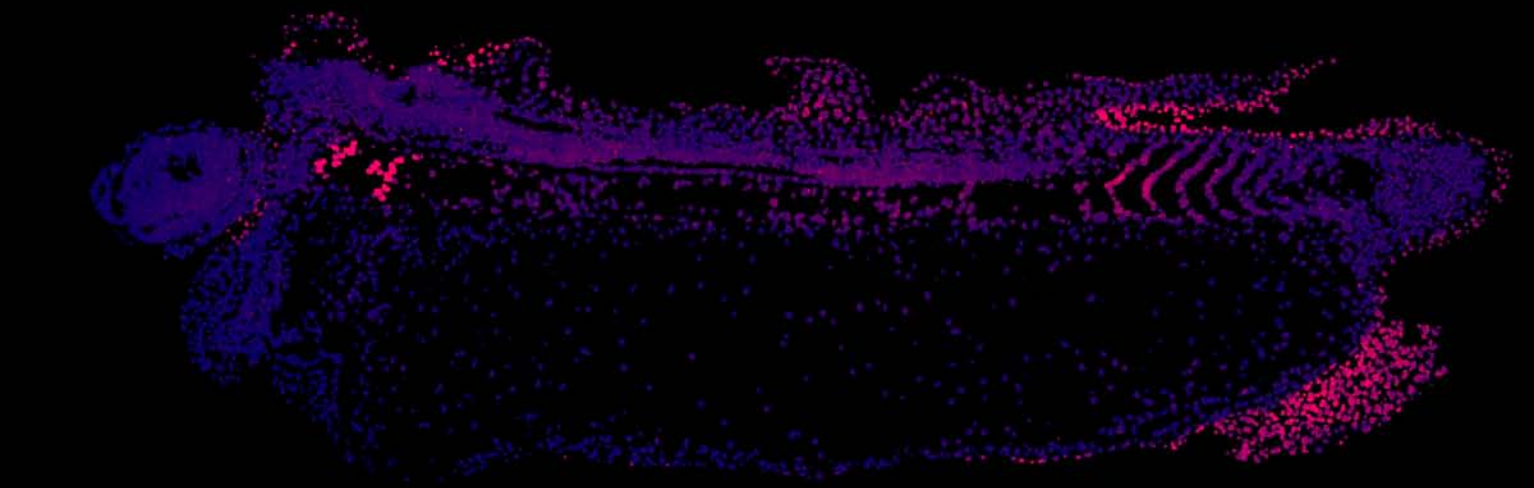

mask: P-MAPK/DAPI

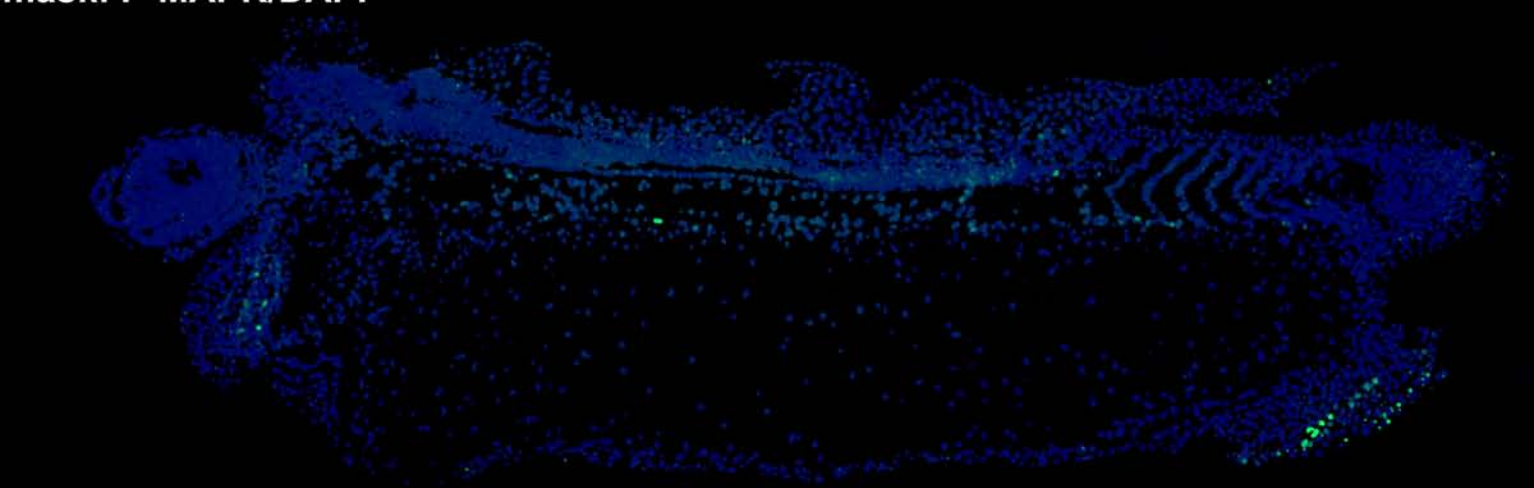

Parasagittal

stage 31, somites

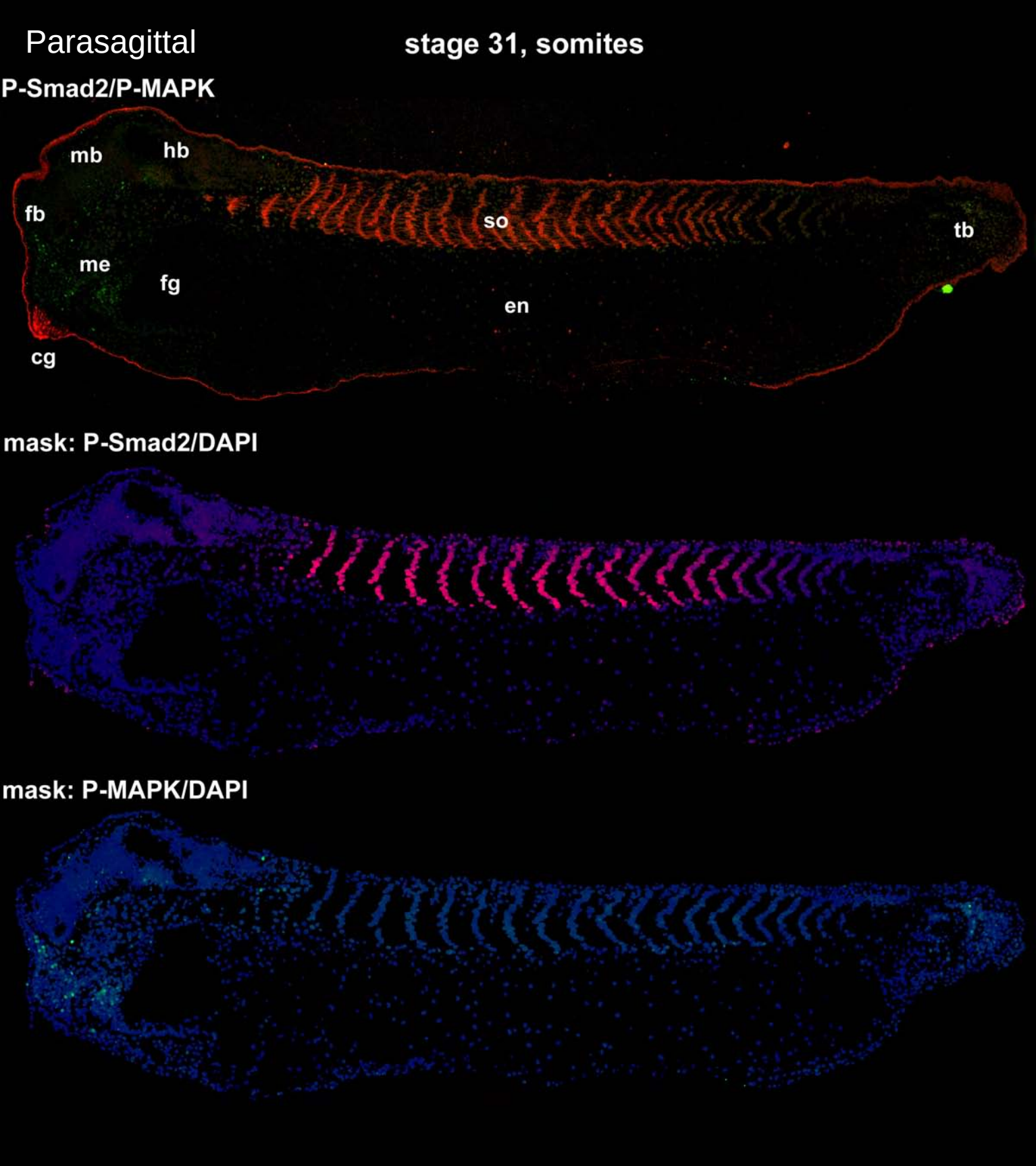

Parasagittal stage 31

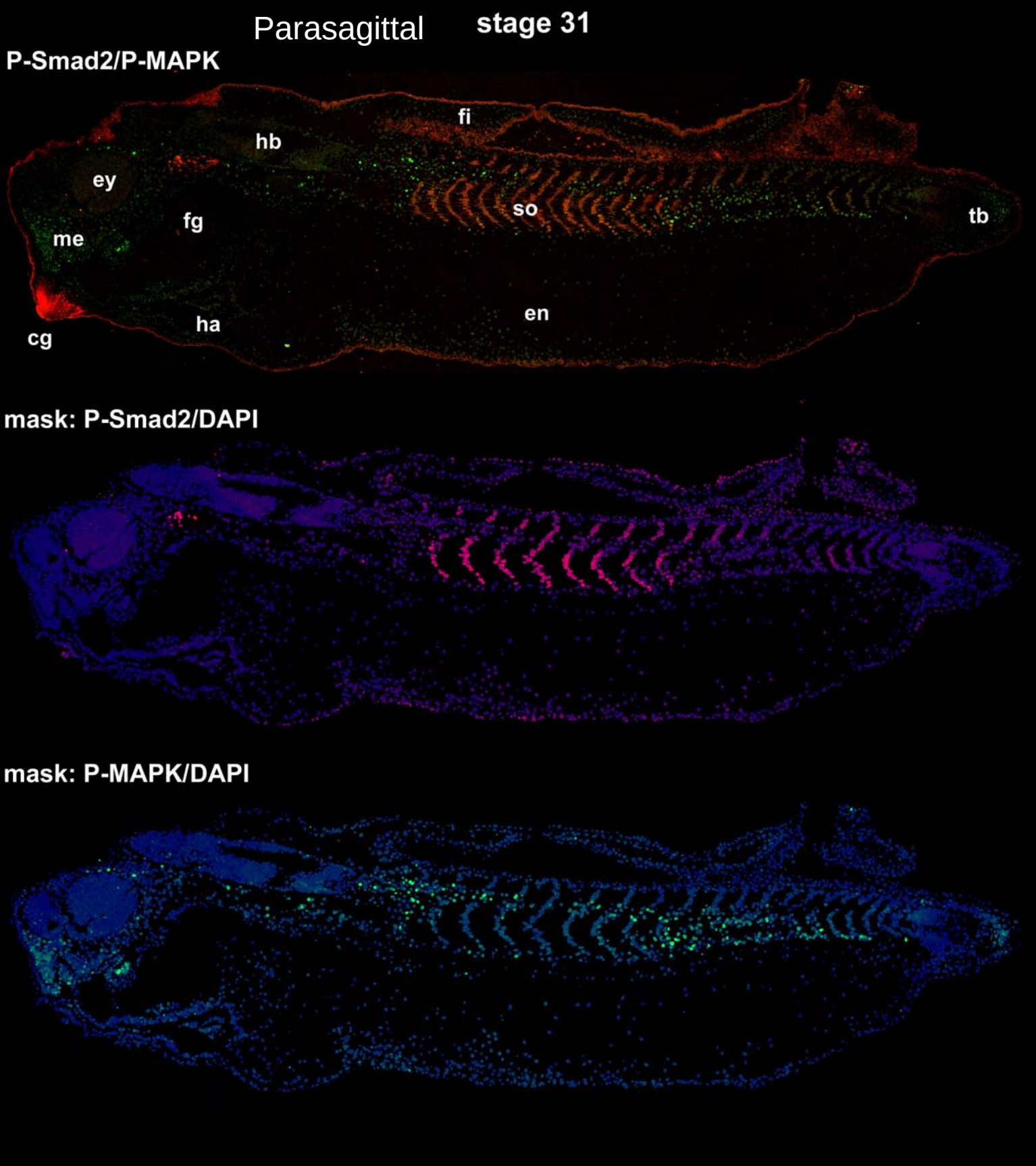

stage 31, head

P-Smad2/P-MAPK

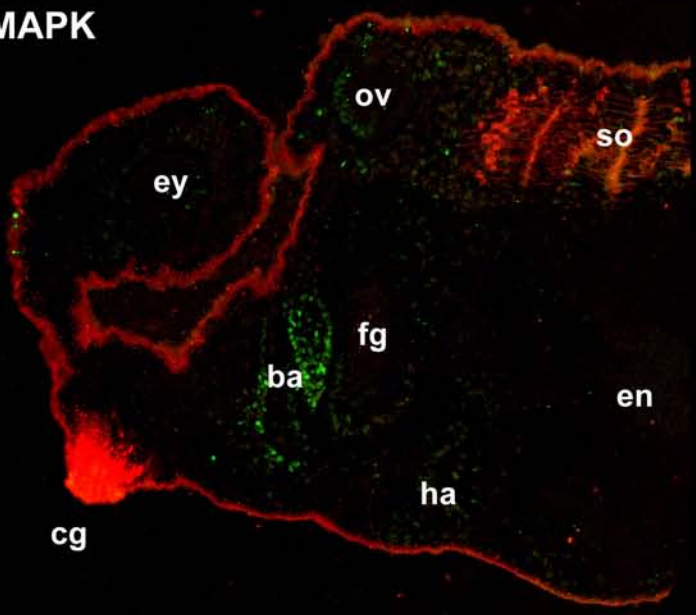

mask: P-Smad2/DAPI

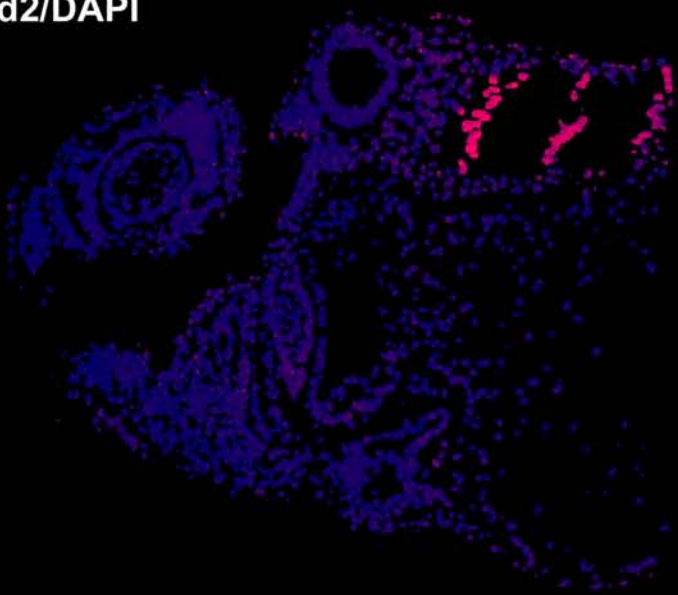

mask: P-MAPK/DAPI